

THE EFFECT OF EPS GEOFOAM BACKFILL ON THE SEISMIC PERFORMANCE  
OF INTEGRAL ABUTMENT BRIDGES

By

MEGAN OOMS

A thesis submitted to the

Graduate School-New Brunswick

Rutgers, The State University of New Jersey

In partial fulfillment of the requirements

For the degree of

Masters of Science

Graduate Program in Civil and Environmental Engineering

Written under the direction of

Dr. Hani H. Nassif

And approved by

---

---

---

New Brunswick, New Jersey

May 2016

# ABSTRACT OF THE THESIS

Seismic Performance of Integral Abutment Bridges with Expanded Polystyrene (EPS)

Geofoam Backfill

By MEGAN OOMS

Thesis Director:

Dr. Hani Nassif

This study was performed to investigate the seismic response of Integral Abutment Bridges (IABs) with Expanded Polystyrene (EPS) geofoam backfill in comparison to IABs with compacted backfill as well as typical jointed bridges. Three-dimensional Finite Element (FE) models of an existing bridge were developed and analyzed using the 1000-year seismic event according to the American Association of State Highway Transportation Officials (AASHTO) Load and Resistance Factor Design (LRFD). Results from existing information were used to determine soil characteristics and site class at the bridge location. Frame elements were utilized to model the piles, girders and diaphragms. Abutments and deck sections were modeled using shell elements to capture the effect of the connection to the girders. Nonlinear soil springs were used to model soil elements according to the Federal Highway Administration Seismic Retrofitting manual. The study shows that the use of EPS has major effects on the seismic performance of IABs. These effects include increasing the fundamental period of the bridge and reducing the forces in the superstructure as well as the integral abutments.

This combination of EPS geofoam backfill and integral abutments provides the benefits of reduced number of joints and bearings, which is highly desirable as it provides reduced maintenance and inspection costs as well as reduced repair costs. It also provides a potential for reduced initial construction costs over integral abutments with compacted backfill as the design forces in the abutments are lower; therefore smaller sections and less reinforcement would be required, although the material and installation costs of EPS geofoam can offset that cost savings.

# **ACKNOWLEDGEMENT**

I would like to express my deepest gratitude to my advisor, Dr. Hani Nassif, for his continuing support throughout my thesis. I would also like to thank my technical advisor, Suhail Albhaisi, for his continued guidance and direction. Lastly, I would like to thank my supervisor and coworkers at Jacobs Engineering Group, who have been understanding and supportive while I work on my thesis and graduate school work.

# TABLE OF CONTENTS

ABSTRACT OF THE THESIS	ii
ACKNOWLEDGEMENT	iv
TABLE OF CONTENTS	v
<b>LIST OF TABLES</b>	vii
<b>LIST OF FIGURES</b>	ix
<b>1 INTRODUCTION</b>	<b>1</b>
1.1 GENERAL	1
1.2 PROBLEM STATEMENT	6
1.3 BRIDGE BACKGROUND	8
1.4 LITERATURE REVIEW	12
1.4.1 EXPANDED POLYSTYRENE GEOFOAM BACKGROUND	12
1.4.2 SEISMIC BACKGROUND	15
1.4.2.1 SEISMICITY IN NEW JERSEY	15
1.4.3 GEOTECHNICAL INFORMATION	21
<b>2 FINITE ELEMENT MODEL</b>	<b>24</b>
2.1 INTRODUCTION	24
2.2 SUPERSTRUCTURE MODELING	28
2.2.1 DECK MODELING	30
2.2.2 GIRDER MODELING	33
2.2.3 DIAPHRAGM MODELING	41
2.3 SUBSTRUCTURE MODELING	46

2.3.1	PIER MODELING	48
2.3.2	ABUTMENT MODELING	52
2.4	SOIL AND BACKFILL MODELING	60
2.5	SOIL-STRUCTURE INTERACTION	61
2.5.1	CALCULATION OF INTEGRAL ABUTMENT SOIL-STRUCTURE INTERACTION	61
2.5.2	CALCULATION OF SOIL-STRUCTURE INTERACTION	79
2.5.3	APPLICATION OF SOIL-STRUCTURE INTERACTION	82
3	FINITE ELEMENT ANALYSIS	85
3.1	SEISMIC ANALYSIS PERFORMED	85
3.2	LOADING AND LOAD COMBINATIONS	88
4	ANALYSIS RESULTS	90
4.1	STRUCTRUAL PERIOD	90
4.2	PIER AND ABUTMENT DISPLACEMENT	99
4.3	PIER FORCES	106
4.4	ABUTMENT FORCES	113
5	SUMMARY AND CONCLUSIONS	130
5.1	SUMMARY	130
5.2	CONCLUSION	131
	Bibliography	134

# LIST OF TABLES

Table 1: Bridge Characteristics.....	11
Table 2: EPS Geofoam Properties .....	14
Table 3: Earthquake History for New Jersey (United States Geological Survey) .....	17
Table 4: Summary of Soil Parameters for Bridge A .....	22
Table 5: Summary of Soil Parameters for Bridge B .....	23
Table 6: Breakdown of Backfill Material and Soil Type by Model Number .....	27
Table 7: Properties of Clay (Rees and Van Impe) (Bowles).....	65
Table 8: Lateral Soil Springs for Cohesionless Backfill.....	66
Table 9: Approximate Soil Densities Used for Soil Spring Calculations of Sand.....	66
Table 10: Equation for $K_{spring}$ of Sand.....	67
Table 11: Lateral Soil Springs for Dense Sand.....	67
Table 12: Lateral Soil Springs for Medium Dense Sand .....	68
Table 13: Lateral Soil Springs for Loose Sand .....	69
Table 14: Average Lateral Soil Springs for Dense Sand Applied to Each Integral Abutment Shell Element .....	70
Table 15: Average Lateral Soil Springs for Medium Dense sand Applied to Each Integral Abutment Shell Element .....	71
Table 16: Average Lateral Soil Springs for Loose Sand Applied to Each Integral Abutment Shell Element .....	72
Table 17: Average Lateral Soil Springs for Dense Sand Applied to Integral Abutment H-Piles ..	73
Table 18: Average Lateral Soil Springs For Medium Dense Sand Applied to Integral Abutment H-Piles .....	75
Table 19: Average Lateral Soil Springs for Loose Sand Applied to Integral Abutment H-Piles ..	77
Table 20: Bridge A Pier Soil Spring Coefficients.....	81
Table 21: Bridge B Pier Soil Spring Coefficients.....	81
Table 22: Seismicity Information .....	88
Table 23: Fundamental Period .....	92
Table 24: Bridge A Longitudinal and Transverse Pier Displacement .....	100
Table 25: Bridge B Longitudinal and Transverse Pier Displacement.....	101
Table 26: Bridge A Maximum Displacement at Top and Bottom of Integral Abutments for Models with Sand Foundation Soils .....	102
Table 27: Bridge A Maximum Displacement at Top and Bottom of Integral Abutments for Models with Clay Foundation Soils.....	103
Table 28: Bridge B Maximum Displacement at Top and Bottom of Integral Abutments for Models with Sand Foundation Soils .....	104
Table 29: Bridge B Maximum Displacement at Top and Bottom of Integral Abutments for Models with Clay Foundation Soils.....	105
Table 30: Summary of Bridge A Pier Column Forces and Moments .....	107
Table 31: Summary of Bridge B Pier Column Forces and Moments .....	108

Table 32: Summary of Bridge A Pier Cap Forces and Moments .....	109
Table 33: Summary of Bridge B Pier Cap Forces and Moments.....	110
Table 34: Summary of Bridge A Pier Footing Forces and Moments .....	111
Table 35: Summary of Bridge B Pier Footing Forces and Moments.....	112
Table 36: Bridge A Maximum Shear and Moment for Compacted Backfill .....	114
Table 37: Bridge A Maximum Shear and Moment for EPS Geofoam Backfill .....	115
Table 38: Bridge A Maximum Shear and Moment for Compacted Backfill .....	116
Table 39: Bridge A Maximum Shear and Moment for EPS Geofoam Backfill .....	117
Table 40: Bridge B Maximum Shear and Moment for Compacted Backfill .....	118
Table 41: Bridge B Maximum Shear and Moment for EPS Geofoam Backfill.....	119
Table 42: Bridge B Maximum Shear and Moment for Compacted Backfill .....	120
Table 43: Bridge B Maximum Shear and Moment for EPS Geofoam Backfill.....	121



# LIST OF FIGURES

Figure 1: Integral Abutment Bridge	2
Figure 2: Conventional Bridge	2
Figure 3: Jointed Bridge Geometric Details for Bridge A	10
Figure 4: Jointed Bridge Geometric Details for Bridge B	10
Figure 5: Pier Geometric Details for Bridge A	11
Figure 6: Pier Geometric Details for Bridge B	11
Figure 7: Stress-Strain Relationship for EPS Geofoam (Geofoam Applications and Uses)	13
Figure 8: EPS Geofoam Being Used as Abutment Backfill (Geofoam Applications and Uses)	13
Figure 9: Geologic Provinces in New Jersey (Dombroski, Jr.)	16
Figure 10: Seismicity Map of NJ (United States Geological Survey)	18
Figure 11: 2-14 Seismic Hazard Map of New Jersey (United States Geological Survey)	20
Figure 12: Bridge Wizard Tool (Computers & Structures, Inc.)	26
Figure 13: Superstructure - Deck Section Definition Tool for Steel Superstructure (Computers & Structures, Inc.)	29
Figure 14: Superstructure - Deck Section Definition for Concrete Superstructure (Computers & Structures, Inc.)	30
Figure 15: Three-Node and Four-Node Shell Elements in CSiBridge (Computers & Structures, Inc.)	33
Figure 16: Definition of Hybrid I-Section (Computers & Structures, Inc.)	38
Figure 17: Definition of Non-Prismatic Section (Computers & Structures, Inc.)	39
Figure 18: Import of Angle Section from AISC Database (Computers & Structures, Inc.)	40
Figure 19: Location of Insertion Points for Frame Elements (Computers & Structures, Inc.)	41
Figure 20: Bridge Diaphragm Property (Computers & Structures, Inc.)	44
Figure 21: Diaphragm Connectivity (Computers & Structures, Inc.)	45
Figure 22: "Substructure - Bents" Definition Tool (Computers & Structures, Inc.)	46
Figure 23: Bridge Object Bent Assignments (Computers & Structures, Inc.)	47
Figure 24: "Bridge Wizard" Abutment Assignments (Computers & Structures, Inc.)	47
Figure 25: Concrete Pier on Spread Footings	50
Figure 26: Connecting Pier to Girder	51
Figure 27: Integral Abutment Geometry	56
Figure 28: Model of Bridge A with Conventional Abutments	58
Figure 29: Model of Bridge B with Conventional Abutments	58
Figure 30: Model of Bridge A with Integral Abutments	59
Figure 31: Model of Bridge B with Integral Abutments	59
Figure 32: Relationship Between Abutment Movement and Earth Pressure (Clough and Duncan)	62
Figure 33: P-y Curve for Soft Clay (Matlock)	64
Figure 34: Bridge A Response Spectra	87
Figure 35: Bridge B Response Spectra	88
Figure 36: 1 <sup>st</sup> Mode Shape for Bridge A with Conventional Abutments	93

Figure 37: 1st Mode Shape for Bridge B with Conventional Abutments	94
Figure 38: 1st Mode Shape for Bridge A with Integral Abutments and Compacted Backfill	95
Figure 39: 1st Mode Shape for Bridge B with Integral Abutments and Compacted Backfill	96
Figure 40: 1st Mode Shape for Bridge A with Integral Abutments and EPS Geofoam Backfill	97
Figure 41: 1st Mode Shape for Bridge B with Integral Abutments and EPS Geofoam Backfill	98
Figure 42: Bridge A Maximum Shear for Dense Sand at Piles	122
Figure 43: Bridge A Maximum Shear for Medium Dense Sand at Piles	122
Figure 44: Bridge A Maximum Shear for Loose Sand at Piles	122
Figure 45: Bridge A Maximum Moment for Dense Sand at Piles	123
Figure 46: Bridge A Maximum Moment for Medium Dense Sand at Piles	123
Figure 47: Bridge A Maximum Moment for Loose Sand at Piles	123
Figure 48: Bridge A Maximum Shear for Stiff Clay at Piles	124
Figure 49: Bridge A Maximum Shear for Medium Stiff Clay at Piles	124
Figure 50: Bridge A Maximum Shear for Soft Clay at Piles	124
Figure 51: Bridge A Maximum Moment for Stiff Clay at Piles	125
Figure 52: Bridge A Maximum Moment for Medium Stiff Clay at Piles	125
Figure 53: Bridge A Maximum Moment for Soft Clay at Piles	125
Figure 54: Bridge B Maximum Shear for Dense Sand at Piles	126
Figure 55: Bridge B Maximum Shear for Medium Dense Sand at Piles	126
Figure 56: Bridge B Maximum Shear for Loose Sand at Piles	126
Figure 57: Bridge B Maximum Moment for Dense Sand at Piles	127
Figure 58: Bridge B Maximum Moment for Medium Dense Sand at Piles	127
Figure 59: Bridge B Maximum Moment for Loose Sand at Piles	127
Figure 60: Bridge B Maximum Shear for Stiff Clay at Piles	128
Figure 61: Bridge B Maximum Shear for Medium Stiff Clay at Piles	128
Figure 62: Bridge B Maximum Shear for Soft Clay at Piles	128
Figure 63: Bridge B Maximum Moment for Stiff Clay at Piles	129
Figure 64: Bridge B Maximum Moment for Medium Stiff Clay at Piles	129
Figure 65: Bridge B Maximum Moment for Soft Clay at Piles	129

# CHAPTER I

## 1 INTRODUCTION

### 1.1 GENERAL

Integral abutment bridges (IABs) have been increasing in popularity over the recent years and as many as 13,000 IABs were reported in service in 2005 based on a survey performed by the Federal Highway Administration (Maruri, P.E. and Petro, P.E.). This growing trend is intuitive given the many advantages that integral abutment bridges have over conventional bridges, which will be discussed in detail later on in this section. Despite the recent increase of IABs being constructed, there is still a lack of information regarding their seismic performance. The purpose of this study is to provide additional information on the seismic performance of integral abutment bridges in various configurations with compacted backfill compared to Expanded Polystyrene Geofoam backfill.

In order to understand the behavior of integral abutment bridges, the difference between conventional bridges and integral abutment bridges must be understood. As shown in Figure 1, conventional or jointed bridges are characterized by having at least one expansion joint and bearings at either end of the bridge to allow for some small amounts of movement in the superstructure and substructure. The bearings act as the

connection between the superstructure and substructure in this case. Integral abutment bridges have no bearings or expansion joints at the ends of the bridge, unlike conventional bridges as shown in Figure 2. The girders are instead constructed integral, or seamlessly, with the abutments.

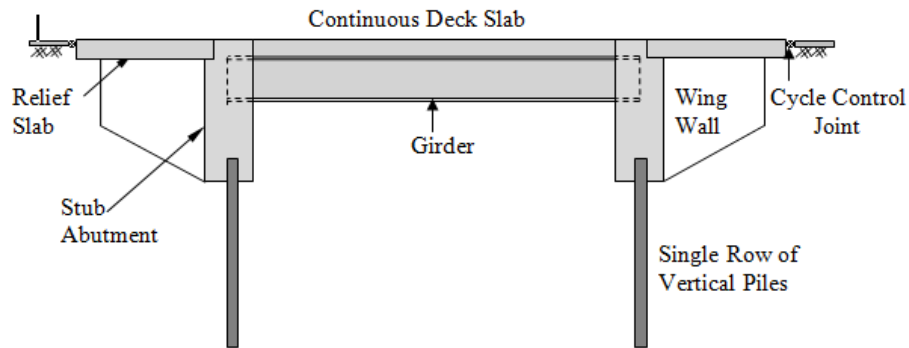


Figure 1: Integral Abutment Bridge

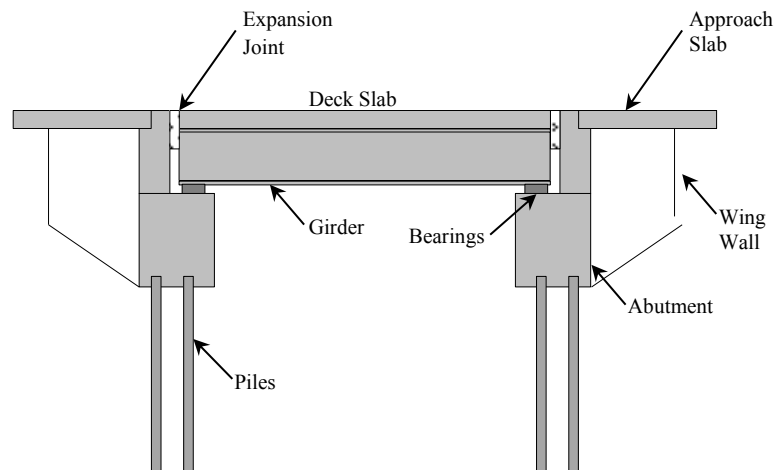


Figure 2: Conventional Bridge

While conventional bridges (or jointed bridges) have been the most common type of bridges constructed in the past, they pose several construction and maintenance complications compared to IABs. The first main complication is that bearings are relatively expensive both for materials and installation costs as well as lifetime maintenance costs. Installing bearings takes a great deal of care to insure that they are set properly in order for them to perform correctly. Additionally, bearings have a high maintenance cost as they can become frozen due to rust and debris, which prevents the bearings from moving as intended (Wasserman and Houston Walker). For this reason, it is important to have regular inspection and maintenance performed on the bearings to ensure that they continue to be free to move as intended. It is also not uncommon for bearings to have to be replaced one or more times during the life of a bridge, which can be very costly. Bearing replacement requires jacking the existing bridge in place so that it is not resting on the bearings that require replacement. Jacking of the bridge can be even more difficult and costly depending on if there is traffic under the bridge where the bearings are as this could require traffic detours or lane shifts which complicate the process significantly.

Similarly, expansion joints are the second main complication of conventional jointed bridges as they are also costly for construction and maintenance. Expansion joints can become filled with debris over time, which prevents proper movement of the joint. If the expansion joint is not allowed to move as intended, this can cause damage to the bridge as well as the expansion joints. The debris can puncture or split the expansion joint, allowing surface runoff water from the roadway and deicing chemicals to leak through the expansion joint onto the superstructure and substructure below the joint. This

can cause corrosion or damage to the structural elements below the expansion joint causing additional maintenance and repairs to be required.

In addition to the cost benefits of not having bearings or expansion joints, the integral abutment bridges have different flexibility and resistance characteristics as a result of the lack of expansion joints and bearings. While conventional bridges have a large degree of flexibility between the girders and the abutments, IABs have more rigid connections. This is a direct result of the fact that there are no bearings at the abutments for IABs, but rather the girders are poured integral with the abutments, and a rigid connection is created at both abutments. The integral abutments are designed to flex enough to account for the expansion and contraction of the superstructure due to temperature loading and seismic demand, which provides some added flexibility in the overall bridge system. Integral abutment bridges as a system are much more rigid than convention abutment bridges. This is due to the fact that that the connection between the superstructure and the integral abutments is a very rigid connection that is not present in conventional bridges. The added flexibility of the integral abutments themselves is relatively small compared to this rigidity of the superstructure to integral abutment connection. This overall rigidity can have a major impact on the structure's performance, particularly during a seismic event.

During a seismic event, a bridge can move both laterally and vertically, which can introduce forces to which the bridge is not normally subjected. Additionally, the bridge supports, whether piers or abutments, move differently from each other, causing the bridge to undergo a wave type motion. For this reason, it is not necessarily the strength of the bridge that is important for seismic design, but rather the flexibility of the

structure. As a result, IABs, which are less flexible than bridges with conventional seat-type abutments, have smaller fundamental periods during a seismic event. This would in turn attract additional forces to the abutments. In most cases the integral abutments can be designed to take these additional loads, however this can lead to larger abutments or would require stronger materials. However, the use of Expanded Polystyrene (EPS) geofoam behind the integral abutments rather than compacted backfill allows for the IABs to be more flexible and therefore have a slightly lower fundamental period. Additionally, this would cause a smaller increase in abutment forces for the IABs as the EPS geofoam takes the additional demand rather than the integral abutments.

In summary, expansion joints and bearings introduce additional construction and maintenance costs throughout the life of the bridge. For this reason it is desirable to reduce or even completely eliminate expansion joints and bearings on a bridge. This can be accomplished by using Integral abutment bridges rather than conventional jointed bridges. However, IABs are more rigid than bridges with conventional abutments, which is not desirable during seismic events. The use of EPS geofoam as backfill may help reduce the rigidity of IABs therefore improving the performance of IABs during seismic events.

## 1.2 PROBLEM STATEMENT

Though integral abutment bridges have many advantages over conventional jointed bridges, the lack of bearings at the abutments introduce a new set of issues. The first issue is that the integral abutment may have to be able to accommodate additional movement during a seismic event that would normally be accommodated for by the bearings and joints in conventional bridges. The second issue is that the bearings and expansion joints present in conventional bridges allow the superstructure to move during a seismic event, which is not the case for integral abutment bridges. Consequently, the foundations of IABs are subjected to additional loading as a result of this additional demand.

By utilizing Expanded Polystyrene (EPS) Geofoam as backfill for the integral abutments, the additional demand on the foundations can be alleviated. This is based on the belief that the EPS geofoam will take the additional demand caused by the abutments being monolithically connected to the superstructure. Because the EPS geofoam can compress when the abutments move during seismic loading, the forces applied to the abutments by the EPS geofoam is less than that which would be applied if it were compacted backfill behind the integral abutments.

This study investigates the effect of EPS geofoam backfill on the seismic performance of IABs in a moderate seismic zone. There are several parameters that affect the performance of IABs including length of spans, number of spans and abutment skew. In particular, this study addresses the effects of these parameters on IABs with EPS geofoam backfill under seismic loading.



In order to investigate the seismic response of IABs, two bridges located in New Jersey were selected to be modeled with both conventional abutments as well as integral abutments. Each of these two bridges have different geometric parameters that are to be included in the analysis to aide in isolating the effects of each parameter on the seismic performance.

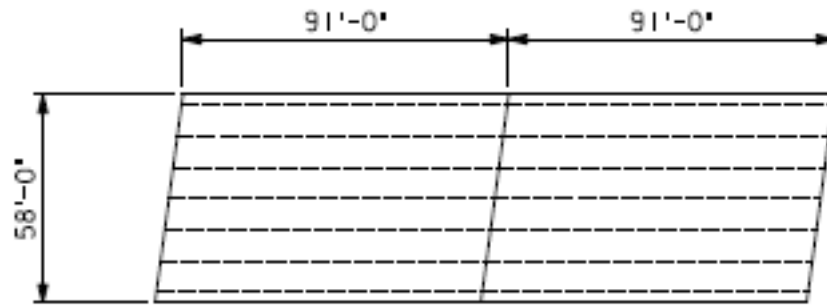
### 1.3 BRIDGE BACKGROUND

Two bridges from New Jersey were selected to be part of this parametric study. A detailed structural finite element model was created for each of these bridges with and without integral abutments. For each bridge, there is one model which is for the conventional bridge configuration and 12 models for the integral abutment bridge configuration for a total of 13 separate models for each of the two bridges and a total of 26 structural finite element bridge models in all. Each of the 12 integral abutment models for each bridge has a different combination of abutment backfill material and in-situ soil at the pile level (refer to Sections 1.4.3 and 2.4 for detailed information on the backfill and in-situ soil used for each model). This is to compare the effect of various soil stiffnesses behind the integral abutment to that of the EPS geof foam backfill for different soil conditions. All 13 models are then analyzed using the multimode response spectrum (MMRS) analysis and accounts for the effects of soil-structure interaction (SSI). The seismic demands with and without integral abutments are then compared to assess the effects of the integral abutment on the seismic response of the bridge for each different abutment backfill scenario. The seismic demands for each different bridge are also compared to assess the effects of the skew, number of spans and span configuration on the performance of the EPS geof foam backfill for integral abutments and on the performance of integral abutment bridges with compacted backfill.

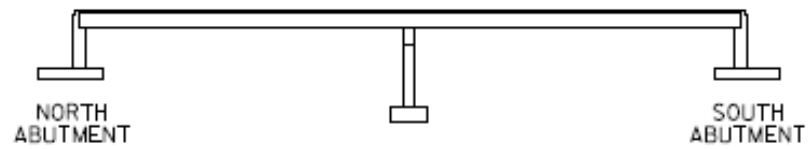
The two bridges selected for this investigation are all located in New Jersey and will be designated Bridge A and B for simplicity. Bridge A is a two-span continuous structure carrying two lanes of traffic. The 58 foot wide cast-in-place concrete deck is supported by steel girders over the two 91 foot long spans as shown in Figure 3. The

steel girders are supported by a central reinforced concrete multi-column pier with a reinforced concrete pier cap. The central pier consists of three columns which each have an approximate height of 17.5 feet, which can be seen in Figure 5. This bridge was constructed with conventional seat-type abutments. The abutments and central pier have a minimal skew of only  $7.63^{\circ}$ . Based on the geometry and configuration of this structure, it represents a typical bridge for the New Jersey area. While this as-built configuration is used for the conventional bridge model, the integral abutment model utilizes this same configuration with exception of the abutment type.

Like Bridge A, Bridge B is a two-span continuous structure but only carries 1 lane of traffic. It has a 30.9 foot wide cast-in-place concrete deck that is supported on steel girders over the approximately 130 foot and 130.75 foot spans as shown in Figure 4. The steel girders are supported by a central reinforced concrete single-column pier and pier cap. The column is approximately 21.25 feet in height. This pier geometry can be seen in Figure 6, below. The bridge was constructed with conventional seat type abutments. The abutments and central pier have no skew.

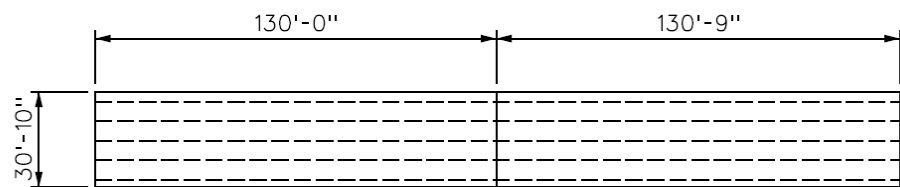


Plan

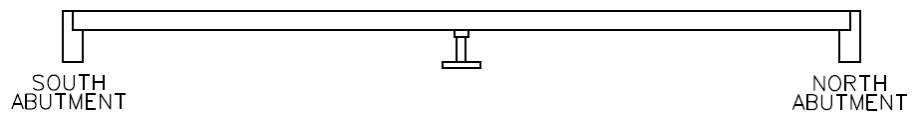


Elevation

**Figure 3: Jointed Bridge Geometric Details for Bridge A**

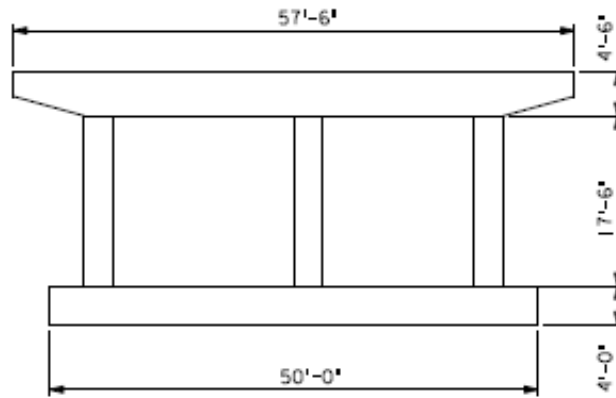


Plan



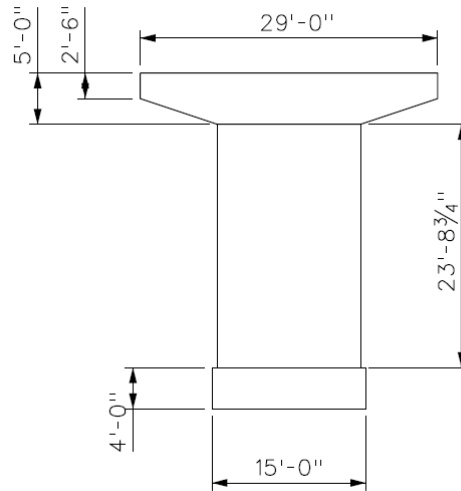
Elevation

**Figure 4: Jointed Bridge Geometric Details for Bridge B**



Elevation

**Figure 5: Pier Geometric Details for Bridge A**



Elevation

**Figure 6: Pier Geometric Details for Bridge B**

**Table 1: Bridge Characteristics**

Bridge	Pier and Abutment Skew	Number of Spans	Total Length (ft)
Bridge A	7.63 <sup>0</sup>	2; continuous	182.00
Bridge B	0 <sup>0</sup>	2; continuous	260.75

## **1.4 LITERATURE REVIEW**

### **1.4.1 EXPANDED POLYSTYRENE GEOFOAM BACKGROUND**

Expanded polystyrene geofoam is often used where backfill is needed for structural elements that would benefit from reduced stresses. EPS geofoam is lightweight and can reduce the loads applied on adjacent soil and structures (Geofoam Applications and Uses). EPS geofoam also provides consistent and predictable mechanical behavior that is beneficial in the design processes and is not affected by the freeze-thaw cycle, moisture or road salts, which makes it a great candidate for abutment backfill material. EPS geofoam behaves as a linear elastic material up to a strain of approximately 1%. Therefore the design loading is typically restricted to the compressive resistance at 1% strain in order to avoid undesirable permanent strains in the geofoam (Expanded Polystyrene Data Sheet).

EPS geofoam is a compressible inclusion, which means that it has a relatively low stiffness. Therefore, it will compress more readily than other materials and hence will result in load reduction through the classical soil mechanics mechanism of shear strength mobilization (Handy).

Additional benefits of EPS geofoam include the relatively short construction times due to the faster placement rates and ease of handling. Both of these characteristics factor in to it also having lower construction costs, despite the somewhat higher material costs as compared to traditional backfill material.

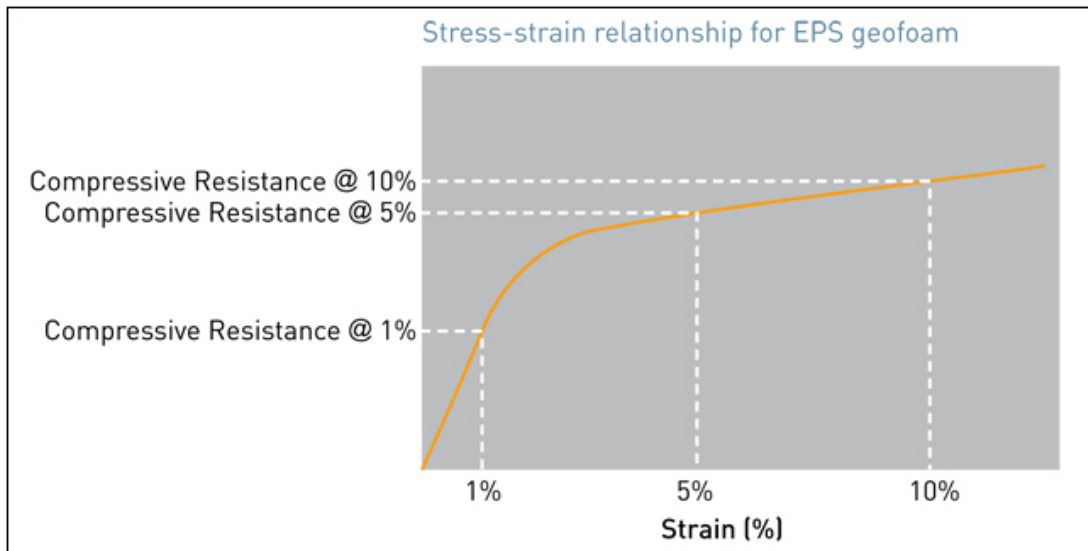


**Figure 7: Stress-Strain Relationship for EPS Geofoam** (Geofoam Applications and Uses)



**Figure 8: EPS Geofoam Being Used as Abutment Backfill** (Geofoam Applications and Uses)

**Table 2: EPS Geofoam Properties**

<b>Property</b>	<b>Units</b>	<b>EPS12 Type XI</b>	<b>EPS15 Type I</b>	<b>EPS19 Type VIII</b>	<b>EPS22 Type II</b>	<b>EPS29 Type IX</b>	<b>EPS39 TypeXIV</b>	<b>EPS46</b>
Density (Min)	Lb/ft <sup>3</sup>	0.70	0.90	1.15	1.35	1.80	2.40	2.85
Compression Resistance @ 10% deformation (min)	psf	840	1,470	2,300	2,820	4,180	5,760	7,200
Compression Resistance @ 5% Deformation (min)	psf	730	1,150	1,890	2,400	3,560	5,040	6,260
Compression Resistance @ 1% Deformation (min)	psf	320	520	840	1,050	1,570	2,160	2,680
Elastic Modulus (min)	psi	220	360	580	730	1,090	1,500	1,860
Flexural Strength (min)	psi	10.0	25.	30.0	40.0	50.0	60.0	75.0

(Expanded Polystyrene Data Sheet)



## **1.4.2 SEISMIC BACKGROUND**

### **1.4.2.1 SEISMICITY IN NEW JERSEY**

New Jersey has four main distinct geologic regions, which consist of the Valley and Ridge Province, Highlands Province, Piedmont Province and Coastal Plain (Witte and Monterverde). The Valley and Ridge Province is characterized by long parallel ridges and wide valleys formed by folded layers of limestone, shale and sandstone, while the Highlands Province to its east is characterized by discontinuous round ridges and deep but narrow valleys and is made up of granite, gneiss and some marble (Kratzer Environmental Services) (Witte and Monterverde). The Piedmont Province is a rolling plain with a series of higher ridges and consists of sandstone, basalt, shale and diabase. It is separated from the Highlands Province by several major faults, including the Ramapo Fault. The Piedmont Province has several ridges and uplands, including the Palisades, Cushtunk Mountain and Rocky Hill which are made up of basalt and diabase, which is much more resistant to erosion than the shale and sandstone, which exists in the valleys and low lands between the ridges (Volkert). The Coastal Plain consists of sediments overlaying the rock of the Piedmont Province and is characterized by being generally flat with few upland areas and hills. Refer to Figure 9 for locations of the four geologic provinces in New Jersey (Dombroski, Jr.).

Both bridges in this study are located in either the Piedmont Province or the Coastal Plain. Bridge A is on the border of the Piedmont Province and the Coastal Plain. While Bridge B is close to the borderline of these two regions, it is located in the Piedmont Province.

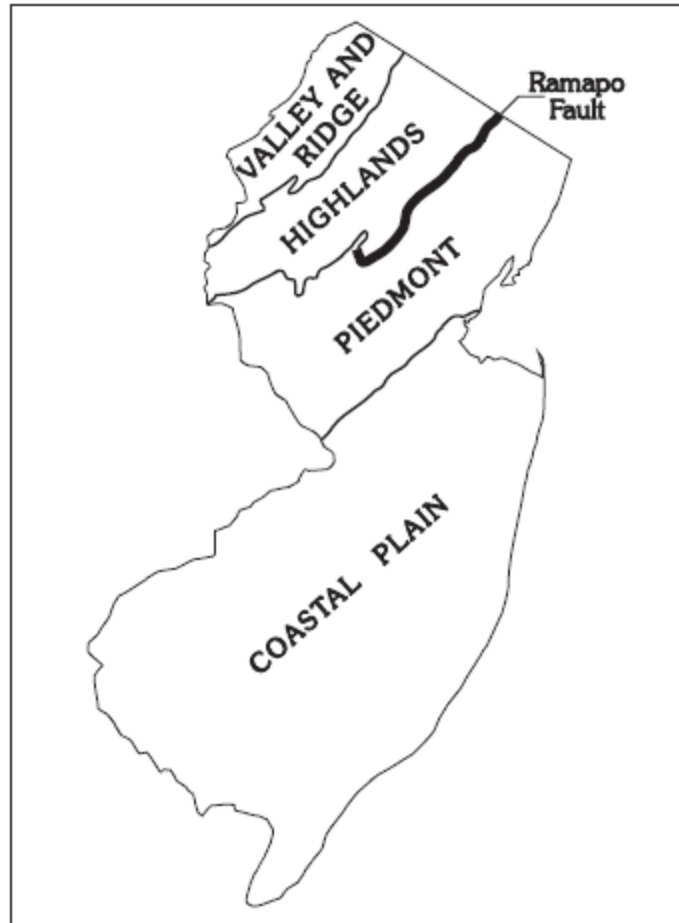


**Figure 9: Geologic Provinces in New Jersey (Dombroski, Jr.)**

Regardless of which region each bridge is located within, they are all subject to the potential effects of a damaging earthquake given that the effects of an earthquake are widespread and earthquakes can occur almost anywhere. New Jersey has experienced several earthquakes since the 1700's, when early historical data was available. The effects of many of these earthquakes were felt by a large portion of the state, and often times by other states as well.

**Table 3: Earthquake History for New Jersey** (United States Geological Survey)

<b>Year</b>	<b>Magnitude</b>	<b>Intensity</b>	<b>Location</b>
1737			NY/NY
1755			MA
1783	5.3	VI	NJ
1811-1812			New Madrid, MI
1860			Riviere-Oulle, Canada
1871		VII	Delaware Border
1884			New York City, NY
1886			Charleston, SC
1895		VI	High Bridge, NJ
1921		V	Moorestown, NJ
1927		VII	Asbury Park, NJ
1933		V	Trenton, NJ
1938		V	Hightstown, NJ
1939			Salem County, NJ
1951			Rockland County, NY
1957		VI	High Bridge, NJ
1961		V	Philadelphia, PA
1968	2.5	V	Burlington County, NJ
1973	3.8	V	Salem County, NJ
2009	3.0		NJ

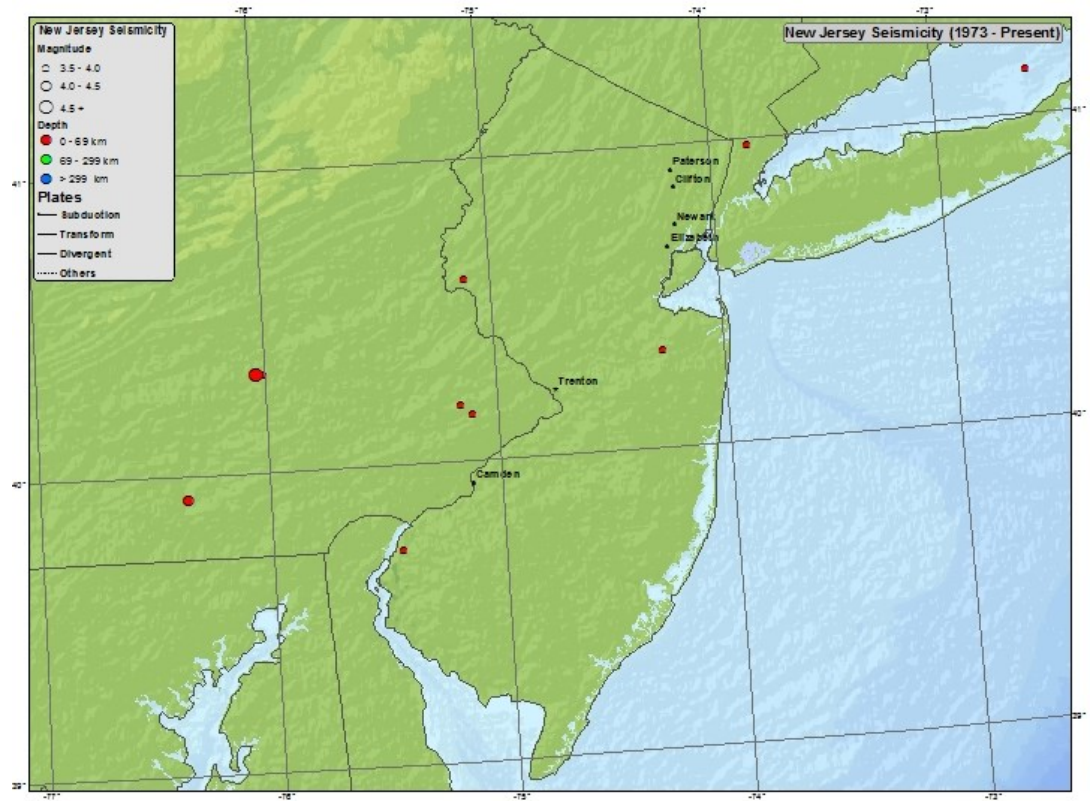


**Figure 10: Seismicity Map of NJ (United States Geological Survey)**

In addition to these earthquakes located in New Jersey, there have been several others that have been located elsewhere but were still felt in New Jersey. In 1939 there was an earthquake near Salem County, New Jersey which was felt as far away as Baltimore, Maryland and Philadelphia, Pennsylvania. In 1973 an earthquake of intensity V was felt in several states, including New Jersey, Delaware, Maryland, Pennsylvania, Connecticut and Virginia. Some of the earthquakes felt in New Jersey were strong enough to cause chimneys, plates, glassware and windows to crack and furniture to become displaced.

Although it is often believed that earthquakes occur at fault lines, this is not necessarily the case for New Jersey. There is no clear relationship between earthquakes

and the geologically mapped faults in most intraplate areas, such as New Jersey (Kafka, 2014). As a result, a bridges' distance to the intraplate fault, such as the Ramapo Fault, illustrated above in **Figure 9**, is not as important as other site-specific factors, such as soil properties and distance from previous epicenters, when considering seismic vulnerability. Additionally, the effects and damage from earthquakes can be felt for miles, often even hundreds of miles. For these reasons, all bridges, regardless of their location, are subject to potentially harmful earthquake effects and should be account for accordingly in their design. Figure 11 shows the 2014 Seismic Hazard Map from USGS for the state of New Jersey.

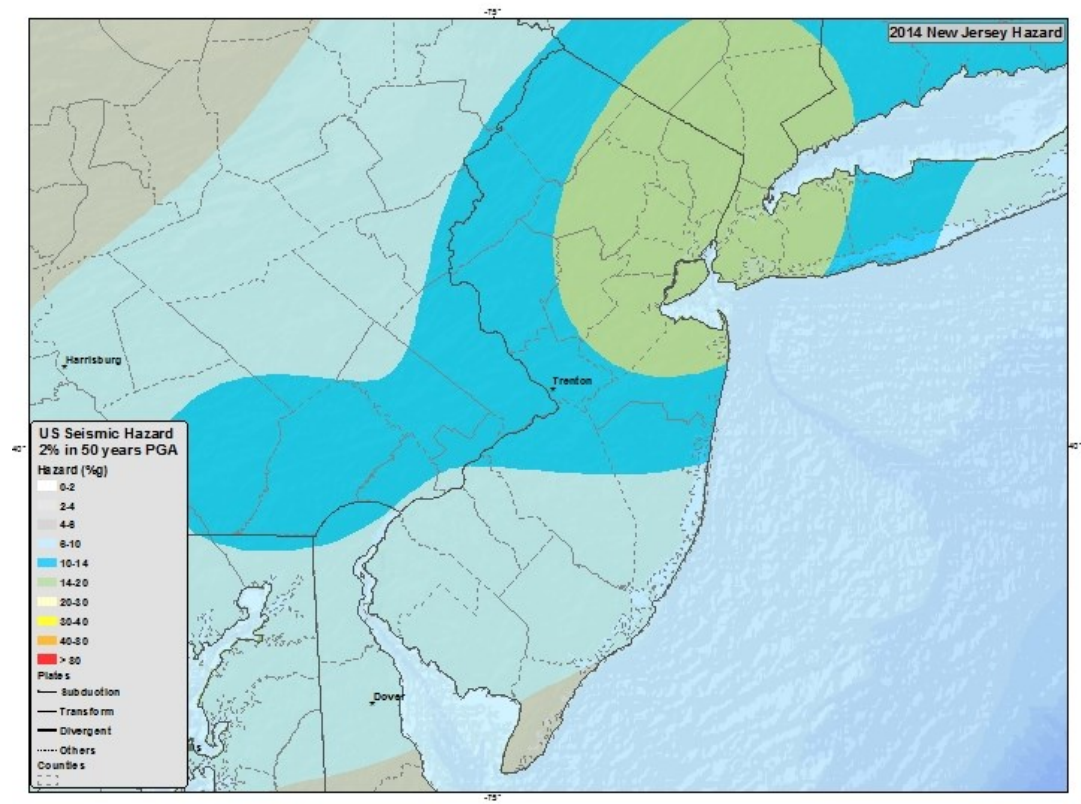


Figure 11: 2-14 Seismic Hazard Map of New Jersey (United States Geological Survey)

### 1.4.3 GEOTECHNICAL INFORMATION

All existing soil information was gathered, which would be needed to create soil profiles and soil springs for each bridge. Information was collected from existing bridge plans, both contract plans and as-built plans, as well as from previous soil boring programs, inspection reports and geotechnical reports. Once existing soil data was gathered and reviewed, it was determined that each of these bridges would have additional borings taken in order to attain adequate information to develop soil profiles for each foundation at each bridge site.

Bridge A had both existing soil data from previous projects as well as two additional SPT borings, with one at each abutment location. The first boring was located just north of the south abutment and the second was located just south of the north abutment. The soil profile developed from these additional borings as well as the existing boring data indicated a layer of fill between 10 and 15 feet thick followed by a 35 foot thick layer of loose sand. Below the loose sand is a 20 foot thick layer of medium dense sand then very dense sand. The soil parameters shown in Table 4 were developed based on the laboratory tests performed on the cores taken at these additional SPT boring locations as well as existing soil data.

**Table 4: Summary of Soil Parameters for Bridge A**

<b>Layer</b>	<b><math>\Phi</math></b>	<b>C/S<sub>a</sub> (ksf)</b>	<b><math>\gamma</math> (pcf)</b>	<b><math>\gamma_{sat}</math> (pcf)</b>
Fill	30°-32°	0	115-120	120-125
Loose Sand	28°-30°	0	110-115	120-125
Medium Dense Sand	32°-35°	0	115-125	120-130
Dense Sand	35°-36°	0	120-125	125-135

Bridge B had one additional boring, located as close to the south abutment as feasible, which was between the south abutment and Pier 1. Based on this additional SPT boring and previous boring data the soil profile was developed. The soil profile shows that the top layer of soil is medium dense sand that is between 15 and 20 feet thick with a dense to medium dense sand layer below. This sand layer is followed by pockets of stiff clay and peat, which are between 10 and 45 feet thick. Below the sand layer and pockets of stiff clay and peat is a layer of dense to very dense sand layer, which is between 25 and 30 feet thick. This is followed by an approximately 20 foot thick layer of loose sand then a layer of very dense sand. The soil parameters shown in Table 5 were determined based on the soil profile and laboratory tests performed on the soil core taken at this location, in conjunction with the previously available boring data.



**Table 5: Summary of Soil Parameters for Bridge B**

<b>Layer</b>	<b><math>\Phi</math></b>	<b>C/S<sub>a</sub> (ksf)</b>	<b><math>\gamma</math> (pcf)</b>	<b><math>\gamma_{\text{sat}}</math> (pcf)</b>
Fill	30°-32°	0	115-120	120-125
Peat		0.25-0.50	105-115	105-115
Soft Clay	0°	0.25-1.00	100-110	105-115
Silt	0°	0.50-0.75	110-115	115-120
Rock	40°-42°	400-725	135-160	135-160

## **CHAPTER II**

### **2 FINITE ELEMENT MODEL**

#### **2.1 INTRODUCTION**

To determine the effect that the integral abutments have on the seismic response of the bridge selected, several models are created as previously discussed. There are a total of 13 models used for each of the bridges for this investigation. For each bridge, the first model is that of the conventional jointed bridge, where the abutments are modeled as supports and no SSI is assume, which is discussed in more detail later on. This model reflects the as-built state of the actual bridge, being that both of the bridges selected were constructed with conventional, seat-type abutments. This model was used as the control specimen for each of the bridges. These two control models were validated by comparing the results to those achieved during a separate evaluation of these bridges in the as-built condition.

The remaining 12 of the 13 models for each bridge have integral abutments in place of the conventional abutments from the first model. These 12 models are all identical, with the exception of the abutment backfill and the in-situ soil properties for the abutment piles. Six of these 12 IAB models have compacted dense sand backfill behind the integral abutments while the other 6 IAB models have EPS geofoam backfill. Each of the six IAB models with compacted backfill, have one of the following in-situ soil types

at the piles is either dense sand, medium dense sand, loose sand, stiff clay, medium stiff clay, or soft clay. Similarly, for each of the six IAB models with EPS geofoam backfill, each model has in-situ soil type as either dense sand, medium dense sand, loose sand, stiff clay, medium stiff clay or soft clay. Table 6 shows a detailed breakdown of the abutment backfill material modeled and soil modeled around the piles that support the integral abutments for each model for a single bridge.

The software CSiBridge 2015 Version 17.1.1 Advanced with Rating was used to create all of the finite element models of these bridges. Frame elements, shell elements, link elements and nodes were used in the creation of these models. The Bridge Wizard tool, shown in Figure 12, was used to generate the general geometry of each bridge. This included the vertical and horizontal layout, deck width, span lengths, girder spacing, diaphragm locations and pier layout. The deck thickness, pier and abutment skews, and pier column spacing as well as the member properties for the girders, pier cap and columns were also defined in the Bridge Wizard tool. Manual modifications were made to incorporate the integral abutments and their supporting piles as well as the pier soil springs.

**Bridge Object Data**

Bridge Object Name: 106.4A      Layout Line Name: BLL1      Coordinate System: GLOBAL      Units: Kip, ft, F

**Define Bridge Object Reference Line**

Span Label	Station ft	Span Type
Start Abutment	50.	Start Abutment
Start Abutment	50.	Start Abutment
Span 1	101.51	Full Span to End Bent
Span 2	205.9675	Full Span to End Bent
Span 3	257.4775	Full Span to End Abutment

Note: 1. Bridge object location is based on bridge section insertion point following specified layout line.

**Bridge Object Plan View (X-Y Projection)**

North

Y

X

Show Enlarged Sketch...

☐ Lock to Prevent Updating the Linked Model

OK      Cancel

**Modify/Show Assignments**

- Spans
- User Discretization Points
- Abutments
- Bents
- In-Span Hinges (Expansion Jt)
- In-Span Cross Diaphragms
- Superelevation
- Prestress Tendons
- Girder Rebar

Modify/Show...

**Figure 12: Bridge Wizard Tool (Computers & Structures, Inc.)**

**Table 6: Breakdown of Backfill Material and Soil Type by Model Number**

<b>Model Number</b>	<b>Abutment Type</b>	<b>Abutment Backfill Material</b>	<b>Foundation Soil</b>
1	Conventional Seat-Type	-	-
2	Integral	Compacted Backfill	Dense Sand
3	Integral	Compacted Backfill	Medium Dense Sand
4	Integral	Compacted Backfill	Loose Sand
5	Integral	Compacted Backfill	Stiff Clay
6	Integral	Compacted Backfill	Medium Stiff Clay
7	Integral	Compacted Backfill	Soft Clay
8	Integral	EPS Geofoam	Dense Sand
9	Integral	EPS Geofoam	Medium Dense Sand
10	Integral	EPS Geofoam	Loose Sand
11	Integral	EPS Geofoam	Stiff Clay
12	Integral	EPS Geofoam	Medium Stiff Clay
13	Integral	EPS Geofoam	Soft Clay

## 2.2 SUPERSTRUCTURE MODELING

The superstructure modeling was broken down in to separate stages; deck, girders and diaphragms. The deck was defined using the “Superstructure – Deck Sections” definition tool, which is shown in **Figure 13** and **Figure 14**. This definition tool within CSiBridge allows the user to define the following details:

- Deck width
- Deck thickness
- Number of girders
- Girder spacing
- Overhang widths

The deck sections defined in the “Superstructure – Deck Sections” definition tool were assigned to the appropriate spans via the “Bridge Wizard” tool. The girders and diaphragms were defined in the Bridge Wizard tool.

Define Bridge Section Data - Steel I Girder

Y  
X

X  Y  ☒ Do Snap

Section is Legal

Girder Output

Modify/Show Properties   Units

OK

**Section Data**

Item	Value
<b>General Data</b>	
Bridge Section Name	BSEC1
Slab Material Property	3500psi
Number of Interior Girders	3
Total Width	371.
Girder Longitudinal Layout	Along Layout Line
Constant Girder Spacing	Yes
Constant Girder Haunch Thickness (t2)	Yes
Constant Girder Frame Section	Yes
<b>Slab Thickness</b>	
Top Slab Thickness (t1)	8.
Concrete Haunch + Steel Flange Thickness (t2)	3.
<b>Girder Section Properties</b>	
Girder Section	Span 1 Girder
<b>Girder Modeling In Area Object Models</b>	
Girders Modeling Object Type	Frame
<b>Fillet Horizontal Dimension Data</b>	
f1 Horizontal Dimension	12.

**Figure 13: Superstructure - Deck Section Definition Tool for Steel Superstructure**  
(Computers & Structures, Inc.)

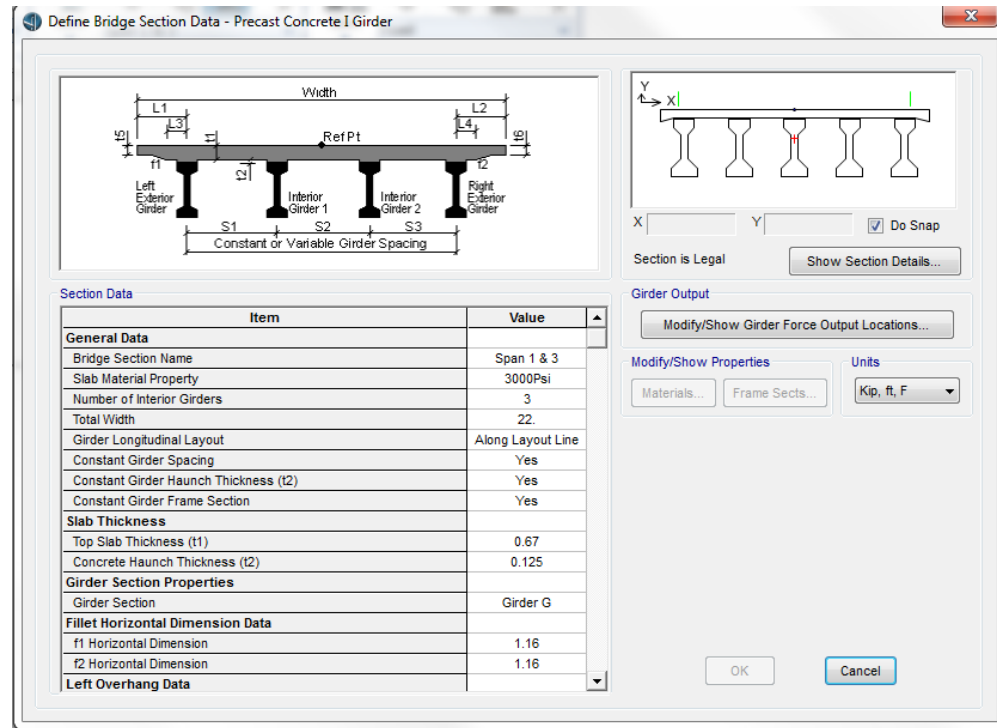


**Figure 14: Superstructure - Deck Section Definition for Concrete Superstructure**  
(Computers & Structures, Inc.)

## 2.2.1 DECK MODELING

For all of the models, the superstructures are modeled in the same manner. The deck is modeled with Three-Dimensional (3-D) shell elements, a type of area object used to model membrane, plate and shell behavior in planar and three-dimensional structures. These 3-D shell elements are capable of supporting both forces and moments, unlike plane or solid areas which are present in CSiBridge. These shell elements combine plate-bending behavior with membrane behavior where these behaviors become coupled if warping is present. The plate-bending behavior includes two-way, out-of-plane, plate rotational stiffness components as well as a translational stiffness component normal to the plate element. CSiBridge has options for both thin-plate and thick-plate shell



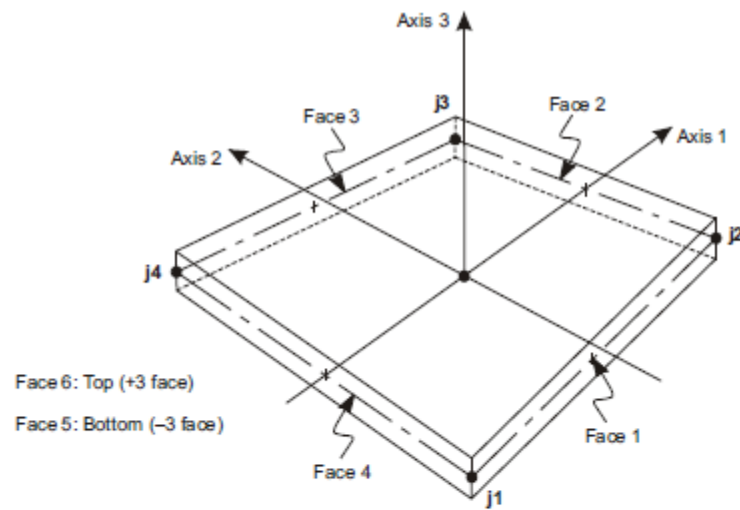
elements. While the thin-plate shell element neglects transverse shearing deformations, the thick-plate shell element includes these effects. The deck was modeled with these thin-plate shell elements as the shearing deformation effects are negligible for the deck sections being as shearing deformations only tend to be important when the thickness is greater than approximately one-tenth to one-fifth the span length, which is not the case in any of these bridges modeled.

These shell elements can be either three-node triangle shaped elements or four-node quadrilateral shaped elements. See Figure 15 for illustration of the three-node and four-node shell elements. Wherever possible, the four-node quadrilateral shell elements were used as they are more accurate. Three-node triangle shell elements were only used where necessary based on geometry and were kept small as they do not account for rapid changes in stresses or in-plane bending as accurately as the quadrilateral shaped shell elements do. CSiBridge allows these shell elements to have either a homogenous material or a material that is layered through the thickness of the shell. For the deck, the material selected was homogenous concrete with a strength defined based on the contract drawings and as-built drawings available for each bridge.

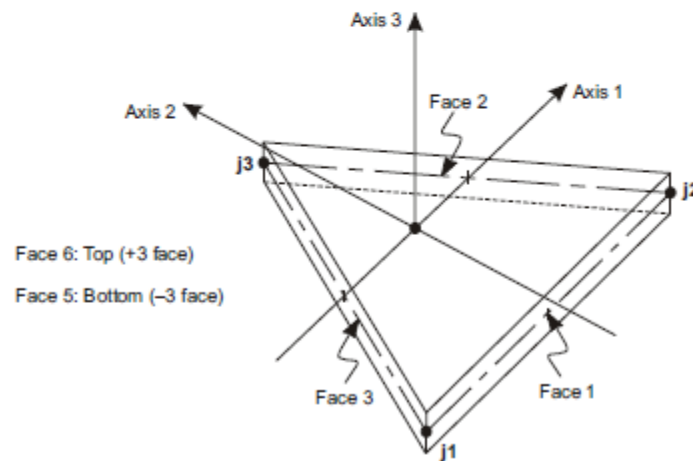
The section properties for shell elements are called shell sections in CSiBridge, which are a set of material and geometric properties that describe the cross-section of one or more shell elements. This is a type of area section property, which is defined independently of the objects then assigned to each appropriate area object. As mentioned above, the deck sections were defined as homogenous throughout the thickness, rather than layered. In order to define the section properties for this the section, the membrane thickness, bending thickness and material property need to be defined.

The membrane thickness is used for calculating the membrane stiffness for full-shell sections as well as for calculating the element volume for the self-weight and mass calculations. The bending thickness is used for calculating the plate-bending and transverse-shearing stiffness for full-shell sections. Both the membrane thickness and bending thickness were taken as one. In order to model the actual deck thickness plus any applicable wearing surface thickness, a property modifier was applied to the shell thicknesses.

The material properties assigned to each shell element are previously defined and may be isotropic, uniaxial or orthotropic. For the deck shell elements, the material property selected was isotropic. Each material property needs the modulus of elasticity, shear modulus, Poisson's ratio, coefficients of thermal expansion, mass density and weight density to be defined as well. These were defined based on information available on existing bridge plans and as-builts for each of these bridges.



Four-node Quadrilateral Shell Element



Three-node Triangular Shell Element

**Figure 15: Three-Node and Four-Node Shell Elements in CSiBridge (Computers & Structures, Inc.)**

## 2.2.2 GIRDER MODELING

The girders are modeled with 3-D Frame elements, which use general 3-D beam-column formulation which includes the effects of biaxial bending, torsion, axial deformation and biaxial shear deformations according to CSiBridge (Computers &

Structures, Inc.). Although nonlinear material behavior is available for frame elements, the girders are defined with linear material behavior as no non-linear analyses are being performed. The shear, axial, torsional, mass and weight properties can all vary linearly over each segment. Frame elements may be loaded by gravity, concentrated loads, distributed loads, strand and deformation loads and loads due to temperature change.

Frame sections are the section properties defined for and applied to frame elements. These section properties can be either prismatic or non-prismatic. For the girders, they are defined as prismatic as they do not vary along the element length. To account for section property change for the girders, the frame elements are modeled to start and end at that section property change. This allows each frame section property to be consistent along its length.

Frame section properties can be defined and generated in a variety of ways. For steel sections, such as the girders in most of the models, the section properties can be imported from the American Institute of Steel Construction (AISC) Steel Construction Manual database that CSiBridge has included in the software. For steel sections not contained in the AISC Steel Construction Manual, there are several other ways to define the frame sections. For sections that are I/wide flange, channel, tee, angle, double angle, double channel, pipe, tube or steel joints, CSiBridge has specialized input wizard that prompts for the relevant information for the given shape, such as flange width, flange thickness, web height and web thickness, for the example of an I/wide flange section. For these nine options, once the prompted information is input, CSiBridge calculates the required section properties automatically. These section properties include the cross-

sectional area, moments of inertia in all three directions, torsional constant and the shear areas.

CSiBridge also offers three types of built-up section definitions which include the cover plated I section, hybrid I section and hybrid U section. Each of these pre-defined inputs prompts for the top flange, bottom flange and web information. For the cover plated I section, it allows the user to select previously defined I section as the base, then define the width, thickness and strength of the top and bottom cover plates. For the hybrid I and I sections, it prompts the user for the web height, thickness and the top and bottom flange widths and thicknesses.

Additionally, there are three other options for defining section properties that do not fall into the previously mentioned categories. First is section designer, which allows the user to draw in various shapes, plates and reinforcing bars to create a built-up section, composite section or a more complex section. Section designer allows the user to combine various shapes and various material properties into one section.

The second option is the non-prismatic section, which allows the user to define a frame section property that varies along the length of the element by defining the variation from one previously defined frame section property to the next. This can include variation between several different section properties along the length of the frame element as well as different types of variation such as parabolic, linear, and cubic variation.

The last method for defining a steel frame section is that for a general section, where CSiBridge prompts for the cross-sectional area, moments of inertia, product of inertia, shear areas, torsional constant, section moduli, plastic moduli, radii of gyration

and shear center eccentricity. In this case, CSiBridge does not calculate any of the section properties, but rather the user is required to input them manually. The tendons are defined in the bridge wizard tool rather than in the frame section property definition as the tendons are not modeled as frame elements or as part of frame elements.

Bridges A and B utilized a combination of steel girder definition methods mentioned above. Most common method used was the hybrid I section definition, not because the sections were hybrid, but because of the ease of input required. The definition of a hybrid I section is shown in Figure 16. The hybrid I section definition option was often used to model plate girders, which could not be input from the AISC database, as they are not rolled sections. In this case, the material properties for the top flange, bottom flange and web were all selected to be the same.

The non-prismatic section input was also used where girder varied along the length of the girder and hence variation along the frame elements. The definition of a non-prismatic section is shown in Figure 17. This was only utilized in a few cases where it was more practical to create non-prismatic sections to model the change in section property over a span rather than start and end frame elements based on the start and end of material properties.

Additionally, some frame sections were imported from the AISC Steel Construction Manual database in CSiBridge. An example of this can be seen in Figure 18, where an I-Section was imported and CSiBridge automatically filled out the dimension section of the I/Wide Flange Section property form automatically, along with the section name and material properties.

The material properties for frame sections are specified by referencing a previously defined material. These materials require the same properties as the shell element materials; modulus of elasticity, shear modulus, coefficient of thermal expansion, mass density and weight density. Material properties will be discussed in further detail below.

For frame elements, the user can define the insertion point, which is the location in the cross section that is located on the frame element line drawn in the model. This is set to the centroid by default but can be specified by the user as any of the following:

- Bottom left
- Bottom center
- Bottom right
- Middle left
- Middle center
- Middle right
- Top left
- Top center
- Top right
- Shear center.

When using the bridge wizard to set up the superstructure, as was done with all of the bridges, the girders all have the insertion point set to centroid as CSiBridge uses this assumed insertion point to calculate the location of the deck shell elements. Figure 19 illustrates the various insertion points for frame elements.

**Built Up Hybrid I-Section**

Section Name: Steel Girder      Display Color:

Section Notes: Modify/Show Notes...

---

**Web Data**

Material (Base): + A588Fy50

Web Height: 4.3333

Thickness: 0.0469

---

**Top Flange Data**

☒ Include Top Plate

Material: + A588Fy50

Width: 1.

Thickness: 0.1042

---

**Bottom Flange Data**

☒ Include Bottom Plate

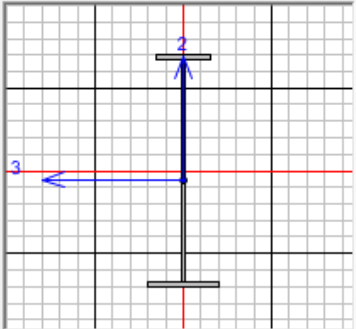
Material: + A588Fy50

Width: 1.3333

Thickness: 0.1042

---

**Section**



**Properties**

Section Properties...

Time Dependent Properties...

**Property Modifiers**

Set Modifiers...

OK Cancel

**Figure 16: Definition of Hybrid I-Section (Computers & Structures, Inc.)**



**Nonprismatic Section Definition**

Nonprismatic Section Name:  Display Color: ☐

Section Notes:

Start Section	End Section	Length	Length Type	EI33 Variation	EI22 Variation
0.5"x64" Web	0.5"x62" R Web	15.	Variable	Parabolic	Linear
0.5"x64" Web	0.5"x62" R Web	15.	Variable	Parabolic	Linear
0.375x62" L Web	0.375"x58" Web	24.	Variable	Parabolic	Linear
0.375"x58" Web	0.375"x48.3" R We	63.	Variable	Parabolic	Linear
0.375"x48.3" L We	0.375"x44" Web	28.75	Variable	Parabolic	Linear

**Figure 17: Definition of Non-Prismatic Section (Computers & Structures, Inc.)**

**I/Wide Flange Section**

Section Name: W36X150      Display Color:

Section Notes: Modify/Show Notes...

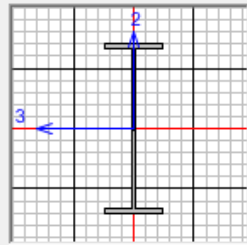
Extract Data from Section Property File

Open File... c:\program files\computers and structures\csibridge Import...

**Dimensions**

Outside height ( t3 )	<span style="border: 1px solid black; padding: 2px;">35.85</span>
Top flange width ( t2 )	<span style="border: 1px solid black; padding: 2px;">11.975</span>
Top flange thickness ( tf )	<span style="border: 1px solid black; padding: 2px;">0.94</span>
Web thickness ( tw )	<span style="border: 1px solid black; padding: 2px;">0.625</span>
Bottom flange width ( t2b )	<span style="border: 1px solid black; padding: 2px;">11.975</span>
Bottom flange thickness ( tfb )	<span style="border: 1px solid black; padding: 2px;">0.94</span>

**Section**



**Properties**

Section Properties...

Time Dependent Properties...

**Material**

+ A992Fy50 ▼

**Property Modifiers**

Set Modifiers...

OK Cancel

**Figure 18: Import of Angle Section from AISC Database (Computers & Structures, Inc.)**

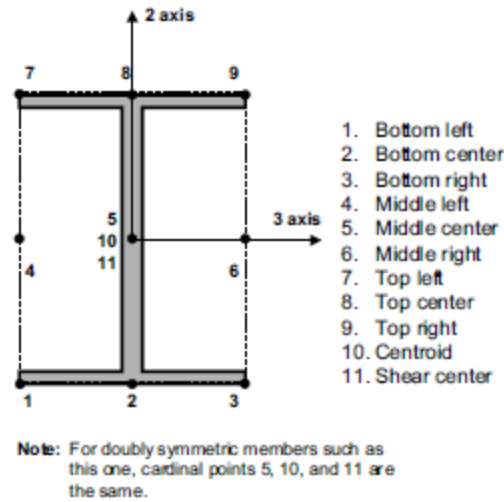


**Figure 19: Location of Insertion Points for Frame Elements (Computers & Structures, Inc.)**

Full composite action between the girders and deck is modeled using joint constraints between the deck and girders, which enforce certain types of rigid-body behavior, to connect together different parts of the model, and to impose certain types of symmetry conditions, according to CSiBridge (Computers & Structures, Inc.). These joint constraints used consist of several sets of two joints, one of which is connected to shell elements for the deck and the other joint is connected to the girders. Each set of joints move together as a 3-D rigid body.

### 2.2.3 DIAPHRAGM MODELING

Diaphragms are modeled with frame elements in the same manner as the girders. When using the Bridge Wizard Tool, as was done in both bridges in this study, the diaphragms are automatically generated based on user input in the wizard. In the Bridge Wizard the user can input the location of each diaphragm by giving the span, diaphragm

property, distance from start of span, bearing and location. The location can be specified as between specific girders only or all girders.

The Bridge Wizard also allows for simplified definition of diaphragm member properties and geometry as shown in Figure 20. The diaphragms are modeled as frame elements, as previously mentioned, but this simplified diaphragm member property definition form allows the user to define the configuration of the diaphragm in addition to the frame element properties to be used. For example, the user can define chord and brace type diaphragms such as V Brace, Inverted V Brace and X brace by selecting that option and defining a corresponding frame element property for top chord, bottom chord and diagonal. Other diaphragm types that can be defined are solid, for the case of concrete bridges, single beam and steel plate, for steel U girder internal diaphragms.

When defining the frame element property for the top chord, bottom chord and diagonal, where applicable, the same process is used as described above in Section 2.2.2 Girder Modeling. Most commonly used frame element property definition process for the diaphragms for these bridges in this study include importing from the AISC database and I/Wide Flange creation.

The diaphragms are connected to the girders in a few different ways, depending on the type of diaphragm. Single beam diaphragms are connected to the girders by sharing common joints. As each diaphragm is only comprised of one member this can be done with no complications. However with the case where there are chord and brace type diaphragms, such as the V Brace or X Brace, this is not the case. In these cases, a link is created at the location where the diaphragm connects to the girder, which represents the girder height between the top and bottom chords. This link is shown in green in Figure

21. The bottom chord then connects to the bottom of these links on either side of the diaphragm, as do the diagonals. These links are defined as rigid links, with fixities in all 3 directions of translation and all 3 directions of rotation.

The user can define end releases for the frame elements for each diaphragm to represent the connectivity between the girder and diaphragm. For the two bridges modeled for this study, the end releases were kept as fixed on both ends for single beam diaphragms as these connections tend to be moment connections. Conversely, for V Brace, Inverted V Brace and X Brace type diaphragms, the ends were released for moment in all three directions on one end and released for two directions, excluding torsion, on the other end. Torsion is not released on the one end in order to provide stability in the system. The ends are released for these three types of diaphragms as they do not tend to have moment connections, therefore this is the most accurate way to reflect that configuration.

**Bridge Diaphragm Property**

Diaphragm Name:  Units:

**Select Diaphragm Type**

☐ Solid (Applies to Concrete Bridges Only)  
☒ Chord and Brace (Applies to Steel Bridges Only)  
☐ Single Beam (Applies to Steel Bridges Only)  
☐ Steel Plate (Applies to Steel U Girder Internal Only)

**Chord and Brace Diaphragm Parameters**

☒ Include Top Chord    
☒ Include Brace    
☐ V Brace  
☐ Inverted V Brace  
☒ X Brace  
☒ Include Bottom Chord    
☐ Include Connection Plates

**Connection Plate Parameters**

Plate Width:   
 Plate Thickness:   
 Material:    
☐ Both Sides of Web

**Brace Work Point Location**

Elevation Change From Top Work Point to Top of Adjacent Girder:   
 Elevation Change From Bottom Work Point to Bottom of Adjacent Girder:

OK Cancel

**Figure 20: Bridge Diaphragm Property** (Computers & Structures, Inc.)

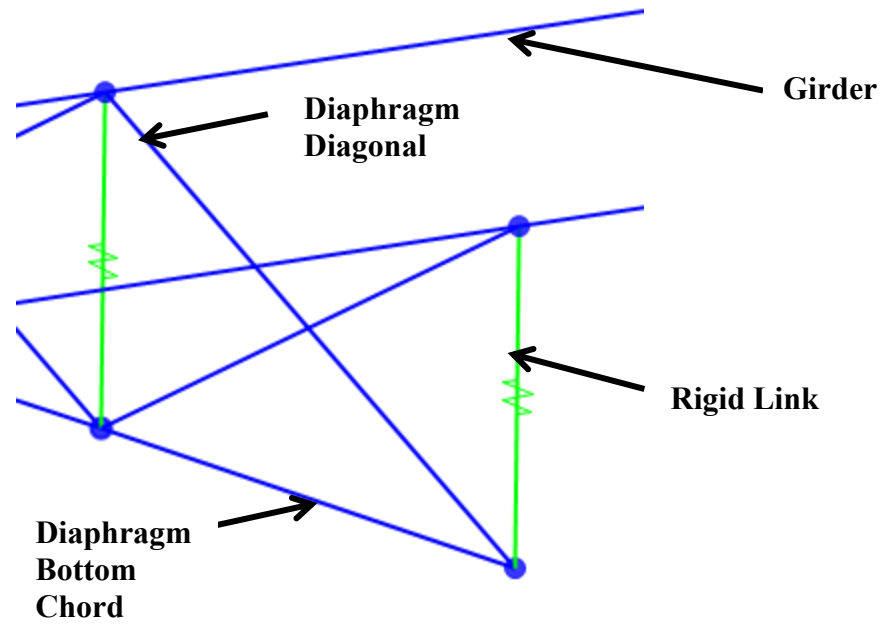


**Figure 21: Diaphragm Connectivity** (Computers & Structures, Inc.)

## 2.3 SUBSTRUCTURE MODELING

The substructure modeling was split into two portions; pier modeling and abutment modeling. The piers were modeled first using the “Substructure – Bents” definition tool in CSiBridge as shown in Figure 22. These bents were assigned using the “Bridge Wizard” as shown in Figure 23. The abutments were defined in two separate ways; using the “Bridge Wizard” for the conventional seat-type abutments, and manually adding for the integral abutments. The abutment assignments are shown in Figure 24.

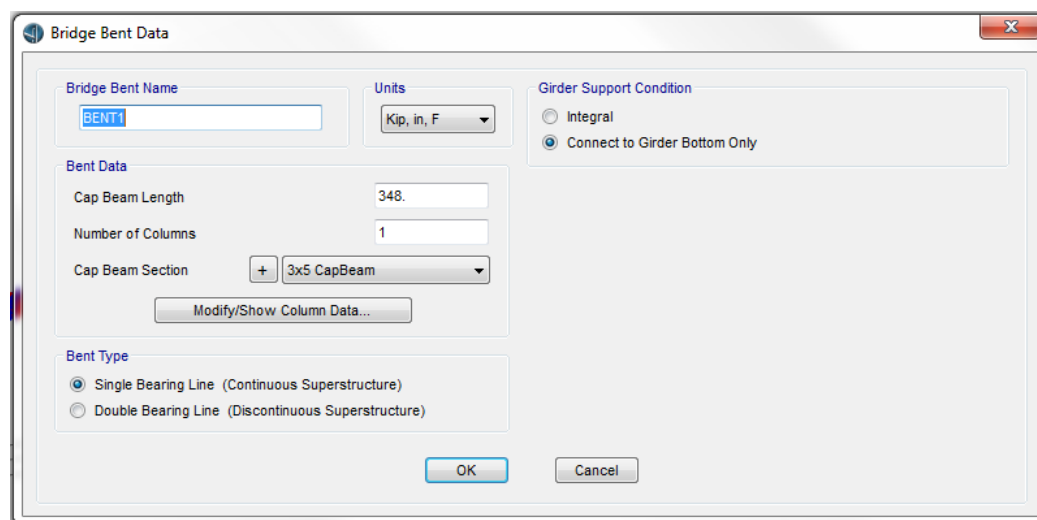
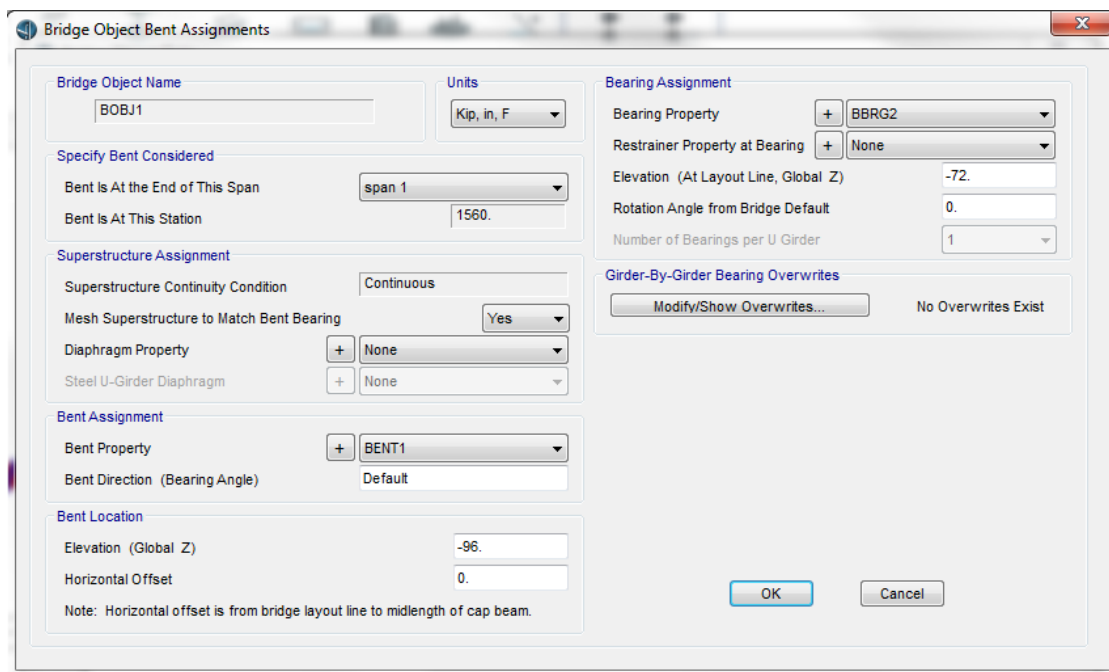


**Figure 22: "Substructure - Bents" Definition Tool (Computers & Structures, Inc.)**





**Bridge Object Bent Assignments**

Bridge Object Name:  Units:

**Specify Bent Considered**

Bent Is At the End of This Span:

Bent Is At This Station:

**Superstructure Assignment**

Superstructure Continuity Condition:

Mesh Superstructure to Match Bent Bearing:

Diaphragm Property:

Steel U-Girder Diaphragm:

**Bent Assignment**

Bent Property:

Bent Direction (Bearing Angle):

**Bent Location**

Elevation (Global Z):

Horizontal Offset:

Note: Horizontal offset is from bridge layout line to midlength of cap beam.

**Bearing Assignment**

Bearing Property:

Restrainer Property at Bearing:

Elevation (At Layout Line, Global Z):

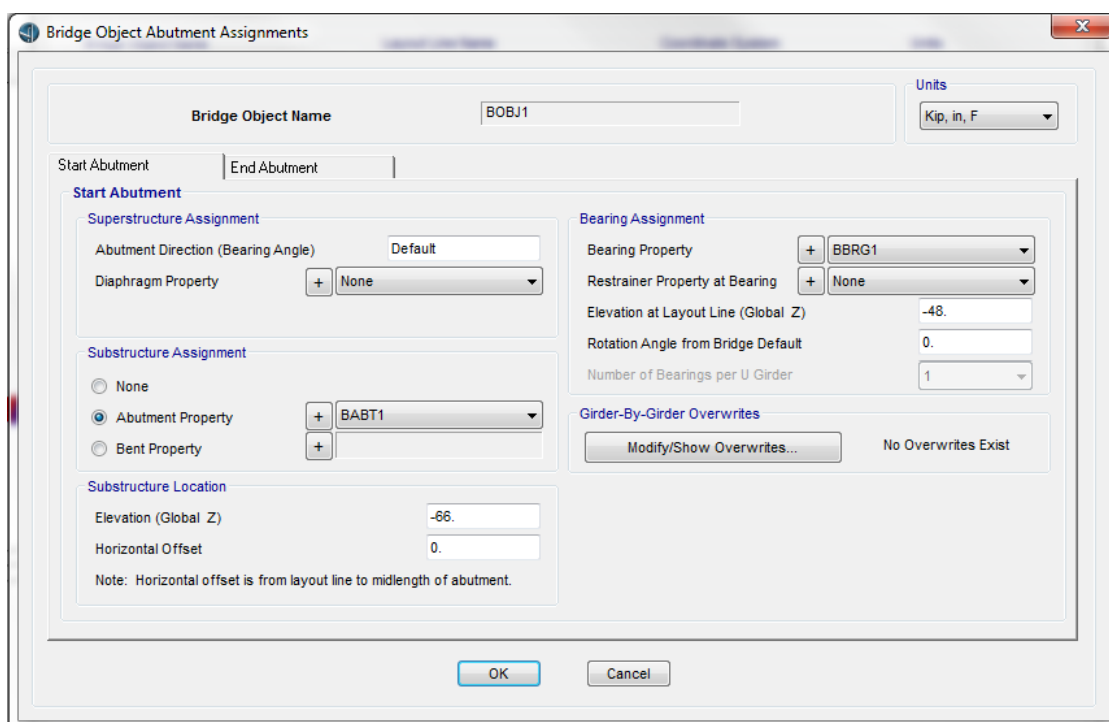
Rotation Angle from Bridge Default:

Number of Bearings per U Girder:

**Girder-By-Girder Bearing Overwrites**

No Overwrites Exist

**Figure 23: Bridge Object Bent Assignments (Computers & Structures, Inc.)**



**Bridge Object Abutment Assignments**

Bridge Object Name:  Units:

Start Abutment:  End Abutment:

**Start Abutment**

**Superstructure Assignment**

Abutment Direction (Bearing Angle):

Diaphragm Property:

**Substructure Assignment**

☐ None

☒ Abutment Property

☐ Bent Property

**Substructure Location**

Elevation (Global Z):

Horizontal Offset:

Note: Horizontal offset is from layout line to midlength of abutment.

**Bearing Assignment**

Bearing Property:

Restrainer Property at Bearing:

Elevation at Layout Line (Global Z):

Rotation Angle from Bridge Default:

Number of Bearings per U Girder:

**Girder-By-Girder Overwrites**

No Overwrites Exist

**Figure 24: "Bridge Wizard" Abutment Assignments (Computers & Structures, Inc.)**

### 2.3.1 PIER MODELING

The piers for both of the bridges are modeled in the same manner in each of the 13 models. 3-D frame elements are used to model the pier cap, columns and footing. The case where the piers consist of columns on spread footings with pier caps, the column starts at the mid height of the footing and ends at the mid height of the pier cap shown in Figure 25. CSiBridge has six concrete frame section definition types. Two of these concrete frame section types are prestressed: prestressed I girder and prestressed U girder. The other four concrete frame section types in CSiBridge are the rectangular section, circular section, pipe section and tube section. The rectangular section option prompts the user for the height and width of a rectangular section as well as the material property to be associated with the frame section definition. It also requires the user to define the section reinforcement including the rebar material for both the longitudinal and confinement bars, reinforcement configuration (circular versus rectangular), type of confinement bars (ties versus spiral), clear cover, number of longitudinal bars on each face, confinement spacing, number of confinement bars and bar sizes to be used.

Bridges A and B defined the capbeams as concrete rectangular sections instead of using the non-prismatic section definition as the overall capbeam geometry for each of these pier caps did not change significantly enough to warrant the use of the non-prismatic section.

The pier columns for Bridge A are also defined using the concrete rectangular frame section definition while the pier columns for Bridge B utilize the concrete circular frame section definition. The concrete circular frame section definition functions the

same way the concrete rectangular section, where the program requires input on the geometry of the section as well as information on the reinforcement provided.

Both bridges have concrete footings. The concrete footings in these bridges are defined utilizing concrete rectangular section properties. The footings are supported by soil springs directly below each column at the center of gravity of the footing.

The springs applied at the bottom of the footings are calculated based on the results of the geotechnical investigation performed at each bridge site and are applied in three directions: vertical, transverse and longitudinal. This site specific data allows for more accurate and realistic results. These soil springs are discussed in more detail in Section 2.5. The spring supports are a way to elastically connect the joint to the ground. Spring support conditions can be specified for any or all of the six degrees of freedom for the given joint for both translation and rotation as necessary.

For the piers, two linear link elements are used to connect each of the girders to the pier cap. This allows the effect and height of the bearings to be captured. It also allows for the offset between the center of gravity of the girders and the center of gravity of the bearings to be accounted for. This is shown in Figure 26. The top link connecting each girder to the pier cap represents the offset between the center of gravity of the girder and the top of the bearing and has properties of being fixed in all six degrees of freedom. The second link connecting each girder to the pier cap represents the height of the bearing and the distance between the center of gravity of the pier cap and the bottom of the bearing and has properties that represent the releases of the actual bearings.

Various types of bearings were included in these models but the most common types were fixed and expansion rocker type bearings. The actual type of bearing was not

important, only its releases, which were modeled by replicating these releases in the lower spring connecting the pier to the girder. Expansion bearings were released in all rotation directions as well as longitudinal translation. Transverse and vertical translations were fixed by applying large stiffness. Fixed bearings had large stiffnesses applied in all three rotation directions and all three translation directions. Typically  $6.852\text{E}+09\text{k/ft}^2$  was used for this large stiffness value.

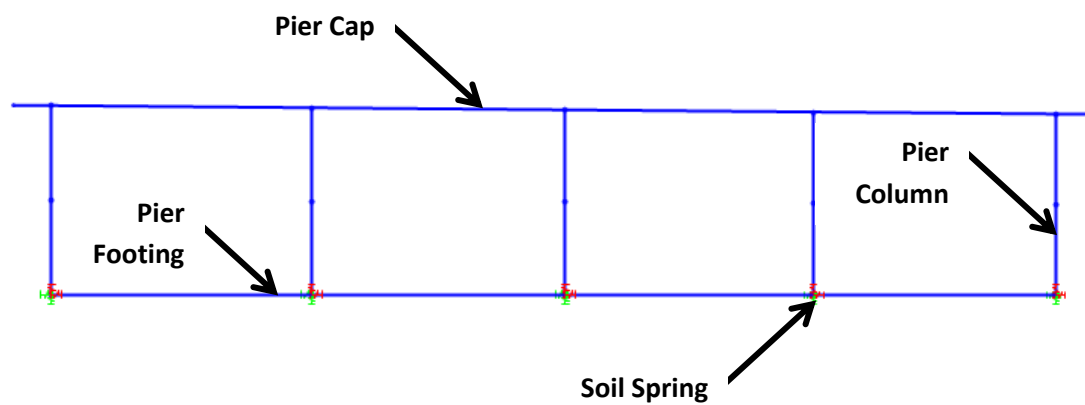


**Figure 25: Concrete Pier on Spread Footings**

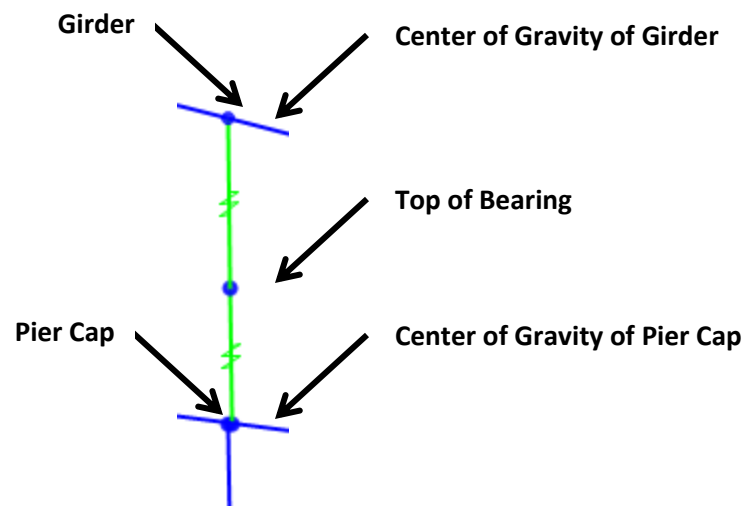


**Figure 26: Connecting Pier to Girder**

### 2.3.2 ABUTMENT MODELING

There are two types of abutments modeled for these bridges: conventional seat-type abutments and integral abutments. The conventional seat type abutments are modeled by fixing the bottom of the linear links that represent the bearings at the abutments. Being as the effect of the seismic event is taken by the bearings not the abutment in these cases, this is a reasonable representation. The ends of the girders at the abutment locations are supported by linear links that reflect the effect of the bearings and the vertical offset between the center of gravity of the girders and the top of the bearings. Conventional seat type abutments do not contribute to the seismic response of the structure as the bearings at the abutments are the controlling factor. Therefore fixing the bottoms of the links representing the bearings is an appropriate way to model this condition.

Since both of the bridges selected were designed and constructed with conventional seat-type abutments, the size, geometry and layout to be used in the models for the integral abutments for each bridge had to be developed. The integral abutment dimensions were selected based on both the New Jersey Department of Transportation (NJDOT) Bridge Design Manual (New Jersey Department of Transportation), as well as other standards set forth by state Departments of Transportation (DOTs) and typical dimensions used in existing bridges with similar span lengths. The Scotch Road Bridge, which carries Scotch Road over Interstate I-95 in New Jersey, was the bridge used as an example for determining the integral abutment dimensions and layout. The Scotch Road Bridge consists of two continuous spans that are each approximately 130 feet long and 40 feet wide. This is a reasonably similar bridge to those in this study, which range from

two 91 foot continuous span bridge to a three span continuous bridge consisting of a 68 foot span, 81 foot span and another 68 foot span. The bridges in this study vary in width from 22 feet wide to 58 feet wide. The Scotch Road Bridge has a length similar to the average length of these bridges as well as a width that's similar to the average width of these bridges. For this reason, the dimensions and layout of the integral abutments for the Scotch Road Bridge are considered a reasonable approximation of the integral abutment size and geometry used for this study in combination with recommendations from the NJDOT Bridge Design Manual.

The dimension of the integral abutment itself had to first be determined. This was based off of several references, including the Scotch Road Bridge. The integral abutments for the Scotch Road Bridge were approximately three feet wide. The NJDOT Bridge Design Manual and standard details recommend a 3.75 foot integral abutment width. Iowa DOT requires a minimum integral abutment width of 1.5 feet. Based on all three of these references, the integral abutments for the bridges in this study were modeled as three foot wide. This allows adequate concrete cover on either side of the H-Piles, while minimizing the width. Wider integral abutments would be stiffer, which is disadvantageous to the seismic performance of the bridge. The length of the integral abutments for these bridges was to be the same as the length of the conventional seat-type abutments that they were constructed with.

The height of the integral abutments for these models was determined based on general recommendations and accepted heights between nine feet and 12 feet high. Both of the bridges were modeled with 10 foot high integral abutments which falls within this accepted range. This height has to account for the depth of the girders, which ranges

from approximately 4.5 feet to 5.5 feet for these bridges included in this parametric study. An additional two feet of height is required to accommodate the embedment length of the piles. NJDOT Bridge Design Manual and standard details requires that the piles be embedded a minimum of two feet into the concrete integral abutments. Additional height is needed between the top of the pile and the bottom of any anchor bolts used to anchor the elastomeric bearings as well as to provide clearance between the reinforcing and the top of the pile. A height of ten feet provides adequate space to account for the girder depth, pile embedment, pile and anchor bolt clearance and pile and rebar clearance. Figure 27 shows the geometry used for the Integral Abutments, including depth and width.

In order to determine the section H-Pile to be used, several references were referred to, including the Scotch Road Bridge. The H-Piles used in the Scotch Road Bridge were HP14 piles. Based on the NJDOT Bridge Design Manual, bridges with spans over 150 feet in length should only be supported on steel H-Piles and for bridges with spans lengths less than 150 feet either cast-in-place, hollow steel pipe piles, prestressed concrete piles or steel H-piles can be used to support the integral abutments. Though only one bridge has spans lengths of 150 feet or more, some of these bridges do have multiple spans each over 100 feet in length in addition to having additional complications including a large degree of skew. As a result, H-piles were used with the web of the piles perpendicular to the centerline of the beams to facilitate bending about the weak axis of the pile. Specifically HP14x89 piles were used for both of the bridges. While HP10x42 and HP12x53 are more common H-Pile sections, the HP14x89 selected



can be used for higher load capacities, which could be necessary given the longer bridge lengths and higher skews found in some of these bridges.

Once the pile section to be used was selected, the pile spacing had to be determined. Looking at the Scotch Road Bridge, which has integral abutments supported on steel H piles, it can be seen that the pile spacing used was that of half of the girder spacing. Although the NJDOT Bridge Design Manual does not have specific recommendations or requirements for pile spacing, Virginia DOT however, does have requirements. Virginia DOT requires a minimum pile spacing of four feet and a maximum pile spacing of the girder spacing. Based on these two examples, and for simplicity of modeling, half the girder spacing was assumed as it meets the Virginia DOT requirements and has been used before in a similar bridge. This also makes the spacing assumption consistent between all of the bridges where using a fixed distance for the spacing could result in pile configurations for each bridge that are not comparable. For example, a bridge with longer spans would not require the same pile spacing as a bridge with much shorter spans as the loading would be completely different. Being as the H-Pile cross section being used is staying constant through-out both bridges, the pile spacing should change for each bridge as each bridge has difference superstructure geometry. By spacing the piles at half the girder spacing, the relationship between the pile spacing for each bridge is a consistent, but the spacing itself changes to reflect the differences of each individual bridge.

Pile depth also had to be determined for the integral abutments. The piles were to be modeled to an approximate fixity location. Based on the work done by Dicleli and Albhaisi (2003) the distance  $x$ , which is measured from the top of the pile to the middle

of the critical length of the pile for integral abutments subject to cyclic loading, was between 6 and 10 times the pile width (Dicleli and Albhaisi). This resulted in a total critical pile length of 12 to 20 times the pile diameter, which is between approximately 14 feet and 23 feet in length for the HP14x89 piles being used in this study. The H-Piles supporting the integral abutments for these bridges were modeled as 25 feet long and fixed at the bottom based on the approximate point of fixity being 20 times the pile diameter. Once this layout was determined, the manner in which to model it was then developed.

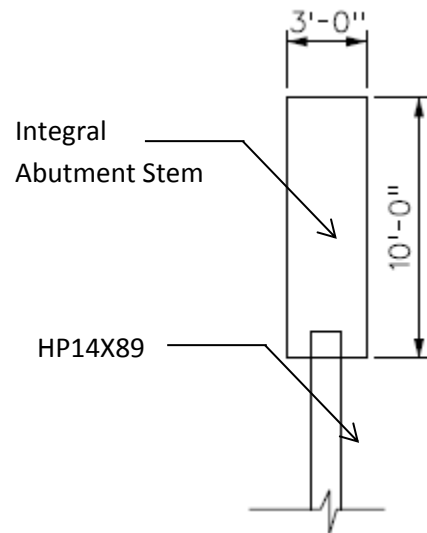


**Figure 27: Integral Abutment Geometry**

The integral abutments are modeled as 3-D shell elements, which are a type of area object that is used to model membrane, plate, and shell behavior in planar and three-dimensional structures. Each abutment 3-D shell element measures one foot in height and half of the girder spacing in length and has four joints. This was done to appropriately apply the variation in spring stiffnesses along the height of the abutment for

the six models with dense sand backfill. As mentioned above, the integral abutments are three feet wide and are 10 feet high and the same length as the conventional seat type abutments in the as-built model. The three foot thickness of the integral abutments was modeled by setting both the bending and membrane thicknesses of the 3-D shell elements to three feet (refer to Section 2.2.1 for more information on shell elements in CSiBridge).

The integral abutments are supported by HP14x89 piles which were defined by importing the properties from the 2014 AISC Steel Construction Manual database in CSiBridge and applied to the pile frame elements spaced at half the girder spacing, which is approximately 4 to 5 feet on center, depending on the girder spacing of each bridge. The piles are modeled by 3-D frame elements and are 25 feet long and fixed at the bottom as mentioned above.

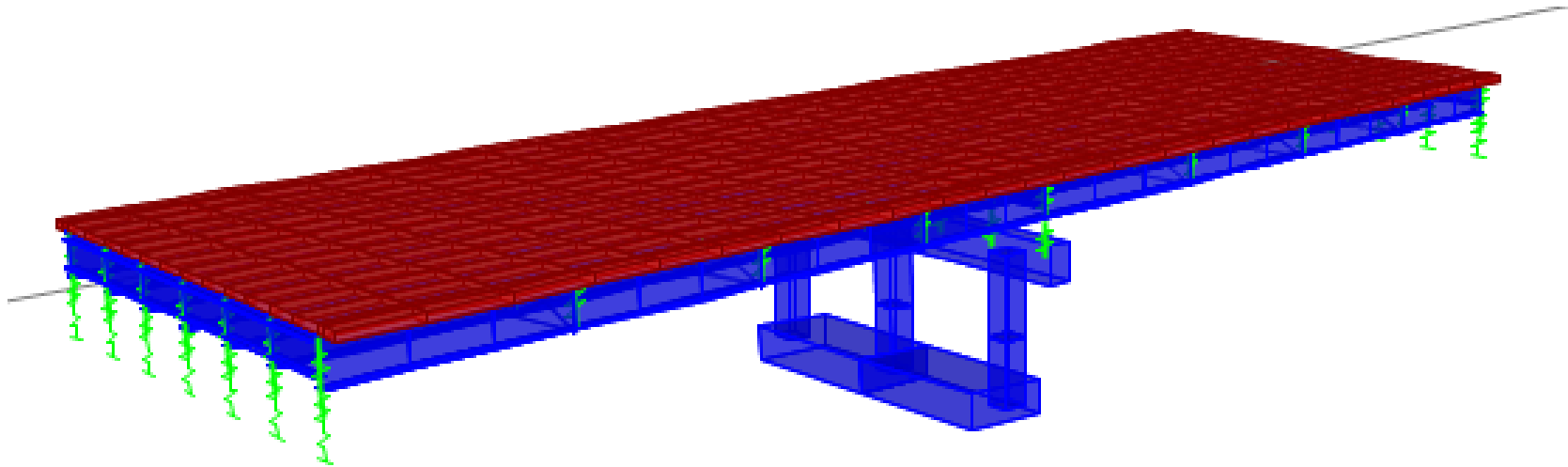


**Figure 28: Model of Bridge A with Conventional Abutments**

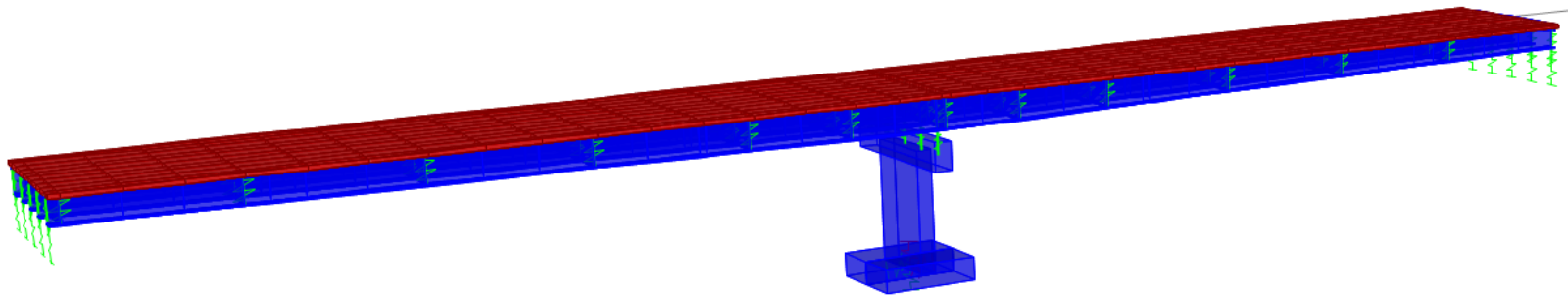


**Figure 29: Model of Bridge B with Conventional Abutments**

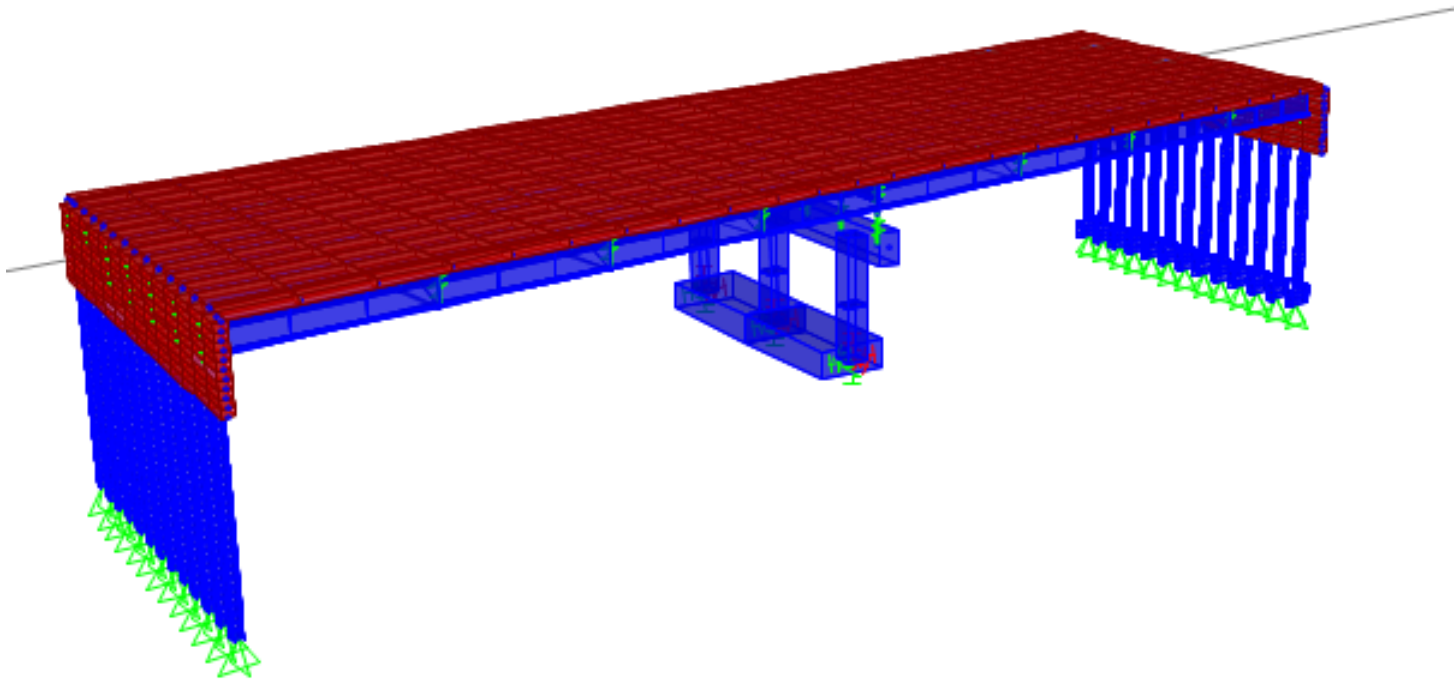


**Figure 30: Model of Bridge A with Integral Abutments**

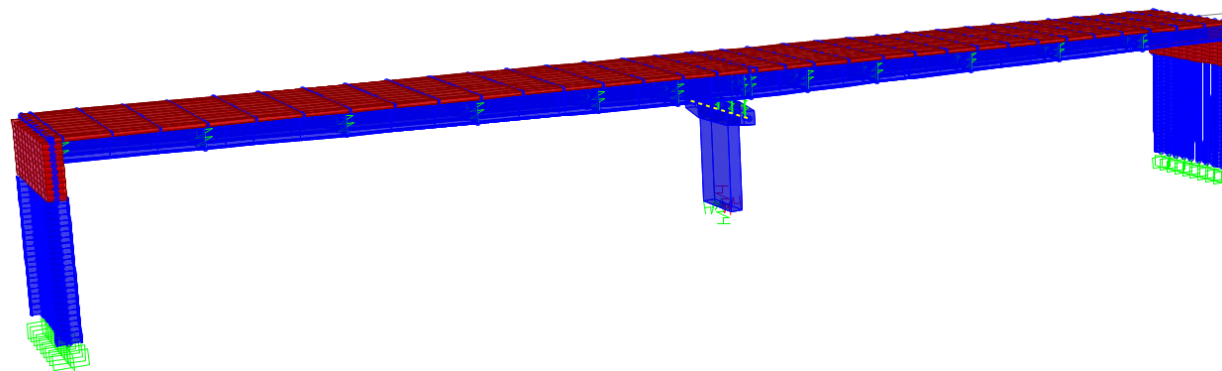


**Figure 31: Model of Bridge B with Integral Abutments**

## **2.4 SOIL AND BACKFILL MODELING**

The dense sand and EPS geofoam backfill were both modeled as area springs that were applied to each shell element that made up the integral abutments. They were defined as either restraining the abutment in compression or tension and either inward or outward movement, depending on the local coordinates and orientation of the integral abutment's shell elements. This allowed the spring constant to be applied to the abutment movement that corresponded to the passive earth pressure that it represents. The area springs for the dense sand and EPS geofoam were specified per unit area of the abutment and calculated as described in Section 2.5.2.

The piles supporting the integral abutments had line springs that were applied to each frame element that made up the piles. They were defined similar to that of the abutment area springs, but they were defined as restraining the piles in both compression and tension. The line springs were specified per unit length of the piles and calculated as described in Section 2.5.2.

## **2.5 SOIL-STRUCTURE INTERACTION**

Soil-structure interaction (SSI) is extremely important when analyzing a structure for seismic performance. SSI accounts for the effects that the ground motions have on the soil and foundation combination. Excluding these effects could result in overly conservative results as it is inaccurate to assume that the bottom of the foundations are fixed. In reality the soil surrounding the foundations will move a small amount and provide a damping effect on the ground motions. In order to capture this effect, soil springs coefficients for X, Y and Z directions are calculated and applied to the base of the piers and abutments. Each pier and abutment can have different soil spring coefficients depending on the surrounding soil properties and foundation properties.

### **2.5.1 CALCULATION OF INTEGRAL ABUTMENT SOIL-STRUCTURE INTERACTION**

Soil-structure interaction at the integral abutments is an essential part of determining the seismic response of the bridge. The earth pressure that the backfill applies on the integral abutment depends on the magnitude and direction of movement of the integral abutment itself. During a seismic event, the integral abutment will undergo both inward and outward movement in quick succession. As a result, static active earth pressure is not applicable and does not need to be considered during a seismic event. Active earth pressure effects are minimal compared to the passive earth pressure and as a result can be ignored. The integral abutment may also move toward the backfill causing there to be passive earth pressure as well, which will be the controlling case. The actual

earth pressure coefficient,  $K$ , will change depending on the movement of the abutment during the seismic event.

Based on past research done with both finite element analysis and experimental data, the variation of the earth pressure coefficient,  $K$ , as a function of the structures displacement,  $\Delta$ , can be determined. (Clough and Duncan) developed a relationship between the earth pressure coefficient and the ratio of the wall movement to wall height for typical backfill soils compacted to a medium dense condition. Figure 32 shows this relationship.

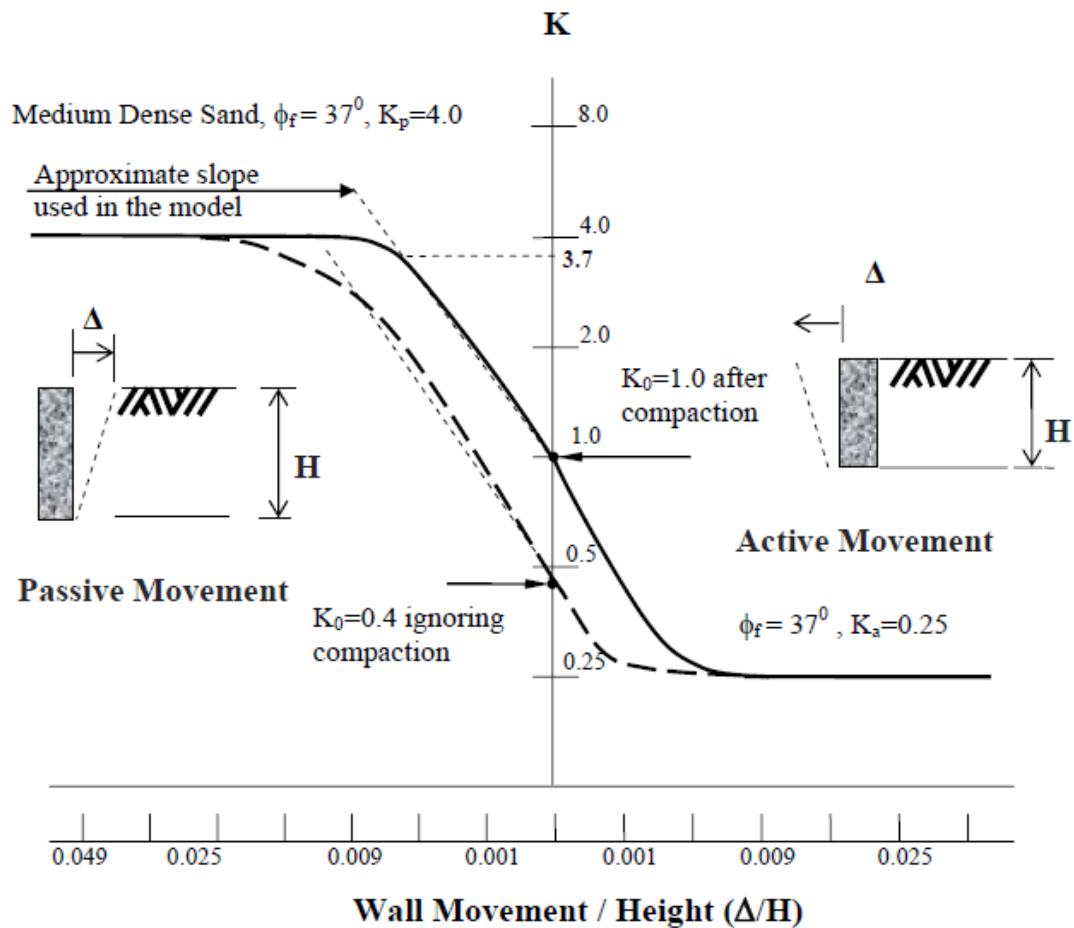


**Figure 32: Relationship Between Abutment Movement and Earth Pressure (Clough and Duncan)**



The passive earth pressure case will control and as a result the passive earth pressure coefficient,  $K$ , was calculated based on the (Clough and Duncan) model in **Figure 32** and applied as linear springs. The spring constant was calculated based on  $dP$ , the change in backfill pressure, and  $\Delta$ , the displacement at the top of the abutment, as follows:

$$K_{spring} = \frac{(dP)}{\Delta}$$

$$dP = (K_p - K_0)\gamma z$$

$\gamma$  is the unit weight of the backfill material, and  $z$  is the spring depth measured from the top of the abutment. Based on the Clough and Duncan model,  $K_0=1$  for compacted backfill. Following the procedure set forth by (Albhaisi and Nassif) by dividing both the numerator and denominator by the abutment height,  $H$ , the equation can be combined with the Clough and Duncan graph shown in Figure 32 to approximate values for  $K_p$  when  $\Delta/H=0.009$ .

$$K_{spring} = \frac{(dP)/H}{\Delta/H}$$

$$K_{spring} = 300\gamma z/H$$

The lateral soil spring constant for cohesive soils is independent of the depth of soil, unlike cohesionless soils. To calculate the soil spring constant for the cohesive foundation soils the modulus for clay,  $E_s$ , and the undrained shear strength of clay,  $C_u$ , are based off the typical p-y curve developed by Matlock (Matlock) as seen in Figure 33.

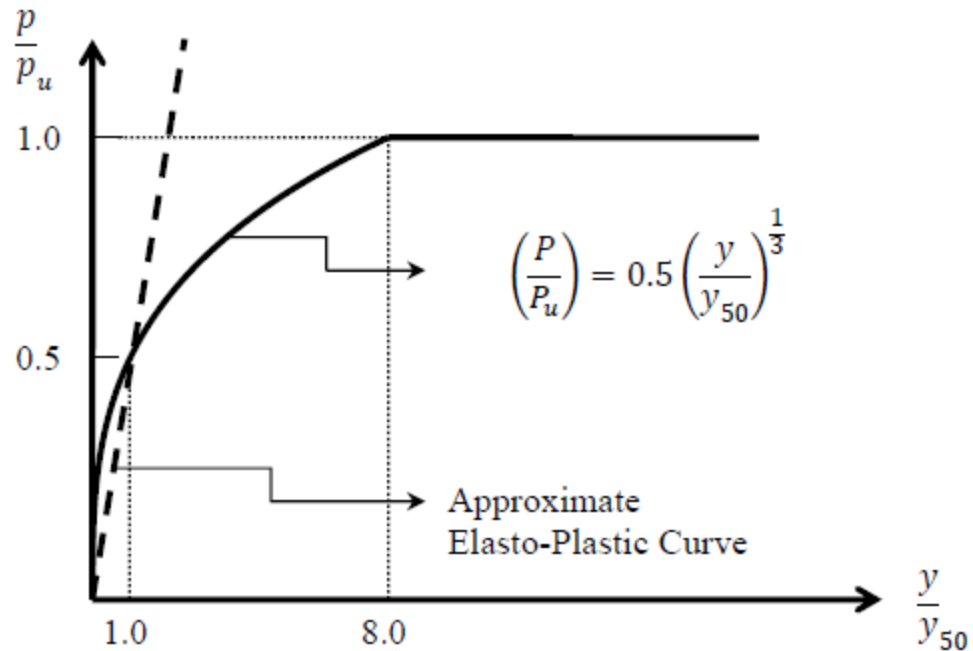


**Figure 33: P-y Curve for Soft Clay (Matlock)**

In order to calculate the ultimate soil resistance, it has to be determined if the soil is behaving as confined soil or unconfined soil as that directly effects the ultimate soil resistance. Soil that is close to the ground surface will act as unconfined soil as there is a lack of confinement whereas soil further away from the ground surface is confined and therefore acts as confined soil. The soil near the ground surface will undergo a wedge action, where the pile may push up a soil wedge due to lateral movement and lack of confinement. This causes a wedge action failure to develop before the regular nonlinear soil failure will develop.

In the case of integral abutments, the soil behaves as confined soil, even near the top of the pile. This is as a result of the backfill behind the abutment and embankment surcharge pressure that is exerted on the foundation soil surrounding the pile. For this reason, only confined soil behavior and ultimate soil resistance of confined soil will be

considered. The ultimate soil resistance for soil behaving as confined soil is calculated as follows:

$$p_u = 9C_u b$$

Skempton's method of calculating the elastic soil modulus,  $E_s$ , can be used in conjunction with the ultimate soil resistance calculated above to determine the lateral soil spring coefficient for cohesive soils (Skempton)

$$E_s = \frac{\frac{p_u}{2}}{2.5\varepsilon_{50}b}$$

$$E_s = \frac{9C_u b}{5\varepsilon_{50}b} = \frac{9C_u}{5\varepsilon_{50}}$$

**Table 7: Properties of Clay (Rees and Van Impe) (Bowles)**

<b>Consistency of Clay</b>	<b>Average Undrained Cohesion, <math>C_u</math> (ksf)</b>	<b><math>\varepsilon_{50}</math></b>
Soft	0.40	0.02
Medium	0.79	0.01
Stiff	1.57	0.07

**Table 8: Lateral Soil Springs for Cohesionless Backfill**

<b>Type of Cohesionless Backfill</b>	<b><math>E_s</math> (k/ft/ft)</b>
Soft Clay	35.71
Medium Clay	142.85
Stiff Clay	436.31
EPS Geofoam	5.76

In order to reduce the variables between each of the bridges, and so as to allow for better comparison of the variables in consideration in this parametric study, the same soil springs for each type of soil were used for both bridges. Refer to Table 14 through Table 16 for the soil springs calculated for each different type of soil used. For dense sand, the soil density used for the soil spring calculation was 127 pcf. This was determined by taking the average soil density for each range provided for dense sand in Table 4 and Table 5 for Bridges A and B. The same was done for medium dense sand and loose sand.

**Table 9: Approximate Soil Densities Used for Soil Spring Calculations of Sand**

<b>Consistency of Sand</b>	<b><math>\gamma</math> (pcf)</b>
Dense Sand	127
Medium Dense Sand	115
Loose Sand	95

**Table 10: Equation for  $K_{\text{spring}}$  of Sand**

<b>Consistency of Sand</b>	<b><math>K_{\text{spring}}</math> (k/ft<sup>2</sup>/ft)</b>
Dense Sand	5.221z
Medium Dense Sand	4.728z
Loose Sand	3.906z

(note that z is the depth to the spring, in feet, measured from the top of abutment)

**Table 11: Lateral Soil Springs for Dense Sand**

<b>Depth (z) (ft)</b>	<b>K (k/ft<sup>2</sup>/ft)</b>	<b>Depth (z) (ft)</b>	<b>K (k/ft<sup>2</sup>/ft)</b>	<b>Depth (z) (ft)</b>	<b>K (k/ft<sup>2</sup>/ft)</b>
0	0	13	72.05	26	150.11
1	5.22	14	78.06	27	156.11
2	10.44	15	84.06	28	162.12
3	15.66	16	90.06	29	168.12
4	20.88	17	96.07	30	174.12
5	26.11	18	102.07	31	180.13
6	31.32	19	108.08	32	186.13
7	36.55	20	114.08	33	192.14
8	41.77	21	120.09	34	198.14
9	46.99	22	126.09	35	204.14
10	52.21	23	132.09	36	210.15
11	60.04	24	138.10		
12	66.05	25	144.10		

**Table 12: Lateral Soil Springs for Medium Dense Sand**

<b>Depth (z) (ft)</b>	<b>K (k/ft<sup>2</sup>/ft)</b>
0	0
1	4.73
2	9.46
3	14.18
4	18.91
5	23.64
6	28.37
7	33.09
8	37.82
9	42.55
10	47.28
11	54.37
12	59.81

<b>Depth (z) (ft)</b>	<b>K (k/ft<sup>2</sup>/ft)</b>
13	65.24
14	70.68
15	76.12
16	81.55
17	86.99
18	92.43
19	97.86
20	103.30
21	108.74
22	114.18
23	119.61
24	125.05
25	130.49

<b>Depth (z) (ft)</b>	<b>K (k/ft<sup>2</sup>/ft)</b>
26	135.92
27	141.36
28	146.80
29	152.23
30	157.67
31	163.11
32	168.54
33	173.98
34	179.42
35	184.86
36	190.29

**Table 13: Lateral Soil Springs for Loose Sand**

<b>Depth (z) (ft)</b>	<b>K (k/ft<sup>2</sup>/ft)</b>	<b>Depth (z) (ft)</b>	<b>K (k/ft<sup>2</sup>/ft)</b>	<b>Depth (z) (ft)</b>	<b>K (k/ft<sup>2</sup>/ft)</b>
0	0	13	53.90	26	112.28
1	3.91	14	58.39	27	116.78
2	7.81	15	62.88	28	121.27
3	11.72	16	67.37	29	125.76
4	15.62	17	71.86	30	130.25
5	19.53	18	76.35	31	134.74
6	23.43	19	80.84	32	139.23
7	27.34	20	85.34	33	143.72
8	31.24	21	89.83	34	148.22
9	35.15	22	94.32	35	152.71
10	39.06	23	9881	36	157.20
11	44.91	24	10330		
12	49.41	25	107.79		

The values shown in Table 11 through Table 13 for each one foot increment were averaged to determine the lateral soil spring constant for each one foot high 3-D shell element to which they are applied. Refer to Table 14 through Table 16 for the average lateral soil spring constant applied to each shell element of which the integral abutments are comprised.

**Table 14: Average Lateral Soil Springs for Dense Sand Applied to Each Integral Abutment Shell Element**

<b>Depth (z) at Top of Shell Element (ft)</b>	<b>Depth (z) at Bottom of Shell Element (ft)</b>	<b>K (k/ft<sup>2</sup>/ft)</b>
0	1	2.61
1	2	7.83
2	3	13.05
3	4	18.27
4	5	23.49
5	6	28.72
6	7	33.94
7	8	39.16
8	9	44.38
9	10	49.60



**Table 15: Average Lateral Soil Springs for Medium Dense sand Applied to Each Integral Abutment Shell Element**

<b>Depth (z) at Top of Shell Element (ft)</b>	<b>Depth (z) at Bottom of Shell Element (ft)</b>	<b>K (k/ft<sup>2</sup>/ft)</b>
0	1	2.36
1	2	7.09
2	3	11.82
3	4	16.55
4	5	21.27
5	6	26.00
6	7	30.73
7	8	35.46
8	9	40.19
9	10	44.91

**Table 16: Average Lateral Soil Springs for Loose Sand Applied to Each Integral Abutment Shell Element**

<b>Depth (z) at Top of Shell Element (ft)</b>	<b>Depth (z) at Bottom of Shell Element (ft)</b>	<b>K (k/ft<sup>2</sup>/ft)</b>
0	1	1.95
1	2	5.86
2	3	9.76
3	4	13.67
4	5	17.58
5	6	21.48
6	7	25.39
7	8	29.29
8	9	33.20
9	10	37.10

**Table 17: Average Lateral Soil Springs for Dense Sand Applied to Integral Abutment H-Piles**

<b>Depth (z) at Top of Shell Element (ft)</b>	<b>Depth (z) at Bottom of Shell Element (ft)</b>	<b>K (k/ft<sup>2</sup>/ft)</b>
10	11	77.23
11	12	84.59
12	13	91.94
13	14	99.30
14	15	106.65
15	16	114.00
16	17	121.36
17	18	128.72
18	19	136.07
19	20	142.43
20	21	150.79
21	22	158.14
22	23	165.49
23	24	172.85
24	25	180.20
25	26	187.56
26	27	194.92
27	28	202.27

28	29	209.62
29	30	216.98
30	31	224.33
31	32	231.69
32	33	239.05
33	34	246.40
34	35	253.75
35	36	261.11

**Table 18: Average Lateral Soil Springs For Medium Dense Sand Applied to Integral Abutment H-Piles**

<b>Depth (z) at Top of Shell Element (ft)</b>	<b>Depth (z) at Bottom of Shell Element (ft)</b>	<b>K (k/ft<sup>2</sup>/ft)</b>
10	11	69.93
11	12	76.59
12	13	83.25
13	14	89.91
14	15	96.57
15	16	103.23
16	17	109.89
17	18	116.55
18	19	123.21
19	20	129.84
20	21	136.53
21	22	143.20
22	23	149.86
23	24	156.52
24	25	163.18
25	26	169.84
26	27	176.50
27	28	183.16

28	29	189.82
29	30	196.50
30	31	203.14
31	32	209.80
32	33	216.46
33	34	223.19
34	35	229.78
35	36	236.44

**Table 19: Average Lateral Soil Springs for Loose Sand Applied to Integral Abutment H-Piles**

<b>Depth (z) at Top of Shell Element (ft)</b>	<b>Depth (z) at Bottom of Shell Element (ft)</b>	<b>K (k/ft<sup>2</sup>/ft)</b>
10	11	57.77
11	12	63.27
12	13	68.77
13	14	74.28
14	15	79.78
15	16	85.28
16	17	90.78
17	18	96.28
18	19	101.79
19	20	107.29
20	21	112.79
21	22	118.29
22	23	123.79
23	24	129.30
24	25	134.80
25	26	140.30
26	27	145.80
27	28	151.30

28	29	156.81
29	30	162.31
30	31	167.81
31	32	173.31
32	33	178.81
33	34	184.31
34	35	189.82
35	36	195.32



### 2.5.2 CALCULATION OF SOIL-STRUCTURE INTERACTION

The soil-structure interaction for the piers in each model was accounted for via soil springs at the bottom of each pier column. These soil springs were calculated based on the Federal Highway Administration (FHWA) Seismic Retrofitting Manual for Highway Structures, 2006, which provides equations shown below for surface stiffness for a rigid plate on a semi-infinite homogenous elastic half-space.

Vertical Translation,  $K_z$ :

$$\frac{GL}{(1 - \nu)} \left[ 0.73 + 1.54 \left( \frac{B}{L} \right)^{0.75} \right]$$

**Equation 1**

Horizontal Translation (toward long side),  $K_y$ :

$$\frac{GL}{(2 - \nu)} \left[ 2 + 2.5 \left( \frac{B}{L} \right)^{0.85} \right]$$

**Equation 2**

Horizontal Translation (toward short side),  $K_x$ :

$$\frac{GL}{(2 - \nu)} \left[ 2 + 2.5 \left( \frac{B}{L} \right)^{0.85} \right] - \frac{GL}{(0.75 - \nu)} \left[ 0.1 \left( 1 - \frac{B}{L} \right) \right]$$

**Equation 3**

Rotation about x axis,  $K_{\theta x}$ :

$$\frac{G}{(1-\nu)} I_x^{0.75} \left(\frac{L}{B}\right)^{0.25} \left(2.4 + -0.5 \frac{B}{L}\right)$$

**Equation 4**

Rotation about y axis,  $K_{\theta y}$ :

$$\frac{G}{(1-\nu)} I_y^{0.75} \left[3 \left(\frac{L}{B}\right)^{0.15}\right]$$

**Equation 5**

Rotation about z axis,  $K_{\theta z}$ :

$$GJ^{0.75} \left[4 + 11 \left(1 - \frac{B}{L}\right)^{10}\right] \frac{1}{L}$$

**Equation 6**

The initial shear modulus,  $G_0$ , for granular soil was calculated based on the effective vertical stress and the normalized corrected blowcount  $(N_1)_{60}$ , which was determined as part of the geotechnical investigations performed at each bridge site. The equation used to calculate  $G$  was from the FHWA Seismic Retrofitting Manual for Highway Structures as follows:

$$G_0 \cong 20,000 \sqrt[3]{((N_1)_{60})} \sqrt{\sigma'_o}$$

**Equation 7**

A summary of the soils springs calculated for each pier is listed below in Table 20 through **Error! Reference source not found.**

**Table 20: Bridge A Pier Soil Spring Coefficients**

$K_z'$	32,861 kip/ft
$K_y'$	34,430 kip/ft
$K_x'$	33,390 kip/ft
$K_{\theta x}$	223,064 kip-ft
$K_{\theta y}$	80,160 kip-ft
$K_{\theta z}$	166,114 kip-ft

**Table 21: Bridge B Pier Soil Spring Coefficients**

$K_z'$	95,076 kip/ft
$K_y'$	78,791 kip/ft
$K_x'$	78,791 kip/ft
$K_{\theta x}$	7,722,799 kip-ft
$K_{\theta y}$	5,562,716 kip-ft
$K_{\theta z}$	6,156,946 kip-ft

### 2.5.3 APPLICATION OF SOIL-STRUCTURE INTERACTION

All 13 models for both bridges include the soil-structure interaction for the piers. However, for the abutments, the soil-structure interaction was only included for the integral abutment models and not for the conventional seat-type abutments. In the models with conventional seat-type abutments, the SSI is assumed to be negligible and therefore not included in the models. This is due to the fact that at the conventional seat-type abutments, the bearings provide a buffer between the abutments and the superstructure. As a result, any displacement or force in the abutment does not get transferred to the superstructure. However, this is not the case for IABs, which is why the SSI for the integral abutments was included in the IAB models. For these modes the SSI plays an important role in the seismic response of the bridge. The SSI for the integral abutments has been accounted for in the models by applying soil springs to the shell elements representing the integral abutments and the frame elements representing the supporting piles.

As mentioned in the previous section, soil springs were calculated for the footing of the piers based on the geotechnical investigations performed at that location. For the case where the piers consist of columns on spread footings, the calculated springs were applied at mid-height of the footing directly below each column. For the case where the piers consist of a drilled shaft with a pier cap, the springs were applied at the bottom of the drilled shaft.

The six IAB models with dense sand compacted backfill have soil springs that vary along the height of the integral abutments. Consequently, these soil springs are calculated at one foot increments where the average spring constant between each one

foot increment is applied to each of the one foot high shell elements that make up the entire integral abutment. This allows the change in soil stiffness with the height of the abutment to be incorporated into the model.

For the six models with EPS geofoam backfill, the soil stiffnesses do not vary over the height of the abutment and therefore there is one only spring coefficient calculated. The spring coefficient calculated for EPS geofoam is applied in a similar manner as the dense sand coefficients were applied to the previous six models; each of the one foot high shell elements that are part of the integral abutments has an EPS geofoam spring coefficient applied.

All 12 of the IAB models have piles on which the integral abutments are supported. These piles also have soil springs applied to them to account for the SSI that they have. The soil stiffnesses applied to these piles are calculated and applied in a manner similar to that used for the integral abutments. However, each of the six IAB models with compacted backfill have different in-situ soil assumptions for the piles; dense sand, medium dense sand, loose sand, stiff clay, medium stiff clay and soft clay. The spring constants for each of these different sand and clay types are calculated and then applied at one foot increments. The spring constants for stiff clay, medium stiff clay and soft clay do not vary over the length of the pile so one spring constant value for each type of clay is calculated and then applied to each of the one foot Frame elements for the entire length of each pile. The spring constants for dense sand, medium dense sand and loose sand are calculated at one foot increments and the average between each increment is then applied to each of the one foot long frame elements that make up the entire length of the piles at the integral abutments.

The spring constants used for cohesive soils are shown in Table 11 through Table 13 and the spring constants used for cohesionless backfill and EPS geofoam are shown in Table 8. The spring constants calculated were based on the Clough and Duncan model for medium sand.

## **CHAPTER III**

### **3 FINITE ELEMENT ANALYSIS**

#### **3.1 SEISMIC ANALYSIS PERFORMED**

Both time history analysis and Multi-modal response spectrum analysis (RSA) are commonly used for the seismic analysis of bridges. The time history analysis is considered a more refined analysis over the multi-modal RSA, which can provide conservative results. The multi-modal RSA is considered a more conservative analysis compared to the time history analysis. This is often adequate for many projects. Time history analysis is generally only used when refined results are required, or when the conservative nature of the multi-modal RSA is not acceptable. For this parametric study the multi-modal RSA was selected to be used for all 13 models for each bridge as it reflects the requirements set forth in the current American Association of State Highway and Transportation Officials (AASHTO) Bridge Design Specifications. Also, the multi-modal RSA provides results for a more general seismic event as it is representative of many design earthquake time history records rather than one specific time history record. Being as a time history analysis requires a great deal more effort during the modeling and analysis with little additional benefit in return, it was deemed unnecessary to refine the results to that degree. The multi-modal RSA will provide results with sufficient accuracy to determine the effects of the various parameters on the seismic response of the bridges. Based on the scope of this parametric study, the additional refinement that can be

achieved from the time history analysis over the multi-modal RSA is not necessary. Therefore the multi-modal response spectrum analysis was used for this study.

For all 13 models for each bridge a multi-modal RSA is performed for a 1000 year return period with 5% structural damping. This was based on AASHTO Bridge Design Specifications, 2012. AASHTO Bridge Design Specifications state that bridges shall have a low probability of collapse when subject to earthquake ground motions that have a seven percent probability of exceedance in 75 years. This equates to a 1000 year return period.

An adequate number of modes were developed in order to achieve 90% mass participation ratio for each model. The response spectrum used for these analyses was generated based on the latitude and longitude of each bridge, the site class and the seismicity information determined from the geotechnical investigations performed at each bridge site. The latitude and longitude coordinates of the bridge were entered into CSiBridge along with the peak ground acceleration (PGA), short period seismic parameter ( $S_{Ds}$ ), and the 1-second period seismic parameter ( $S_{D1}$ ), which utilizes the AASHTO Hazard Maps in the development of the response spectra. Refer to Figure 34 and Figure 35 for the response spectra used for each bridge.

The modal load case in CSiBridge was defined based on the input response spectrum as described above and utilizes the eigenvector modal type rather than the Ritz vector analysis. Eigenvector analysis is used to determine the natural modes or the undamped free-vibration mode shapes and frequencies of the system (Computers & Structures, Inc.) which provide insight into the behavior of the structure. The alternative to eigenvector analysis is Ritz vector analysis, which is used when dealing with modal



superposition or time-history analysis, neither of which is the case for the models in this parametric study.

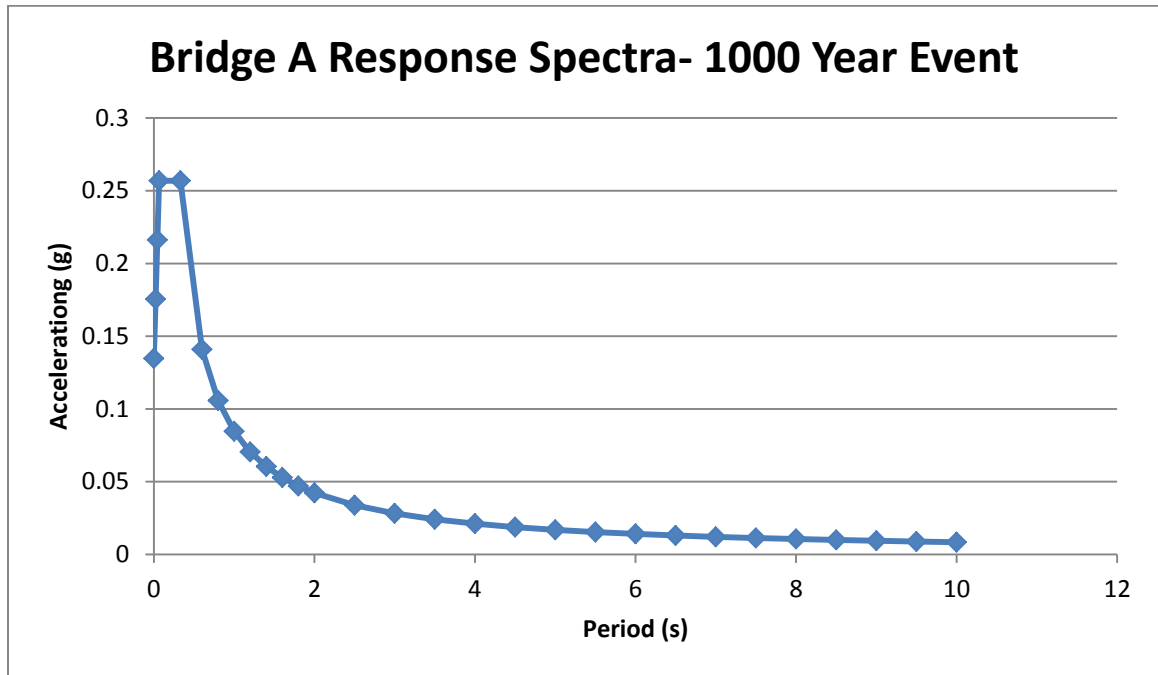


**Figure 34: Bridge A Response Spectra**

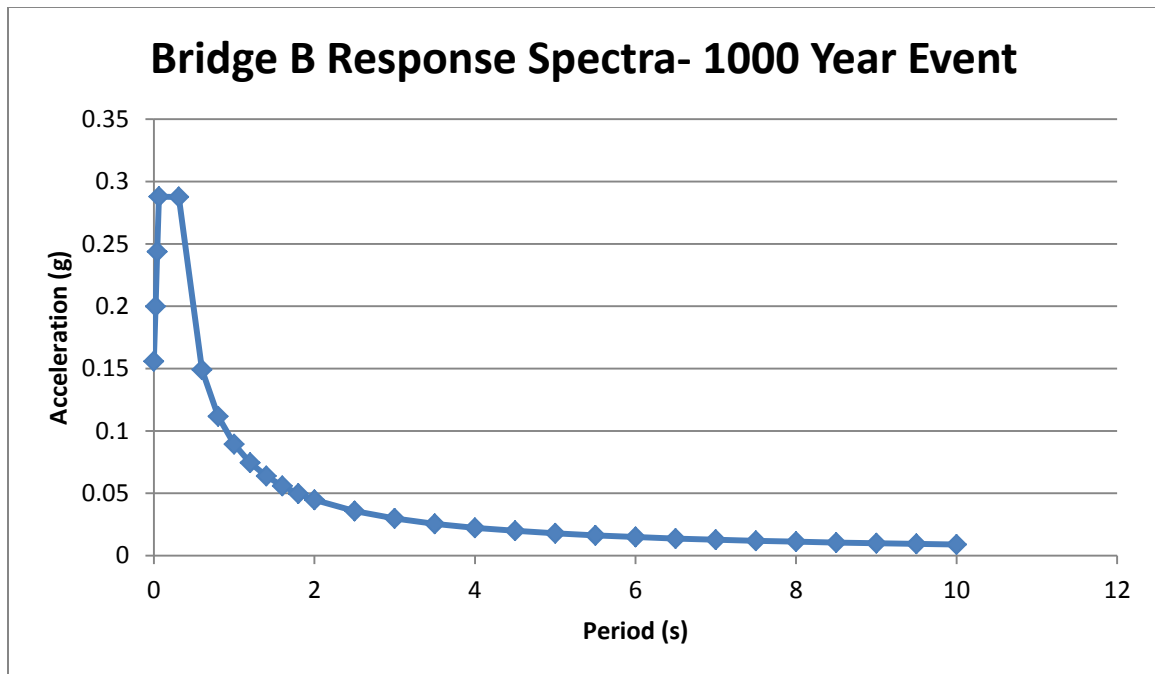


**Figure 35: Bridge B Response Spectra**

**Table 22: Seismicity Information**

Bridge	Site Class	Pga	$S_s^1$	$S_1^2$
Bridge A	D	0.087	0.165	0.036
Bridge B	D	0.098	0.180	0.037

### 3.2 LOADING AND LOAD COMBINATIONS

The load cases used for each model were Extreme Event I, from AASHTO Bridge Construction Specifications. The following were the two equations used for Extreme Event I load combinations.

$$1.25DL+0.5LL+1.0EQ_L+0.3EQ_T$$

**Equation 8**

$$1.25DL+0.5LL+0.3EQ_L+1.0EQ_T$$

**Equation 9**

$EQ_L$  is the longitudinal earthquake loading from the multi-mode analysis and  $EQ_T$  is the transverse earthquake loading from the multi-mode analysis.  $DL$  is the dead load and includes the existing wearing surface.  $LL$  is the live load as calculated by CSiBridge Live Load Optimizer.

CSiBridge utilizes a feature called the Live Load Optimizer. The Live Load Optimizer uses the definition of the lanes and vehicles, such as the HS-20 and accompanying lane loading in order to calculate the influence lines. CSiBridge uses these calculated influence lines along with the appropriate multiple presence factor as defined in the AASHTO Bridge Construction Specifications to determine the worst case live load scenario.

## **CHAPTER IV**

### **4 ANALYSIS RESULTS**

Various measures are used to determine the overall seismic response of the bridge in each model. This includes the dominant structural period as well as the longitudinal and transverse displacement of the top of the pier, top of the integral abutments and conventional abutments and bottom of the integral abutments. Note that displacements at the bottom of the conventional abutments are not available based on the modeling assumptions utilized, as the conventional abutments are not modeled in their entirety. Refer to Section 2.3.2 for more information on how the abutments are modeled. Other metrics used includes pier column, cap and footing maximum moments and shears as well as base reactions and mode shapes.

#### **4.1 STRUCTURAL PERIOD**

The dominant structural period for the bridge is a direct reflection of structure's overall stiffness. The higher the dominant structural period, the more flexible the structure is. The flexibility of a structure influences the distribution of loads to the piers and abutments. The fundamental structural period for each model is shown below in Table 23, where the (CB) following the model number indicates the model is for an IAB with compacted backfill and (EPS) following the model number indicated the model is for an IAB with EPS geof foam backfill. From the structural periods listed below in Table

23 it can be seen that the typical jointed bridge is the most flexible with the highest dominant structural period. Of the IABs, the model with the EPS Geofoam backfill and soft clay at the piles is the most flexible while the IAB with compacted backfill and stiff clay at the piles is the stiffest with the lowest period. The dominant structural period from each model indicates that the EPS geofoam backfill allows for a more flexible structure than those with compacted backfill.

The mode shapes for a bridge are also used as an indication of the structure's stiffness and the structure's overall seismic response. The first mode shape is the dominant mode shape for that bridge. Figure 36 through Figure 41 shows the first mode shape for each traditional jointed bridge model, IAB model with Compacted Backfill and Dense Sand at Piles and IAB model with EPS Geofoam and Dense Sand at Piles.

**Table 23: Fundamental Period**

<b>Model Number</b>	<b>Model Description</b>	<b>Structural Period</b>	
		<b>Bridge A</b>	<b>Bridge B</b>
1	Jointed Bridge	1.555	1.213
2 (CB)	Dense Sand	0.812	1.079
3 (CB)	Medium Dense Sand	0.815	1.086
4 (CB)	Loose Sand	0.820	1.087
5 (CB)	Stiff Clay	0.752	1.045
6 (CB)	Medium Stiff Clay	0.799	1.073
7 (CB)	Soft Clay	0.842	1.093
8 (EPS)	Dense Sand	1.226	1.118
9 (EPS)	Medium Dense Sand	1.242	1.126
10 (EPS)	Loose Sand	1.274	1.127
11 (EPS)	Stiff Clay	0.988	1.074
12 (EPS)	Medium Stiff Clay	1.167	1.110
13 (EPS)	Soft Clay	1.417	1.136

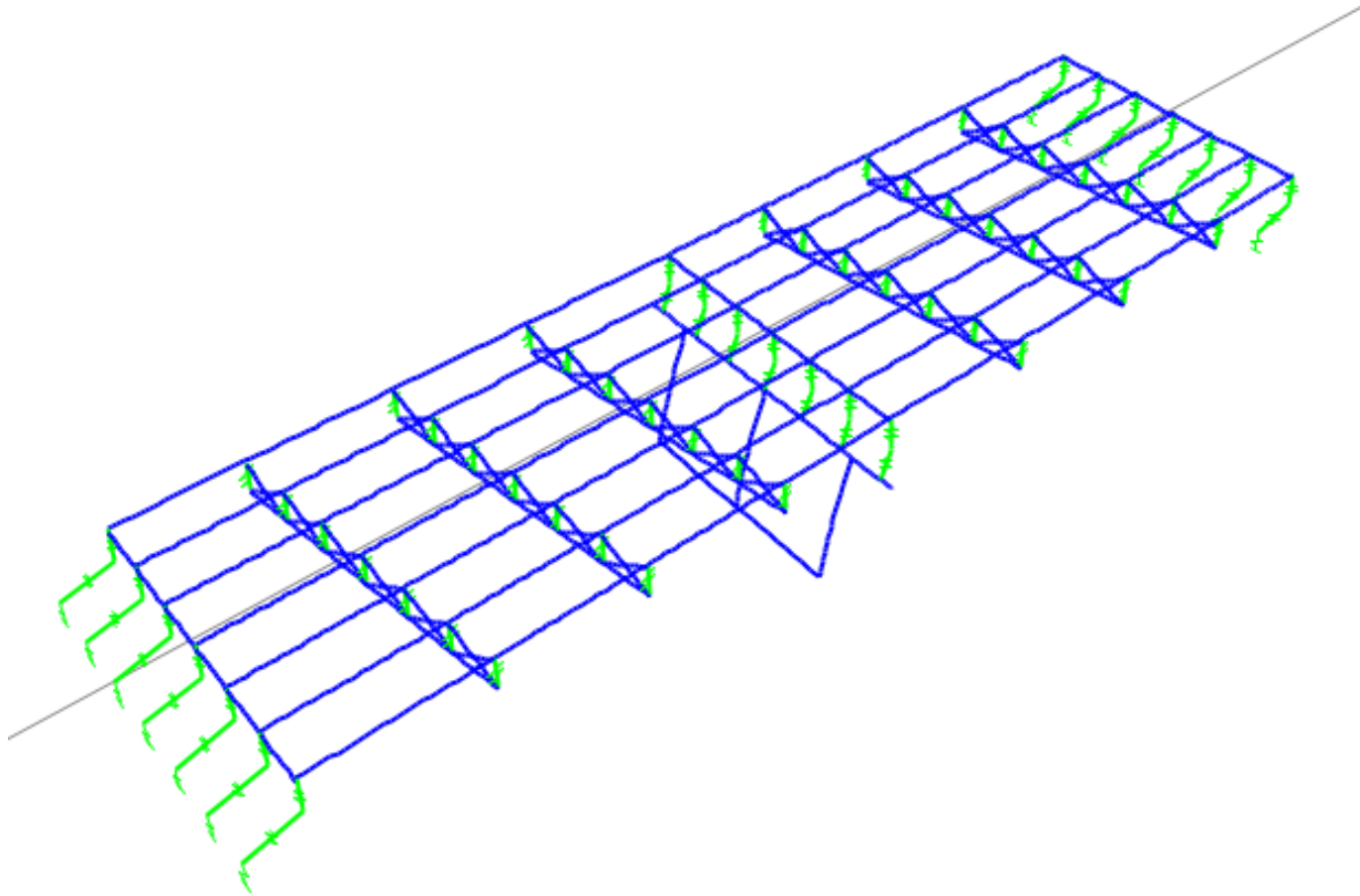


**Figure 36: 1<sup>st</sup> Mode Shape for Bridge A with Conventional Abutments**

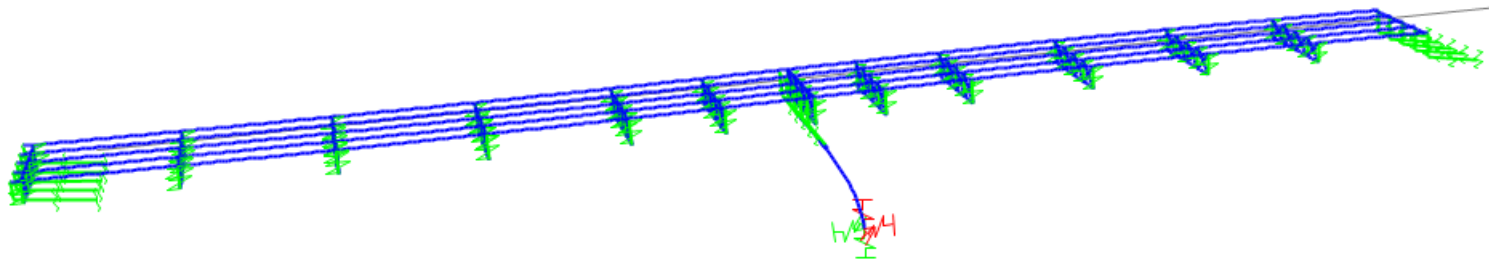


**Figure 37: 1st Mode Shape for Bridge B with Conventional Abutments**



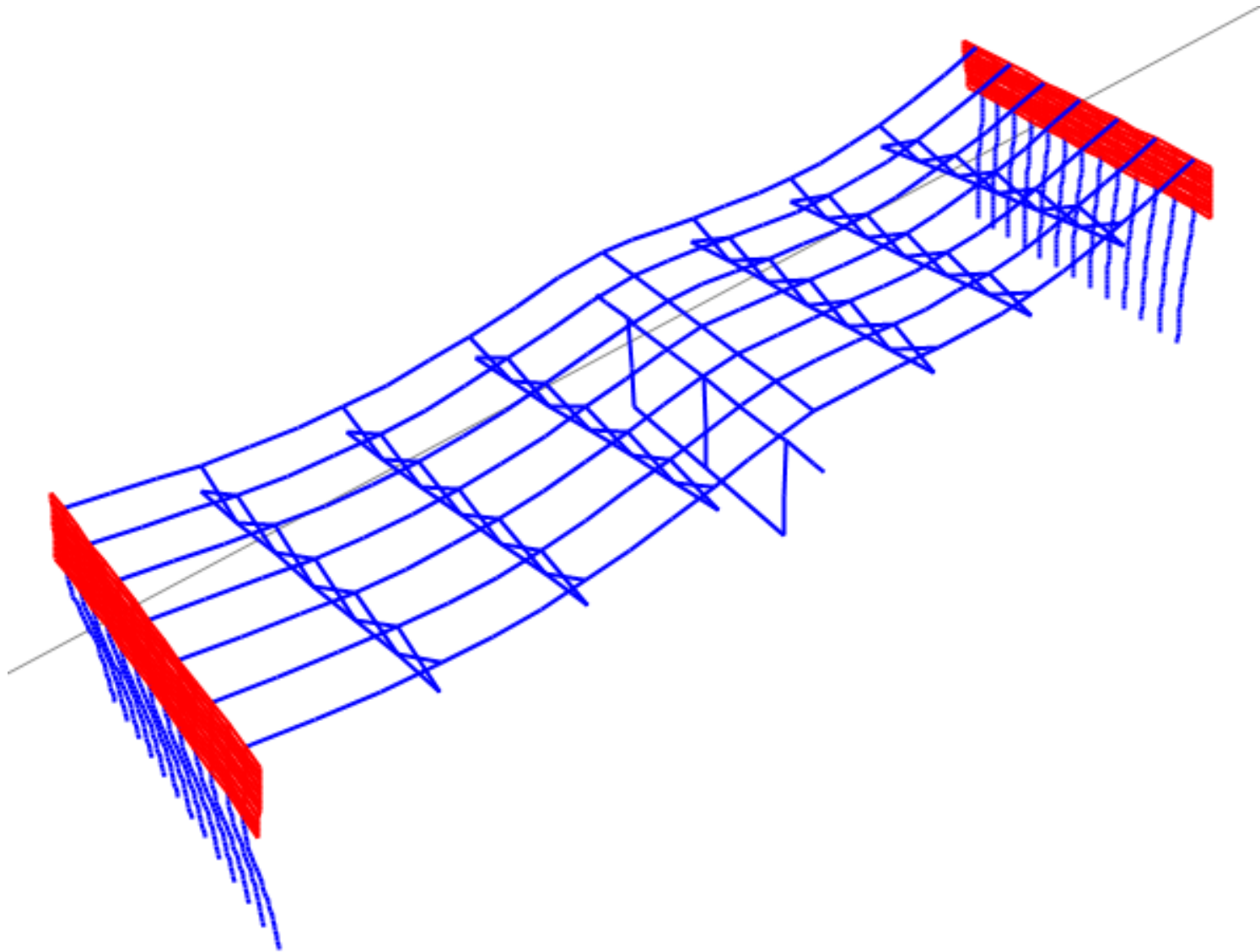


**Figure 38: 1st Mode Shape for Bridge A with Integral Abutments and Compacted Backfill**

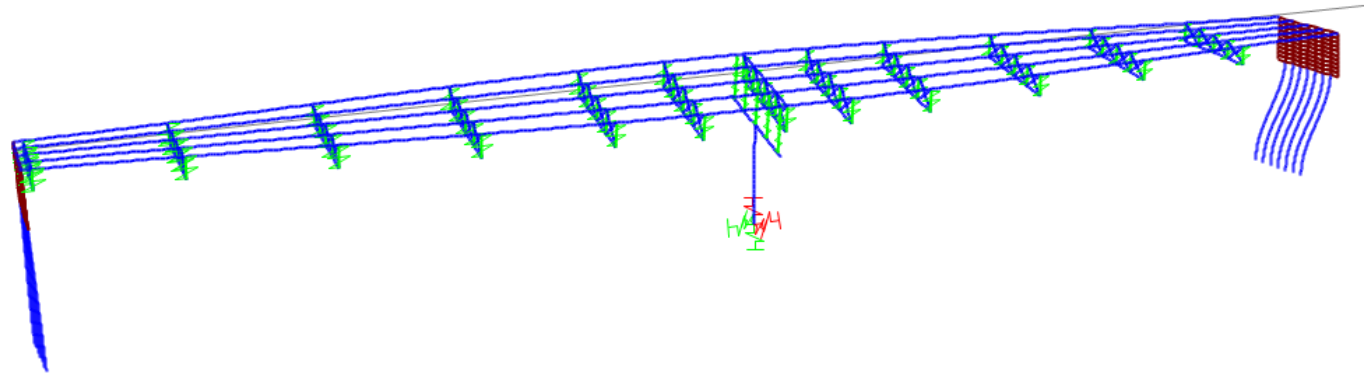


**Figure 39: 1st Mode Shape for Bridge B with Integral Abutments and Compacted Backfill**

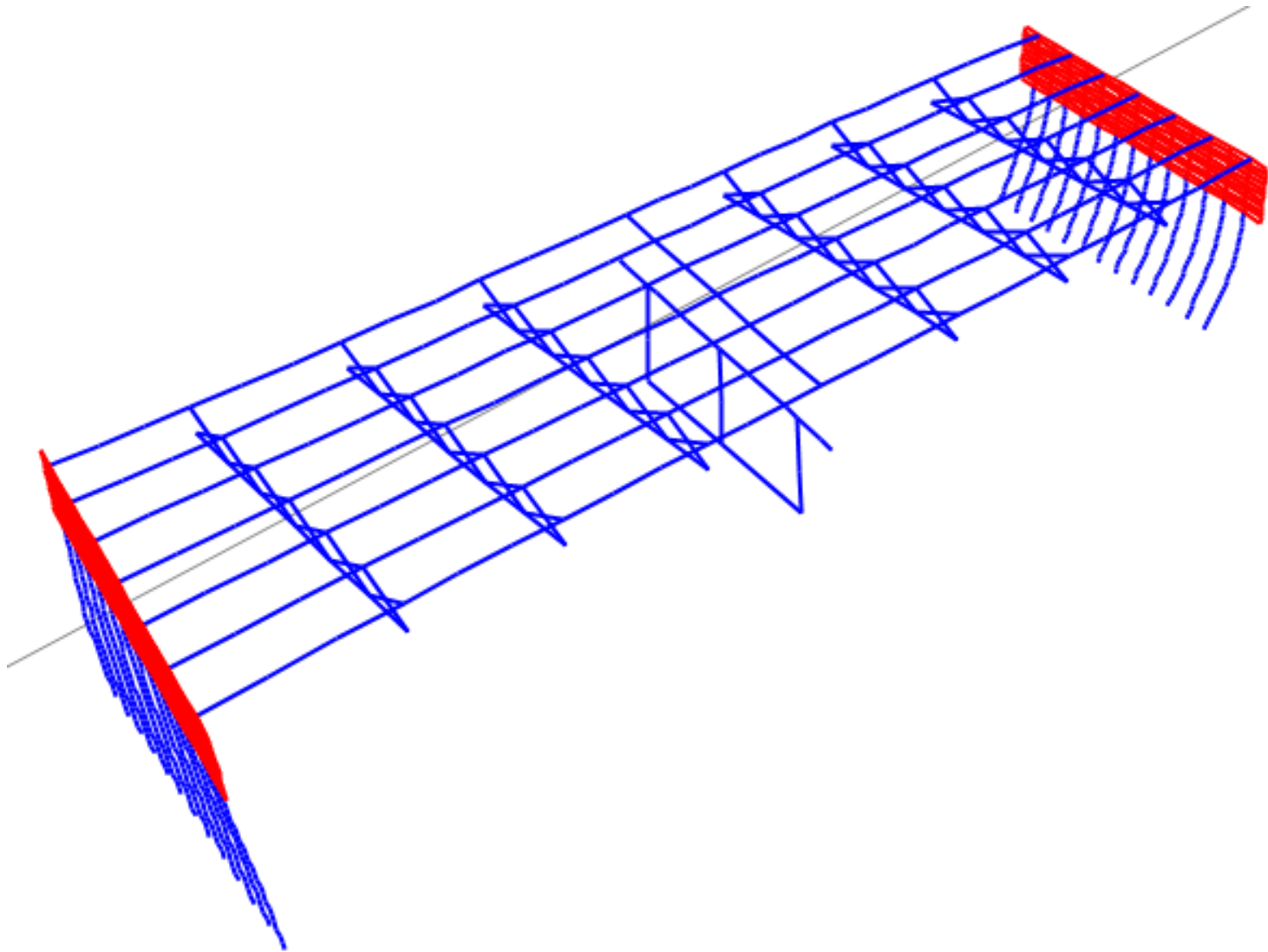


**Figure 40: 1st Mode Shape for Bridge A with Integral Abutments and EPS Geofoam Backfill**

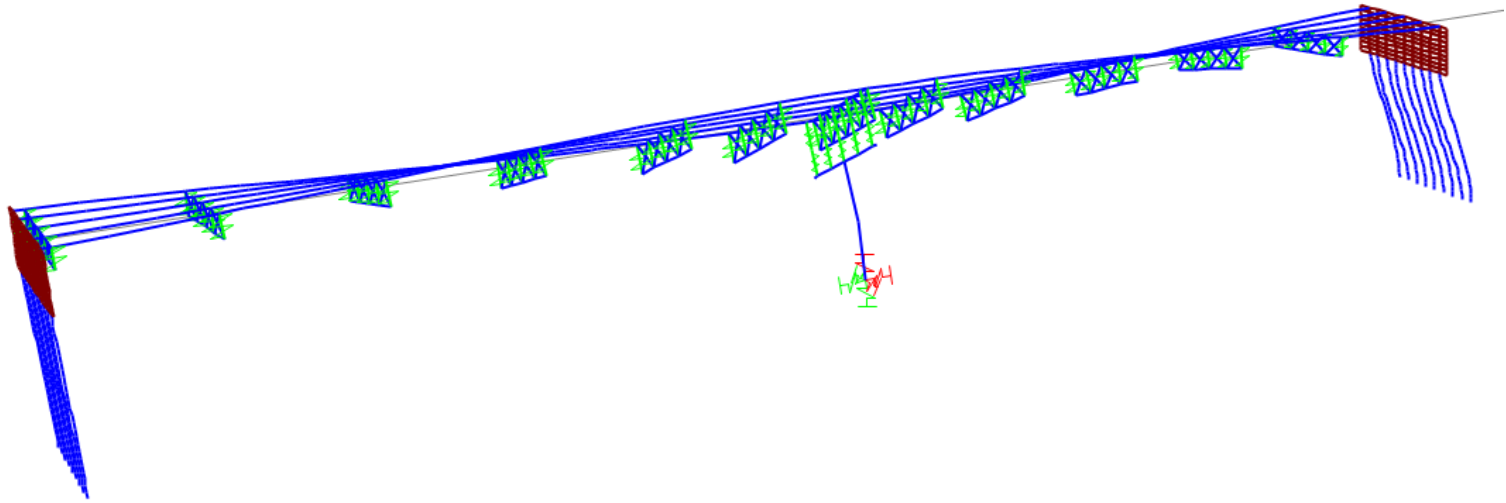


**Figure 41: 1st Mode Shape for Bridge B with Integral Abutments and EPS Geofoam Backfill**

## 4.2 PIER AND ABUTMENT DISPLACEMENT

Pier and abutment displacement in both the longitudinal and transverse directions are important part of determining the seismic response of the structure. Piers and abutments are only capable of handling a certain amount of displacement in either direction.

For traditional seat-type abutments, the bearings take a large percentage of the displacement therefore a majority of the displacement does not transfer to the abutments themselves. This is not the case for integral abutments as there are no bearings to reduce the transfer of displacement to the abutment. Integral abutments are designed to handle a certain amount of displacement to account for expansion and contraction of the superstructure due to temperature changes, however are not normally designed to accommodate excessive displacement due to a seismic event. For this reason, the displacement seen in the abutments in each model can be used to determine the best backfill and soil combination for integral abutments under the effect of seismic loading.

Similar to abutments, piers are only designed to accommodate a certain amount of displacement. Piers in IABs can be subject to more displacement than piers in traditional jointed bridges as a result of the increased stiffness of the structure. For this reason it is important to evaluate the amount of displacement at the pier for each combination of abutment backfill and soil at the piles.

The longitudinal and transverse pier displacement is measured at the pier cap and shown in Table 24 and Table 25. The displacements for the integral abutments are measured at both the top and the bottom of the abutment. They are measured in the

longitudinal and transverse directions and shown in Table 26 through Table 29 where (T) refers to top and (B) refers to bottom of the abutment.

**Table 24: Bridge A Longitudinal and Transverse Pier Displacement**

<b>Model Number</b>	<b>Model Description</b>	<b>Longitudinal Displacement (in)</b>	<b>Transverse Displacement (in)</b>
1	Jointed Bridge	-0.190	0.690
2 (CB)	Dense Sand	-0.474	0.250
3 (CB)	Medium Dense Sand	-0.475	0.253
4 (CB)	Loose Sand	-0.476	0.260
5 (CB)	Stiff Clay	-0.464	0.191
6 (CB)	Medium Stiff Clay	-0.472	0.256
7 (CB)	Soft Clay	-0.481	0.289
8 (EPS)	Dense Sand	-0.482	0.365
9 (EPS)	Medium Dense Sand	-0.483	0.374
10 (EPS)	Loose Sand	-0.485	0.390
11 (EPS)	Stiff Clay	-0.469	0.234
12 (EPS)	Medium Stiff Clay	-0.479	0.332
13 (EPS)	Soft Clay	-0.494	0.432

**Table 25: Bridge B Longitudinal and Transverse Pier Displacement**

<b>Model Number</b>	<b>Model Description</b>	<b>Longitudinal Displacement (in)</b>	<b>Transverse Displacement (in)</b>
1	Jointed Bridge	0.838	0.183
2 (CB)	Dense Sand	-0.666	-1.969
3 (CB)	Medium Dense Sand	-0.666	-1.969
4 (CB)	Loose Sand	-0.611	-1.754
5 (CB)	Stiff Clay	-0.625	-0.222
6 (CB)	Medium Stiff Clay	-0.628	-0.249
7 (CB)	Soft Clay	-0.632	-0.271
8 (EPS)	Dense Sand	-0.670	-1.965
9 (EPS)	Medium Dense Sand	-0.670	-1.966
10 (EPS)	Loose Sand	-0.670	-1.966
11 (EPS)	Stiff Clay	-0.625	0.278
12 (EPS)	Medium Stiff Clay	-0.628	-0.340
13 (EPS)	Soft Clay	-0.633	-0.488

**Table 26: Bridge A Maximum Displacement at Top and Bottom of Integral Abutments for Models with Sand Foundation Soils**

<b>Model Number</b>	<b>Model Description</b>	<b>Longitudinal Displacement (in)</b>	<b>Transverse Displacement (in)</b>
2 (CB)	Dense Sand	-0.043 (T) -0.043(B)	0.286(T) 0.334(B)
3 (CB)	Medium Dense Sand	-0.043(T) -0.043(B)	0.292(T) 0.342(B)
4 (CB)	Loose Sand	-0.043(T) -0.043 (B)	0.301(T) 0.356(B)
8 (EPS)	Dense Sand	-0.042(T) -0.041 (B)	0.446(T) 0.472(B)
9 (EPS)	Medium Dense Sand	-0.041(T) -0.041(B)	0.458(T) 0.488(B)
10 (EPS)	Loose Sand	-0.041(T) -0.041 (B)	0.479(T) 0.519(B)



**Table 27: Bridge A Maximum Displacement at Top and Bottom of Integral Abutments for Models with Clay Foundation Soils**

<b>Model Number</b>	<b>Model Description</b>	<b>Longitudinal Displacement (in)</b>	<b>Transverse Displacement (in)</b>
5 (CB)	Stiff Clay	-0.044(T) -0.044(B)	0.218(T) 0.222(B)
6 (CB)	Medium Stiff Clay	-0.044(T) -0.044(B)	0.271(T) 0.312(B)
7 (CB)	Soft Clay	-0.043(T) -0.043(B)	0.337(T) 0.422(B)
11 (EPS)	Stiff Clay	-0.044(T) -0.044(B)	0.279(T) 0.256(B)
12 (EPS)	Medium Stiff Clay	-0.042(T) -0.042(B)	0.403(T) 0.417(B)
13 (EPS)	Soft Clay	-0.040(T) -0.040(B)	0.542(T) 0.641(B)

**Table 28: Bridge B Maximum Displacement at Top and Bottom of Integral Abutments for Models with Sand Foundation Soils**

<b>Model Number</b>	<b>Model Description</b>	<b>Longitudinal Displacement (in)</b>	<b>Transverse Displacement (in)</b>
2 (CB)	Dense Sand	-0.081(T) -0.078(B)	1.051(T) -0.301(B)
3 (CB)	Medium Dense Sand	-0.081(T) -0.078(B)	1.053(T) -0.302(B)
4 (CB)	Loose Sand	-0.131(T) -0.131(B)	0.819(T) -1.189(B)
8 (EPS)	Dense Sand	-0.109(T) -0.105(B)	0.020(T) 0.001(B)
9 (EPS)	Medium Dense Sand	-0.109(T) -0.105(B)	0.020(T) 0.001(B)
10 (EPS)	Loose Sand	-0.109(T) -0.105(B)	0.020(T) 0.001(B)

**Table 29: Bridge B Maximum Displacement at Top and Bottom of Integral Abutments for Models with Clay Foundation Soils**

<b>Model Number</b>	<b>Model Description</b>	<b>Longitudinal Displacement (in)</b>	<b>Transverse Displacement (in)</b>
5 (CB)	Stiff Clay	-0.107(T) -0.107(B)	0.905(T) 0.422(B)
6 (CB)	Medium Stiff Clay	-0.044(T) -0.045(B)	-0.355(T) 0.385(B)
7 (CB)	Soft Clay	-0.105(T) -0.105(B)	0.940(T) -0.834(B)
11 (EPS)	Stiff Clay	-0.107(T) -0.107(B)	0.410(T) -0.364(B)
12 (EPS)	Medium Stiff Clay	-0.044(T) -0.045(B)	-0.463(T) -0.471(B)
13 (EPS)	Soft Clay	-0.106(T) -0.102(B)	0.519(T) -0.393(B)

Based on the displacements shown in Table 24 and Table 25, the pier displacement for the IABs is significantly less than that for the typical jointed bridges. The displacement at the abutments for the IABs with compacted backfill is approximately 60% less than that for the IABs with EPS geofoam backfill.

### **4.3 PIER FORCES**

For each model, the maximum moment and maximum shear at the pier column, pier cap and pier footing (where applicable) are reported in Table 30 to Table 35. For the models where more than one pier exists, the maximum moment and shear reported for the pier cap, pier column and pier footings is the maximum for all piers in the model.

**Table 30: Summary of Bridge A Pier Column Forces and Moments**

<b>Model Number</b>	<b>Model Description</b>	<b>Maximum Moment (kip-ft)</b>	<b>Maximum Shear (kip)</b>
1	Jointed Bridge	895.259	-49.320
2 (CB)	Dense Sand	1026.428	121.630
3 (CB)	Medium Dense Sand	-1025.789	-121.555
4 (CB)	Loose Sand	1028.594	121.886
5 (CB)	Stiff Clay	1015.157	120.298
6 (CB)	Medium Stiff Clay	1023.437	121.278
7 (CB)	Soft Clay	1032.854	122.400
8 (EPS)	Dense Sand	1060.738	125.726
9 (EPS)	Medium Dense Sand	-1063.524	-126.050
10 (EPS)	Loose Sand	-1069.075	-126.706
11 (EPS)	Stiff Clay	-1031.651	-122.289
12 (EPS)	Medium Stiff Clay	-1051.564	-124.638
13 (EPS)	Soft Clay	-1097.163	-130.024

**Table 31: Summary of Bridge B Pier Column Forces and Moments**

<b>Model Number</b>	<b>Model Description</b>	<b>Maximum Moment (kip-ft)</b>	<b>Maximum Shear (kip)</b>
1	Jointed Bridge	-5743.320	172.788
2 (CB)	Dense Sand	-6531.145	188.581
3 (CB)	Medium Dense Sand	-6532.802	188.642
4 (CB)	Loose Sand	-6531.268	188.608
5 (CB)	Stiff Clay	-6541.783	188.843
6 (CB)	Medium Stiff Clay	-6533.217	188.625
7 (CB)	Soft Clay	-6527.238	188.510
8 (EPS)	Dense Sand	-6520.877	188.055
9 (EPS)	Medium Dense Sand	-6522.130	188.105
10 (EPS)	Loose Sand	-6520.632	188.064
11 (EPS)	Stiff Clay	-6532.717	188.433
12 (EPS)	Medium Stiff Clay	-6523.020	188.133
13 (EPS)	Soft Clay	-6516.861	187.940

**Table 32: Summary of Bridge A Pier Cap Forces and Moments**

<b>Model Number</b>	<b>Model Description</b>	<b>Maximum Moment (kip-ft)</b>	<b>Maximum Shear (kip)</b>
1	Jointed Bridge	-1378.867	456.612
2 (CB)	Dense Sand	-1820.513	523.410
3 (CB)	Medium Dense Sand	-1822.767	524.205
4 (CB)	Loose Sand	-1827.721	525.858
5 (CB)	Stiff Clay	-1781.326	509.976
6 (CB)	Medium Stiff Clay	-1813.185	521.032
7 (CB)	Soft Clay	-1848.007	533.003
8 (EPS)	Dense Sand	-1860.347	532.868
9 (EPS)	Medium Dense Sand	-1864.637	534.115
10 (EPS)	Loose Sand	-1873.042	536.517
11 (EPS)	Stiff Clay	-1804.267	515.484
12 (EPS)	Medium Stiff Clay	-1847.516	529.313
13 (EPS)	Soft Clay	-1914.575	548.246

**Table 33: Summary of Bridge B Pier Cap Forces and Moments**

<b>Model Number</b>	<b>Model Description</b>	<b>Maximum Moment (kip-ft)</b>	<b>Maximum Shear (kip)</b>
1	Jointed Bridge	-4370.522	627.353
2 (CB)	Dense Sand	-4139.348	579.675
3 (CB)	Medium Dense Sand	-4142.389	580.141
4 (CB)	Loose Sand	-4147.707	581.016
5 (CB)	Stiff Clay	-4098.323	572.940
6 (CB)	Medium Stiff Clay	-4132.223	578.496
7 (CB)	Soft Clay	-4170.891	584.777
8 (EPS)	Dense Sand	-4146.288	580.973
9 (EPS)	Medium Dense Sand	-4149.807	581.519
10 (EPS)	Loose Sand	-4156.188	582.565
11 (EPS)	Stiff Clay	-4104.510	573.592
12 (EPS)	Medium Stiff Clay	-4137.816	579.575
13 (EPS)	Soft Clay	-4185.918	587.375



**Table 34: Summary of Bridge A Pier Footing Forces and Moments**

<b>Model Number</b>	<b>Model Description</b>	<b>Maximum Moment (kip-ft)</b>	<b>Maximum Shear (kip)</b>
1	Jointed Bridge	-510.079	113.395
2 (CB)	Dense Sand	-852.433	152.604
3 (CB)	Medium Dense Sand	-852.868	152.631
4 (CB)	Loose Sand	-854.403	152.739
5 (CB)	Stiff Clay	-842.661	151.927
6 (CB)	Medium Stiff Clay	-849.862	152.423
7 (CB)	Soft Clay	-858.728	153.025
8 (EPS)	Dense Sand	-883.535	154.937
9 (EPS)	Medium Dense Sand	-885.745	155.110
10 (EPS)	Loose Sand	-890.212	155.458
11 (EPS)	Stiff Clay	-860.141	153.140
12 (EPS)	Medium Stiff Clay	-876.110	154.361
13 (EPS)	Soft Clay	-912.808	157.234

**Table 35: Summary of Bridge B Pier Footing Forces and Moments**

<b>Model Number</b>	<b>Model Description</b>	<b>Maximum Moment (kip-ft)</b>	<b>Maximum Shear (kip)</b>
1	Jointed Bridge	5743.319	-173.163
2 (CB)	Dense Sand	-6531.145	-188.834
3 (CB)	Medium Dense Sand	6532.802	-188.895
4 (CB)	Loose Sand	6531.268	-188.861
5 (CB)	Stiff Clay	6541.440	-189.096
6 (CB)	Medium Stiff Clay	6533.217	-188.878
7 (CB)	Soft Clay	6527.238	-188.764
8 (EPS)	Dense Sand	6520.877	-188.310
9 (EPS)	Medium Dense Sand	6522.130	-188.358
10 (EPS)	Loose Sand	6520.632	-188.318
11 (EPS)	Stiff Clay	6532.717	-188.686
12 (EPS)	Medium Stiff Clay	6523.020	-188.367
13 (EPS)	Soft Clay	6516.861	-188.194

#### **4.4 ABUTMENT FORCES**

For each integral abutment model, the maximum moments and maximum shears at the abutments are reported in Table 36 to Table 43. These values are the maximum shear and moment at each row of abutment area shells. Each abutment area shell measures one foot high and half the width of the girder spacing. Location 1 is the first row of area shells at the top of the abutment, which measures from the top of the integral abutment to one foot below the top of the integral abutment. Similarly, location 2 is the second row of area shells, where the top of these area shells are located one foot down from the top of the integral abutments and the bottom of the area shells are two feet down from the top of integral abutment.. For the maximum shears and moments, the maximum magnitudes were used, regardless of direction.

**Table 36: Bridge A Maximum Shear and Moment for Compacted Backfill**

<b>Abutment Location (ft)</b>	<b>Dense Sand at Piles</b>		<b>Medium Dense Sand at Piles</b>		<b>Loose Sand at Piles</b>	
	<b>Max Shear (K-ft)</b>	<b>Max Moment (K-ft)</b>	<b>Max Shear (K-ft)</b>	<b>Max Moment (K-ft)</b>	<b>Max Shear (K-ft)</b>	<b>Max Moment (K-ft)</b>
1	161.21	-295.85	161.21	-295.85	160.45	-294.48
2	59.48	-138.40	59.48	-138.40	59.19	-137.77
3	24.71	-79.24	25.17	-79.24	25.05	-78.90
4	13.24	-54.05	13.24	-54.05	13.18	-53.83
5	9.11	-42.15	9.11	-42.15	9.06	-41.99
6	7.99	-34.12	7.99	-34.12	7.95	-34.01
7	7.30	-26.09	7.30	-26.09	7.27	-26.02
8	6.74	-19.14	6.74	-19.14	6.72	-19.07
9	7.33	-14.59	7.33	-14.59	7.31	-14.54
10	11.29	-14.37	11.29	-14.37	11.29	-14.37

**Table 37: Bridge A Maximum Shear and Moment for EPS Geofoam Backfill**

<b>Abutment Location (ft)</b>	<b>Dense Sand at Piles</b>		<b>Medium Dense Sand at Piles</b>		<b>Loose Sand at Piles</b>	
	<b>Max Shear (K-ft)</b>	<b>Max Moment (K-ft)</b>	<b>Max Shear (K-ft)</b>	<b>Max Moment (K-ft)</b>	<b>Max Shear (K-ft)</b>	<b>Max Moment (K-ft)</b>
1	-97.28	-183.91	-97.12	-183.61	-93.09	-175.70
2	34.56	-90.26	34.50	-90.11	33.03	-86.38
3	13.90	-55.45	13.87	-55.36	13.28	-53.17
4	6.69	-41.26	6.68	-41.19	6.38	-39.69
5	4.33	-34.41	4.32	-34.36	4.07	-33.28
6	3.80	-30.70	3.79	-30.70	3.65	-29.86
7	4.40	-26.72	4.39	-26.72	4.27	-26.14
8	5.85	-24.38	5.85	-24.38	5.75	-24.42
9	9.78	-22.37	9.79	-22.36	9.77	-22.82
10	20.06	-29.14	20.07	-29.15	20.35	-30.84

**Table 38: Bridge A Maximum Shear and Moment for Compacted Backfill**

<b>Abutment Location (ft)</b>	<b>Stiff Clay at Piles</b>		<b>Medium Stiff Clay at Piles</b>		<b>Soft Clay at Piles</b>	
	<b>Max Shear (K-ft)</b>	<b>Max Moment (K-ft)</b>	<b>Max Shear (K-ft)</b>	<b>Max Moment (K-ft)</b>	<b>Max Shear (K-ft)</b>	<b>Max Moment (K-ft)</b>
1	164.13	-301.28	161.60	-296.62	161.85	-297.11
2	60.54	-140.96	59.62	-138.78	59.72	139.03
3	25.62	-80.71	25.23	-79.47	25.27	-79.62
4	13.48	-55.03	13.27	-54.22	13.29	-54.32
5	9.28	-43.05	9.13	-42.28	9.14	-42.36
6	8.12	-35.56	8.00	-34.23	8.02	-34.29
7	7.42	-27.82	7.32	-26.17	7.33	-26.20
8	6.90	-20.42	6.76	-19.09	6.78	-8.75
9	7.73	-15.07	7.30	-14.46	7.24	-14.15
10	11.76	-14.52	11.21	-14.26	11.16	-14.26

**Table 39: Bridge A Maximum Shear and Moment for EPS Geofoam Backfill**

<b>Abutment</b>	<b>Stiff Clay</b>		<b>Medium Stiff Clay</b>		<b>Soft Clay</b>	
<b>Location (ft)</b>	<b>Max Shear (K-ft)</b>	<b>Max Moment (K-ft)</b>	<b>Max Shear (K-ft)</b>	<b>Max Moment (K-ft)</b>	<b>Max Shear (K-ft)</b>	<b>Max Moment (K-ft)</b>
1	-101.15	-191.32	-97.63	-184.62	77.94	-146.70
2	35.98	-93.84	34.72	-90.58	27.44	-71.52
3	14.97	-57.59	13.97	-55.61	11.76	-43.28
4	7.30	-42.78	6.63	-41.34	5.78	-31.18
5	4.73	-35.60	4.30	-34.45	3.74	-25.26
6	4.06	-31.71	3.82	-30.72	3.12	-22.31
7	4.58	-27.49	4.42	-26.66	3.39	-19.22
8	6.00	-24.83	5.82	-24.26	4.14	-16.49
9	9.84	-22.68	9.71	-22.24	6.80	-15.14
10	20.12	-29.08	19.88	-28.91	13.88	-19.91

**Table 40: Bridge B Maximum Shear and Moment for Compacted Backfill**

<b>Abutment Location (ft)</b>	<b>Dense Sand at Piles</b>		<b>Medium Dense Sand at Piles</b>		<b>Loose Sand at Piles</b>	
	<b>Max Shear (K-ft)</b>	<b>Max Moment (K-ft)</b>	<b>Max Shear (K-ft)</b>	<b>Max Moment (K-ft)</b>	<b>Max Shear (K-ft)</b>	<b>Max Moment (K-ft)</b>
1	587.521	866.438	580.260	856.799	566.971	837.432
2	-137.089	346.448	-135.603	342.554	-132.265	334.178
3	-42.345	211.517	-41.916	209.075	-42.842	204.251
4	-23.656	174.489	-23.381	172.270	-23.277	164.670
5	-23.268	151.807	-22.994	149.855	-22.984	146.741
6	-18.822	133.380	-18.603	131.718	-16.334	128.650
7	-19.962	116.665	-19.712	115.224	-18.742	112.894
8	-23.656	101.880	-23.353	100.669	-23.144	98.503
9	-36.086	89.312	-35.674	88.348	-35.074	86.514
10	107.970	-94.395	-93.669	107.431	-92.152	105.959



**Table 41: Bridge B Maximum Shear and Moment for EPS Geofoam Backfill**

<b>Abutment Location (ft)</b>	<b>Dense Sand at Piles</b>		<b>Medium Dense Sand at Piles</b>		<b>Loose Sand at Piles</b>	
	<b>Max Shear (K-ft)</b>	<b>Max Moment (K-ft)</b>	<b>Max Shear (K-ft)</b>	<b>Max Moment (K-ft)</b>	<b>Max Shear (K-ft)</b>	<b>Max Moment (K-ft)</b>
1	535.889	779.384	43.765	763.106	505.924	734.864
2	-120.145	315.486	-9.796	309.005	-112.407	296.394
3	-35.569	197.078	-2.896	193.143	-34.241	185.654
4	-18.727	166.266	-1.522	163.172	-18.484	154.226
5	-18.988	148.390	-1.548	145.735	-18.252	140.623
6	-15.569	133.543	-1.265	131.149	-13.034	126.778
7	-17.789	120.311	-1.448	118.306	-16.279	114.937
8	-23.092	108.281	-1.887	106.652	-22.083	103.774
9	-38.456	97.632	-3.158	96.373	-37.002	94.078
10	-105.733	121.171	-8.738	120.457	-103.174	118.849

**Table 42: Bridge B Maximum Shear and Moment for Compacted Backfill**

<b>Abutment Location (ft)</b>	<b>Stiff Clay at Piles</b>		<b>Medium Stiff Clay at Piles</b>		<b>Soft Clay at Piles</b>	
	<b>Max Shear (K-ft)</b>	<b>Max Moment (K-ft)</b>	<b>Max Shear (K-ft)</b>	<b>Max Moment (K-ft)</b>	<b>Max Shear (K-ft)</b>	<b>Max Moment (K-ft)</b>
1	684.991	994.274	608.244	892.018	504.141	753.771
2	-158.660	396.748	-140.844	355.935	-119.651	300.099
3	-50.552	242.719	-45.487	217.604	-39.359	182.542
4	-28.255	197.710	-24.950	175.776	-21.321	146.378
5	-28.143	175.261	-24.712	156.544	-20.766	129.293
6	-20.747	152.818	-17.872	136.975	-14.706	112.819
7	-23.073	132.765	-20.238	119.704	-16.676	98.645
8	-27.857	113.801	-24.752	103.701	-20.384	85.912
9	-40.152	113.801	-36.741	89.990	-30.718	75.628
10	-96.149	104.801	-93.286	105.158	-81.626	95.259

**Table 43: Bridge B Maximum Shear and Moment for EPS Geofoam Backfill**

<b>Abutment</b>	<b>Stiff Clay</b>		<b>Medium Stiff Clay</b>		<b>Soft Clay</b>	
<b>Location</b>	<b>Max</b>	<b>Max</b>	<b>Max</b>	<b>Max</b>	<b>Max</b>	<b>Max</b>
<b>(ft)</b>	<b>Shear</b>	<b>Moment</b>	<b>Shear</b>	<b>Moment</b>	<b>Shear</b>	<b>Moment</b>
<b>(K-ft)</b>	<b>(K-ft)</b>	<b>(K-ft)</b>	<b>(K-ft)</b>	<b>(K-ft)</b>	<b>(K-ft)</b>	<b>(K-ft)</b>
1	691.235	996.857	568.842	826.341	424.586	621.276
2	-157.336	398.103	-128.278	333.397	-94.913	252.039
3	-48.223	246.335	-39.281	207.805	-28.783	158.425
4	-26.918	203.832	-21.211	171.227	-15.416	131.108
5	-26.842	182.799	-20.939	155.350	-15.041	120.039
6	-20.091	160.981	-15.299	139.341	-10.646	109.244
7	-23.075	141.899	-18.696	124.962	-13.571	99.835
8	-28.954	123.507	-24.566	111.270	-18.875	91.043
9	-43.610	106.689	-39.489	99.091	-32.571	83.566
10	-106.809	116.223	-104.927	118.597	-93.639	109.404

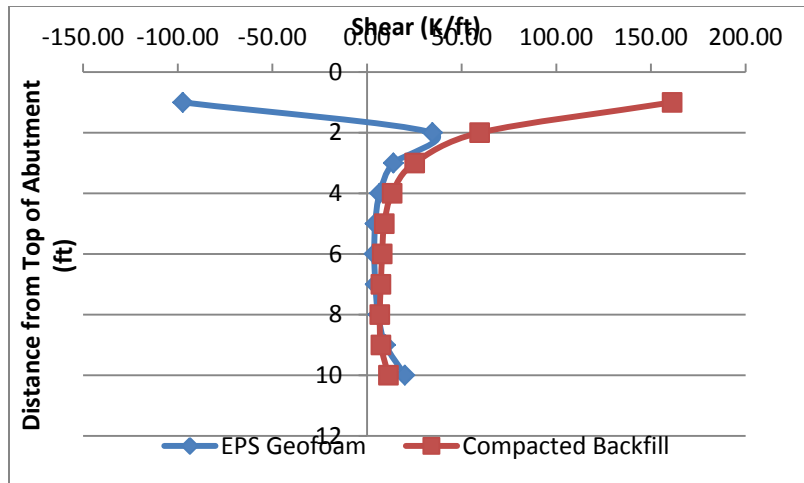


**Figure 42: Bridge A Maximum Shear for Dense Sand at Piles**

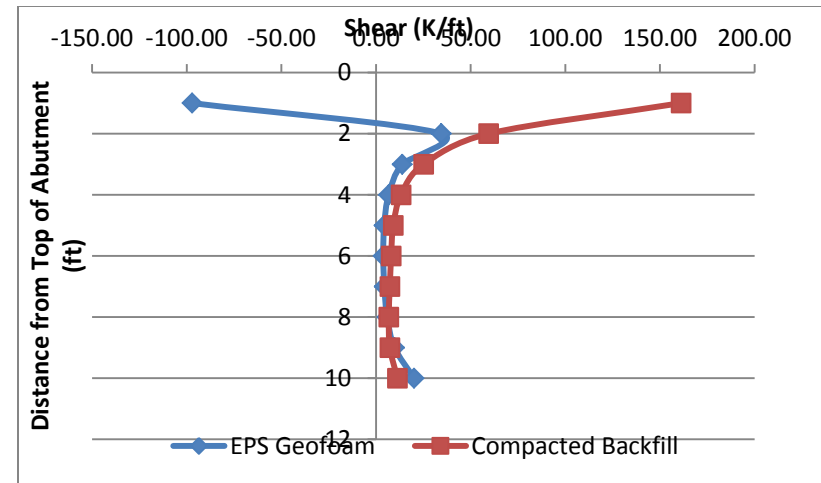


**Figure 43: Bridge A Maximum Shear for Medium Dense Sand at Piles**

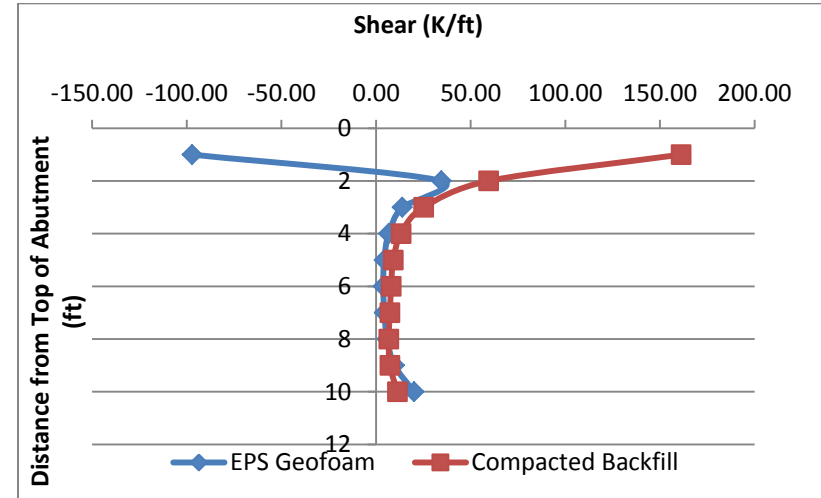


**Figure 44: Bridge A Maximum Shear for Loose Sand at Piles**

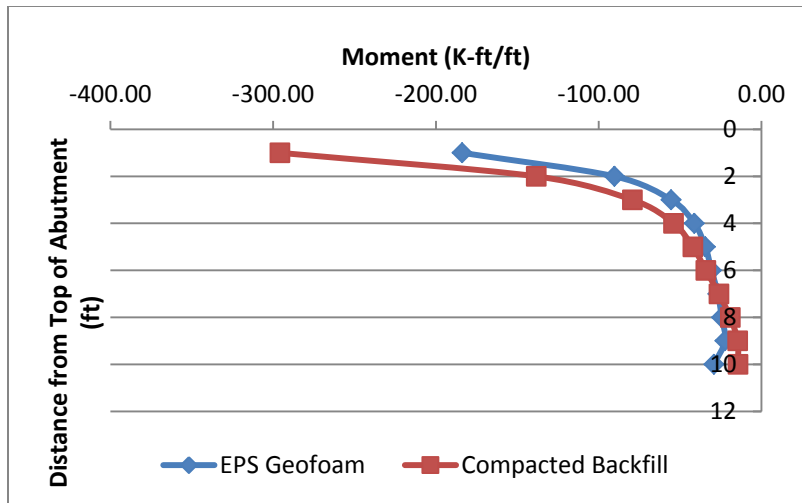


**Figure 45: Bridge A Maximum Moment for Dense Sand at Piles**

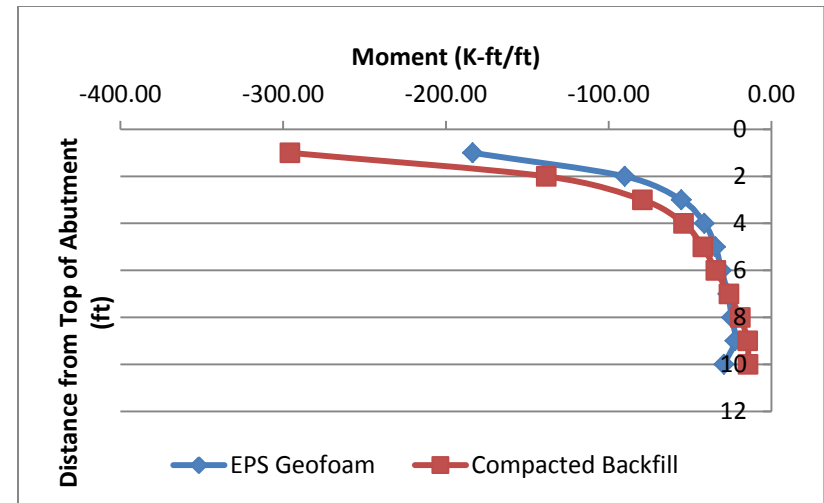


**Figure 46: Bridge A Maximum Moment for Medium Dense Sand at Piles**

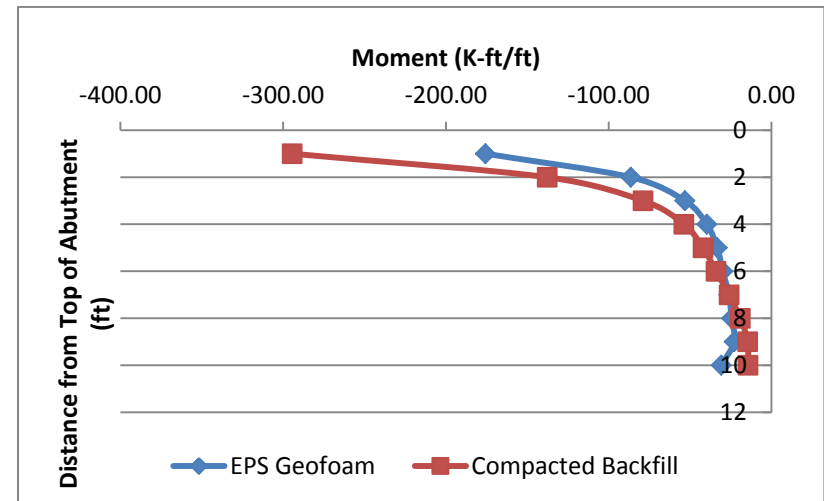


**Figure 47: Bridge A Maximum Moment for Loose Sand at Piles**

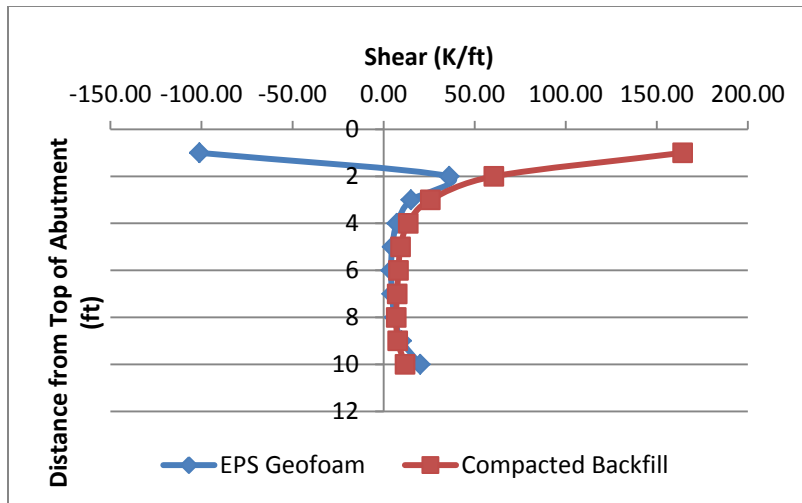


**Figure 48: Bridge A Maximum Shear for Stiff Clay at Piles**

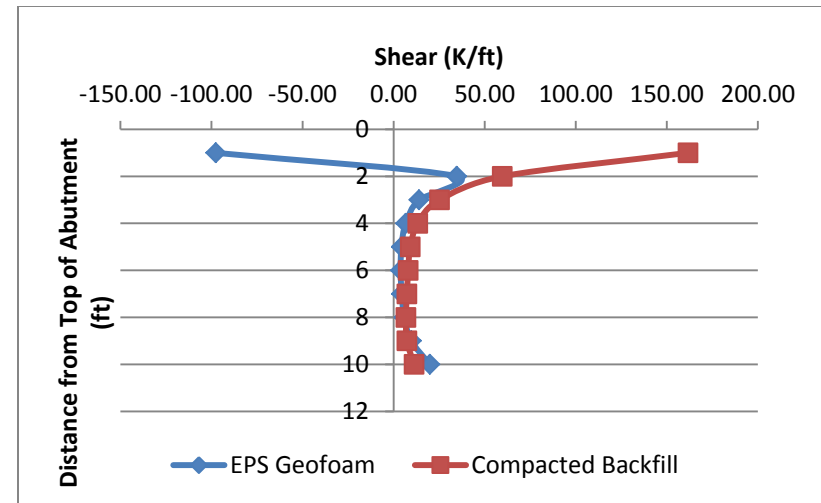


**Figure 49: Bridge A Maximum Shear for Medium Stiff Clay at Piles**

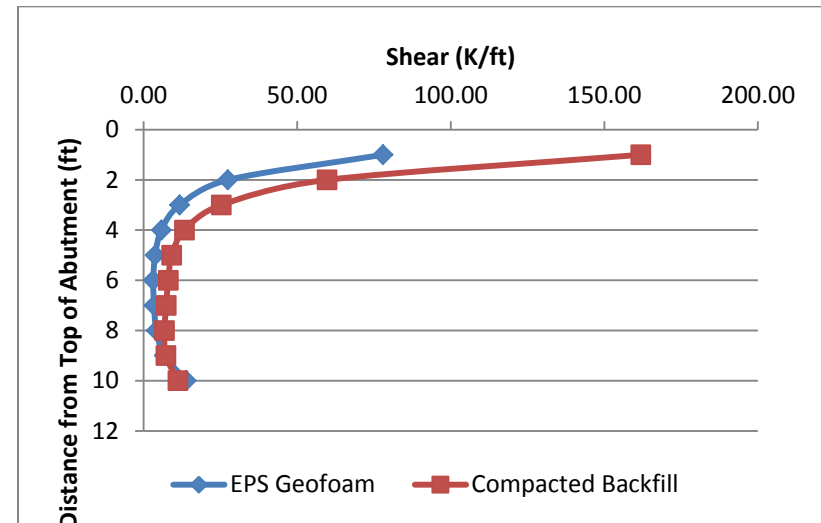


**Figure 50: Bridge A Maximum Shear for Soft Clay at Piles**

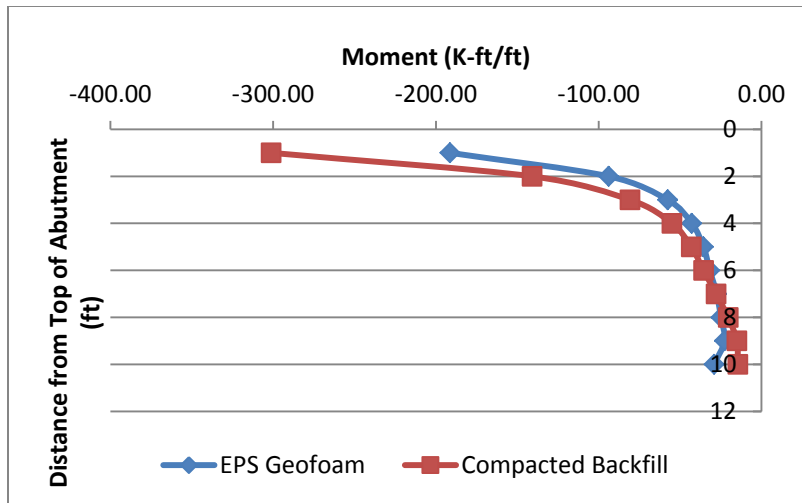


**Figure 51: Bridge A Maximum Moment for Stiff Clay at Piles**

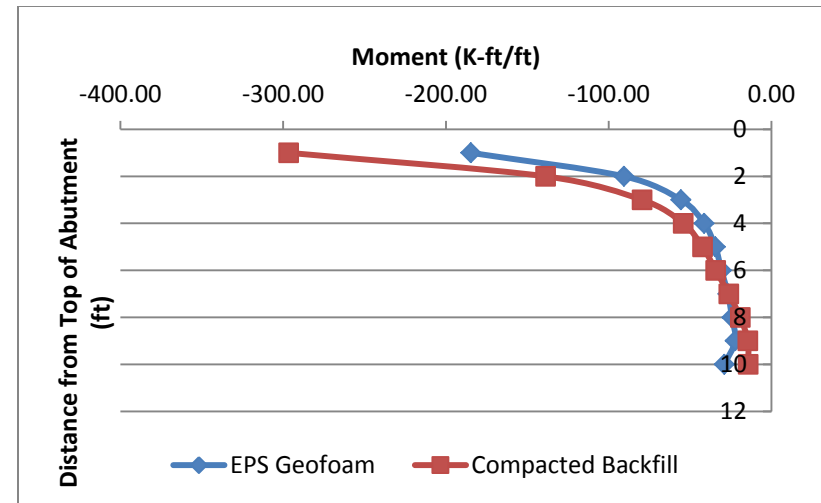


**Figure 52: Bridge A Maximum Moment for Medium Stiff Clay at Piles**

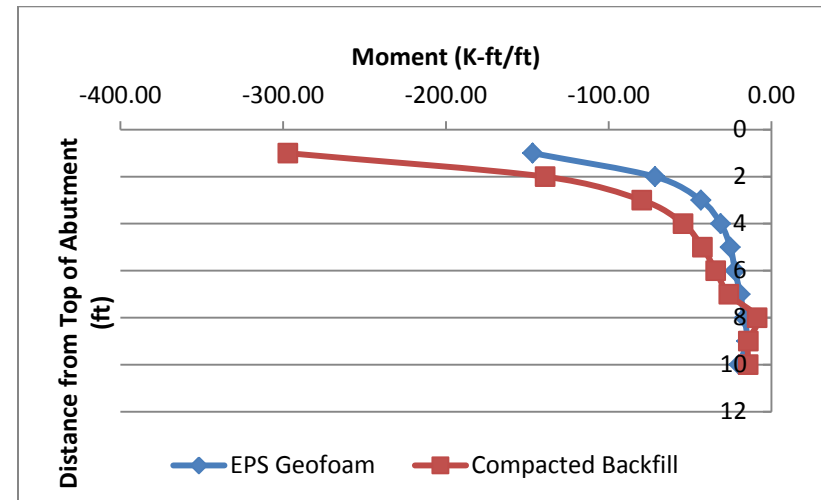


**Figure 53: Bridge A Maximum Moment for Soft Clay at Piles**

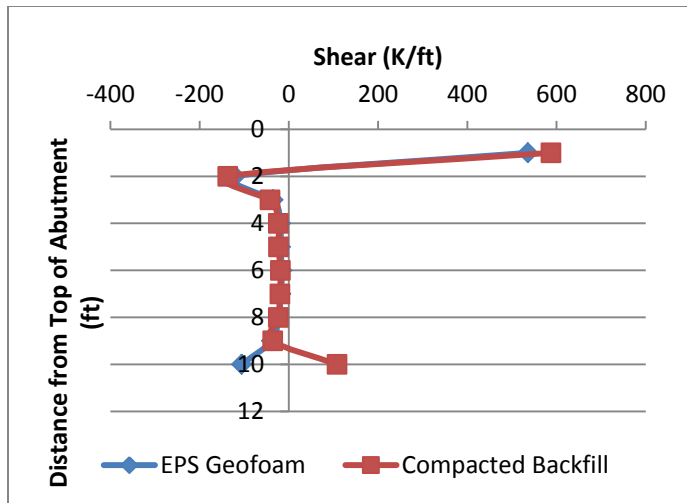


**Figure 54: Bridge B Maximum Shear for Dense Sand at Piles**

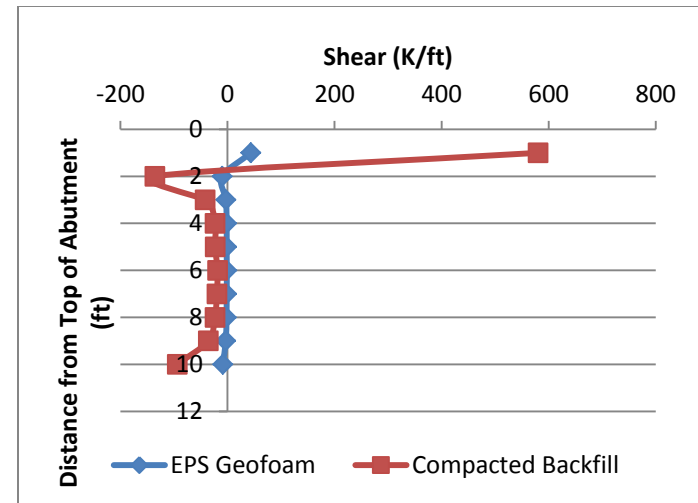


**Figure 55: Bridge B Maximum Shear for Medium Dense Sand at Piles**

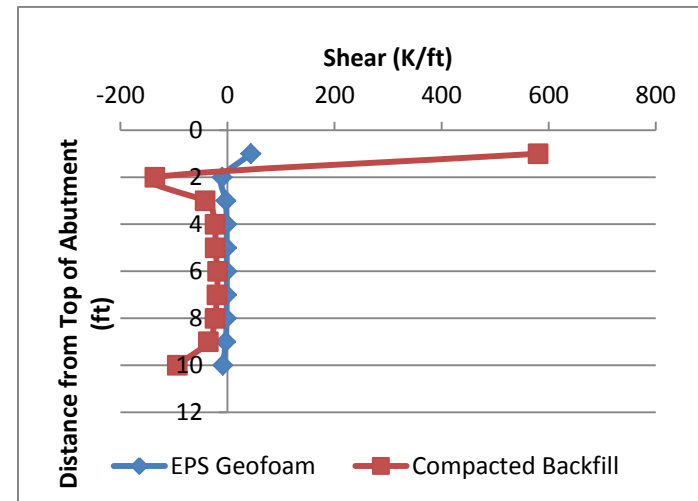


**Figure 56: Bridge B Maximum Shear for Loose Sand at Piles**



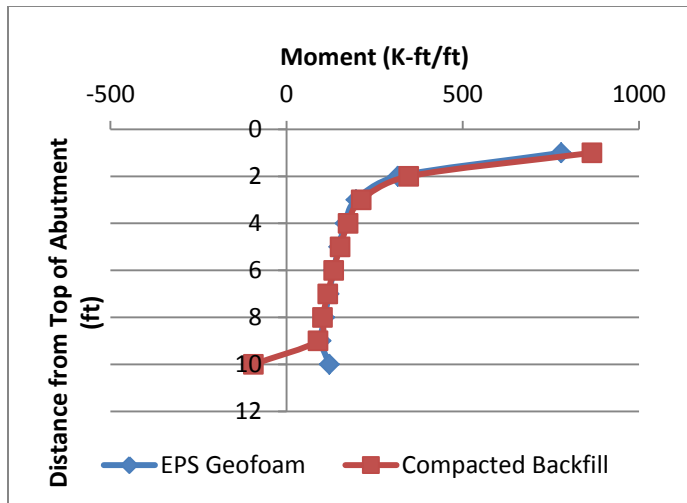


**Figure 57: Bridge B Maximum Moment for Dense Sand at Piles**

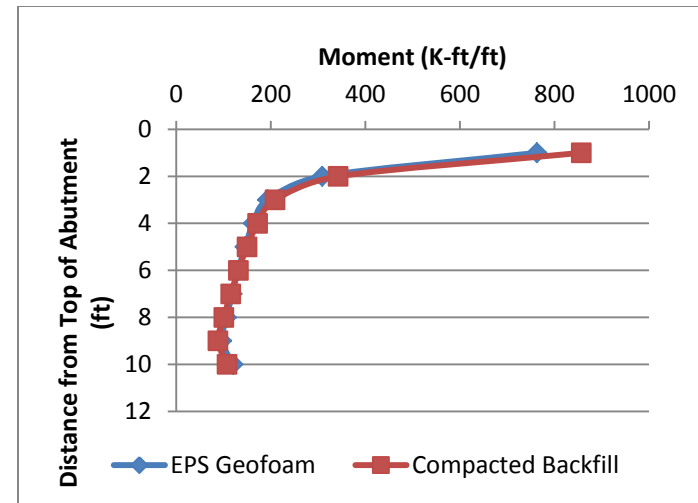


**Figure 58: Bridge B Maximum Moment for Medium Dense Sand at Piles**

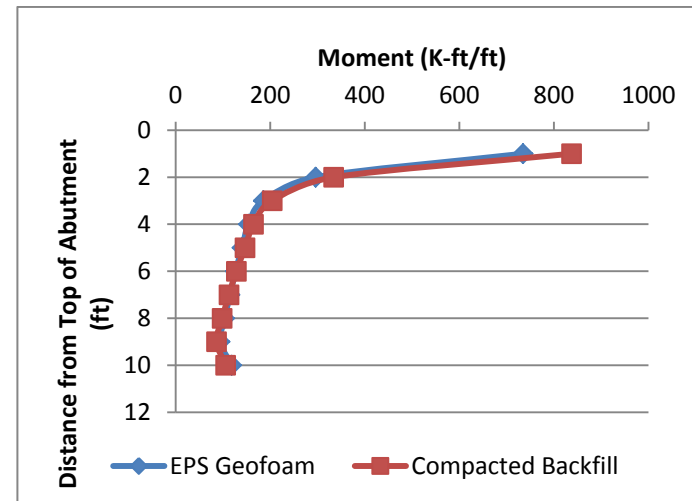


**Figure 59: Bridge B Maximum Moment for Loose Sand at Piles**

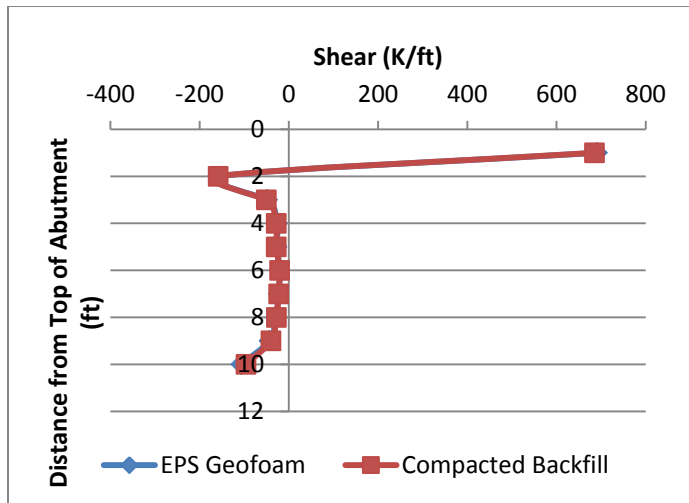


Figure 60: Bridge B Maximum Shear for Stiff Clay at Piles

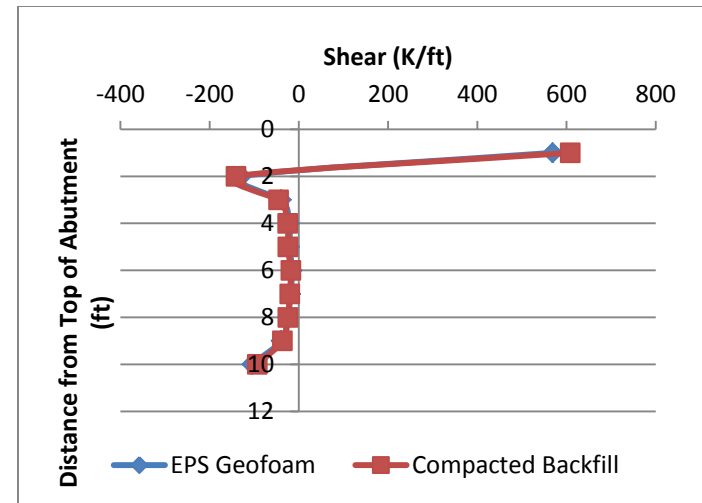


Figure 62: Bridge B Maximum Shear for Soft Clay at Piles

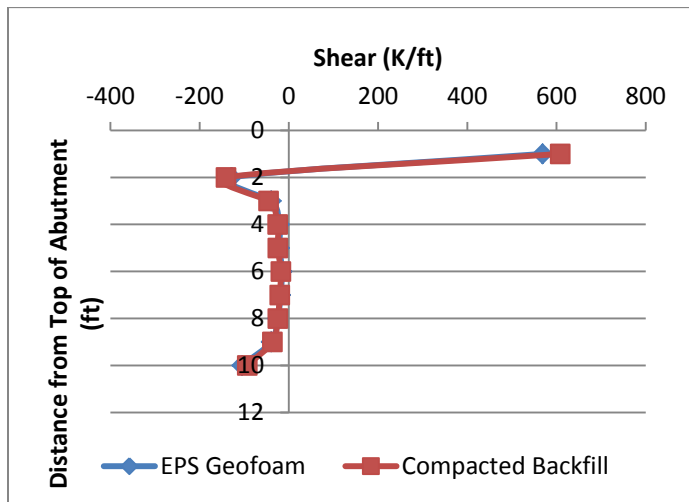
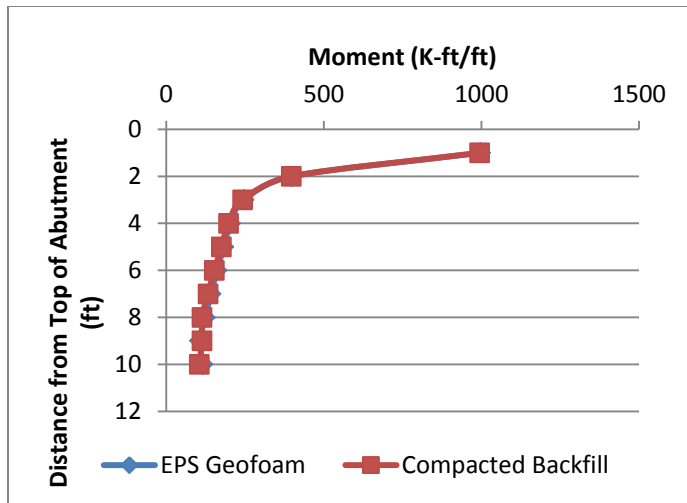
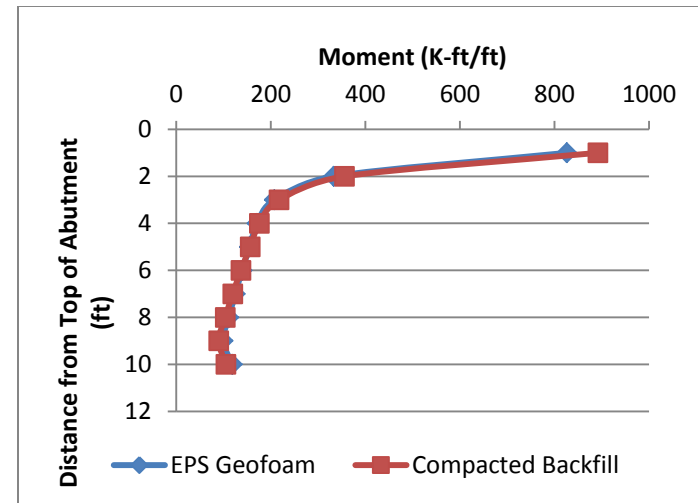


Figure 61: Bridge B Maximum Shear for Medium Stiff Clay at Piles



**Figure 63: Bridge B Maximum Moment for Stiff Clay at Piles**



**Figure 64: Bridge B Maximum Moment for Medium Stiff Clay at Piles**

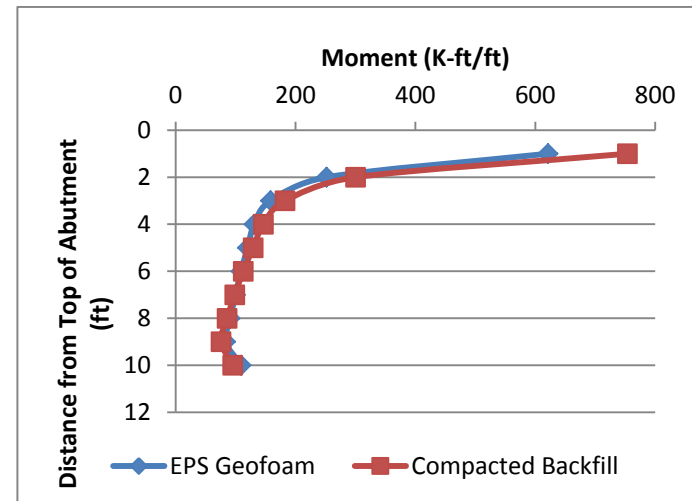


**Figure 65: Bridge B Maximum Moment for Soft Clay at Piles**

## **CHAPTER V**

### **5 SUMMARY AND CONCLUSIONS**

#### **5.1 SUMMARY**

Integral abutment bridges provide many advantages over bridges with conventional abutments. This includes reduced or no bridge joints and reduced quantity of bearings. Both of these provide construction and maintenance cost savings. Additionally, reduced number of bearings and joints means less maintenance over the life of the structure.

With these benefits, many agencies are pushing towards using integral abutment bridges where possible. As a result, integral abutment bridges are being designed for seismic loading in medium seismic zones more frequently. Integral abutment bridges tend to be more rigid than bridges with conventional abutments due to the stiff connection between the superstructure and the abutment. When designing for seismic loading, this additional rigidity can cause the structure to attract more forces, which could require using larger sections, which in turn costs more in labor and materials.

It would be beneficial to be able to reduce the stiffness of integral abutment bridges and therefore reduce the seismic loading on certain members. The use of EPS Geofoam backfill with integral abutment bridges can offer great benefits, including reduced stiffness. This can help reduced abutment forces under seismic loading and increase bridge flexibility as a whole.

## 5.2 CONCLUSION

Based on the analysis of the 13 models per bridge, 1 traditional jointed bridge with seat-type abutments and 12 with integral abutments and various types of backfill and surrounding soil, several conclusions can be made. The following are the main conclusions:

- The fundamental period is significantly smaller for bridges with integral abutment, which means the bridges are less flexible than bridges with conventional abutments.
- The bridge length may affect the amount by which EPS geof foam increases abutment displacement compared to using compacted backfill.
- Bridge length may affect the change in pier footing moments and shears. The longer the bridge the smaller the percent change in pier footing moments and shears when using EPS Geofoam backfill in place of compacted backfill. It is not clear if this is a direct correlation or if other factors affect this change.
- EPS Geofoam backfill reduces both the moment and the shear in the integral abutments compared to compacted backfill. This is true for all cases including, dense sand, medium dense sand and loose sand at piles as well as stiff clay, medium stiff clay and soft clay at piles. This was seen to be true for both Bridge A and Bridge B.
- EPS Geofoam backfill allows the integral abutments to displace slightly more than the case with compacted backfill. This, in turn, causes the pier to displace slightly more as well.

Increasing the displacement of the integral abutments and central pier under seismic loading is an acceptable side effect as the small amount of increased displacement can be accounted for in the design of the integral abutments and pier. This

minimal amount of increased displacement, however, allows for the moments and shears in the abutments under seismic loading to be reduced, which is an important benefit. This makes designing the integral abutments easier as there are smaller forces that need to be accounted for which can result in potentially smaller cross-sections. Additionally, the reduction in moment in the integral abutments is important, as this reduces the amount of rotation that the integral abutment needs to be designed for during a seismic event.

Both the increase in pier cap forces and the increase in pier footing forces when using EPS Geofoam backfill in place of compacted backfill do not have a significant impact on the overall structure. This increase is not a benefit or detriment to the overall design of the structure, but rather a side effect for the other benefits gained from using EPS Geofoam backfill in place of compacted backfill.

When designing bridges for seismic loading in moderate seismic zone, integral abutments should be considered as a valid option, especially when coupled with EPS geofoam backfill. Although the integral abutments in these models attracted more seismic force than the conventional seat-type abutments did, these additional forces were within a range that was still designable.

This combination of EPS geofoam backfill and integral abutments provides the benefits of reduced number of joints and bearings, which is highly desirable as it provides reduced maintenance and inspection costs as well as reduced repair costs. It also provides a potential for reduced initial construction costs over integral abutments with compacted backfill as the design forces in the abutments are lower; therefore smaller

sections and less reinforcement would be required, although the material and installation costs of EPS geofoam can offset that cost savings.

## Bibliography

- Albhaisi, Suhail M. and Hani Nassif. "Effect of Substructure Stiffness on the Performance of Integral Abutment Bridges Under Thermal Loads." (2012): 325.
- American Association of State Highway Transportation Officials. *AASHTO LRFD Bridge Design Specifications, Sixth Edition*. Washington, D.C., 2012.
- American Institute of Steel Construction (AISC). *Manual of Steel Construction, 14th Edition*. Chicago, IL, 2011.
- Bowles, J.E. *Foundation Analysis and Design, 5th Edition*. New York, NY: McGraw-Hill, 1996.
- Clough, G. W. and J. M. Duncan. "Earth Pressures." Fang, Hsai-Yang. *Foundation Engineering Handbook*. Springer, 1991. 923.
- Computers & Structures, Inc. *CSI Analysis Reference Manual for SAP2000, ETABS, SAFE and CSiBridge*. Berkeley, California, 2014.
- . *CSiBridge 2015 Advanced w/Rating Version 17.1.1 Build 1099*. 2014.
- Dicleli, Murat, P. Eng and M. Suhail Albhaisi. "Maximum Length of Integral Bridges Supported on Steel H-Piles Driven in Sand." *Elsevier* (2003): 14.
- Dombroski, Jr., Daniel R. "Earthquake Risk in New Jersey." 2005.
- Expanded Polystyrene Data Sheet*. 2015. 15 August 2015.  
<<http://universalconstructionfoam.com/resources/expanded-polystyrene-data-sheet.php>>.
- Frosch, J. Robert, et al. "Jointless and Smoother Bridges: Behavior and Design of Piles." Perdue University, 2004.
- Geofoam Applications and Uses*. 2015. 2015. <<http://www.geofoam.com/applications/>>.
- Insulated Building Systems. "GeoTech TerraFlex Product Specifications." n.d.
- "Integral Abutment and Jointless Bridges." *The 2005 - FHWA Conference*. Baltimore, MD: Federal Highway Administration, 2005. 343.
- Iowa Department of Transportation, Office of Bridges and Structures. "Commentary Appendix for Technical Documents." *LRFD Bridge Design Manual Commentary*. 2009.
- Kafka, Alan L. *Why Does the Earth Shake in New England?* 15 February 2014. 3 June 2015.  
<<http://universalconstructionfoam.com/resources/expanded-polystyrene-data-sheet.php>>.



- Kratzer Environmental Services. "Physiography, Topography and Geology." 2006.
- Maruri, P.E., Rodolfo F. and Samer H. Petro, P.E. "Integral Abutments and Jointless Bridges (IAJB) 2004 Survey Summary." *The 2005 - FHWA Conference: Integral Abutment and Jointless Bridges (IAJB 2005)*. Baltimore, MD: Federal Highway Administration, 2005. 19.
- Matlock, H. "Correlation for Design of Laterally Loaded Piles in Soft Clay." *Proceedings of the II Annual Offshore Technology Conference*. Houston, Texas, 1970. 577-594.
- New Jersey Department of Transportation. *Design Manual for Bridges and Structures*. 2009.
- Rees, L.C. and W.F. Van Impe. *Single Piles and Pile Group under Lateral Loading*. Rotterdam: A.A. Balkema, 2001.
- Skempton, A. W. "The Bearing Capacity of Clays." *Building Research Congress*. London, England, 1951. 180-189.
- United States Geological Survey. *New Jersey 2014 Seismic Hazard Map*. 30 October 2014. 15 May 2015. <[http://earthquake.usgs.gov/earthquakes/states/new\\_jersey/hazards.php](http://earthquake.usgs.gov/earthquakes/states/new_jersey/hazards.php)>.
- . *New Jersey Earthquake History*. 14 January 2015. 15 May 2015. <[http://earthquake.usgs.gov/earthquakes/states/new\\_jersey/history.php](http://earthquake.usgs.gov/earthquakes/states/new_jersey/history.php)>.
- . *New Jersey Seismicity Map - 1973 to March 2012*. 18 April 2014. 15 May 2015. <[http://earthquake.usgs.gov/earthquakes/states/new\\_jersey/seismicity.php](http://earthquake.usgs.gov/earthquakes/states/new_jersey/seismicity.php)>.
- Volkert, Rich. "Geology of the Piedmont Province (Newark Basin)." 2008. *Rutgers*. 15 May 2015. <<http://envirostewards.rutgers.edu/Lecture%20Resource%20Pages/2008Lecture%20Notes/ECEC%20Piedmont%20geology.pdf>>.
- Witte, Ron W. and Don H. Monterverde. "Geologic History of New Jersey's Valley and Ridge Physiographic Province." *New Jersey Geological and Water Survey Information Circular* 2012: 8.